DEVELOPMENT AND PERFORMANCE ANALYSIS OF POROUS RADIANT BURNERS FOR COOKING APPLICATIONS

A Thesis

Submitted by

VIJAYA KUMAR PANTANGI

For the award of the degree

of

DOCTOR OF PHILOSOPHY

DEPARTMENT OF MECHANICAL ENGINEERING

INDIAN INSTITUTE OF TECHNOLOGY GUWAHATI

MAY 2010

CERTIFICATE

It is certified that the work contained in the thesis entitled **Development and Performance Analysis of Porous Radiant Burners for Domestic Cooking Applications** by **Vijaya Kumar Pantangi**, a student in the Department of Mechanical Engineering, Indian Institute of Technology Guwahati, India, for the award of the degree of the **Doctor of Philosophy** has been carried out under our supervision and that this work has not been submitted elsewhere for the degree.

Dr. Subhash C. Mishra
Professor
Department of Mechanical Engineering
Indian Institute of Technology Guwahati
Guwahati – 781039, Assam, India.

Dr. P. Muthukumar
Assistant Professor
Department of Mechanical Engineering
Indian Institute of Technology Guwahati
Guwahati – 781039, Assam, India.

Dedicated to my parents

Dr. P. V. Rama Rao and Mrs. Uma Devi,

sister Rajeswari and her family.

Acknowledgements

I am deeply indebted to my thesis supervisors, **Prof. Subhash C. Mishra** and **Dr. P. Muthukumar**, for their invaluable guidance and steady encouragement throughout my Ph.D. program. The vigour and attention bestowed by them in taking my research ahead in difficult times will never be forgotten. Starting from formulating the problems to the final experimental results and their physical interpretations, they remained deeply involved in my thesis work. They provided me with most innovative ideas, helpful books and journals that were very helpful in successfully completing the present thesis. I have immensely benefited from each and every moment of my association with them. I am highly inspired by their intellectual prowess and exemplary professionalism.

I am also deeply indebted to **Prof. Dr. Dr. h. c. F. Durst**, one of the pioneers in the porous medium combustion, for giving an opportunity to work with him at FMP Technology GmbH and University of Erlangen, Erlangen, Germany on my Ph.D. problem. The thing which likes me about Prof. Durst is the way he approaches the problem. It is simply unsurpassed. I would also thank **FMP Technology GmbH** and **PROMEOS** for providing the necessary scholarship for my stay at Germany. I would also like to thank **Dr. Ausmeier** and a **Turkey friend** for providing the necessary instrumentation.

I would like to thank **Petroleum Conservation and Research Association (PCRA), New Delhi** for their financial support for the Second phase developments. I am thankful to my doctoral committee members: **Dr. Manmohan Pandey** (Currently at IIT Gandhinagar, Gujarat), **Dr. U. K. Saha** and **Dr. Anugrah Singh** for providing insightful comments and

valuable suggestions during the annual progressive seminars as part of the Ph.D. program. Their suggestions helped me work in a focused manner and improve my communication skills. I am grateful to all of them. I would like to express my sincere thanks to the highly skilled workshop personnel for making components in time and making the experiments a success. I would like to express my sincere thanks to **Prof. U. S. Dixit** and **Prof. S. K. Dwivedy** and other faculty members of the Department of Mechanical Engineering for their encouragement and support. I am also thankful to the **Center for Energy**, **administrative staff** of IIT Guwahati who directly and indirectly helped to complete the thesis work.

I am sincerely thankful to **Mr. S. Rajesh Reddy**, **Mr. Subir Das** and **Mr. Ratan** for their help during the experiments. **Mrs. M. K. Sharma** needs a special mention for being a colleague all the way from M.Tech (2 years) and Ph.D (5 years). In the same way **Dr. E. V Rao, Dr. Ramaraju, Dr. K. Veerababu, Dr. B. Mondal, Dr. Muthukumaran, D. Santhosh, S.P. Laxmanan, D.A. Perumal, A. Satheesh, C. Subramanian, S. Anbarasu, Ratnakar Das, Suresh, Buljit Burgohain, Arpana Nath, S. Shukla and R Chopdae** gave me a remarkable moral support with out which it would have been difficult for me to stay 2500 km far away from home. And how can I forget my parents? I venerate their patience, wishes and the enormous trust they repose in my abilities at all times. I would also like to thank my friends **Anupam Sengupta**, **Milani**, **Zrinka Buhin**, **Nagi reddy**, **Sheila Christina, Gautham** and **Ayan** for making my stay a memorable one at Erlangen, Germany. I would like to extend my sincere thanks to who are all helped me directly and indirectly for the successful completion of the thesis.

May 2010 **Vijaya Kumar Pantangi**

Abstract

For cooking, liquefied petroleum gas (LPG) is one of the most commonly used fuels in India and many other countries. LPG being a clean fuel burns with no soot and has high calorific value than kerosene and wood. In India, as the living standard of the people is improving, the number of LPG consumers is also increasing. The increase is very high in the urban sector. In the year 2004, the dependency of Indian urban domestic sector on LPG fuel was about 48% and for the period of 2010 - 2011, the same had been projected to be about 90%. The total domestic consumption of LPG in India is almost comparable with other petroleum products used in industrial applications. The thermal efficiencies of the current LPG cooking stoves available in the Indian market are in the range of 60 - 65% and at the same time the CO (90 - 1050 mg/m^3) and NO_X (162 - 216 mg/m^3) emissions levels are above the world health organization standards. Moreover, these burners operate in a very low thermal power modulation. Considering the energy conservation, environmental issues and increase in demand on LPG in the near future, there is a need to explore the ways to further improve the thermal efficiency and the emission characteristics of the LPG cooking stoves.

In order to overcome the above mentioned disadvantages in the existing cooking burners, this thesis proposes the applicaton of porous medium combustion (PMC) and porous surface combustion (PSC) technologies in domestic cooking stoves. The aim of the present work is to develop the porous burners using PMC and also the combination of PMC and PSC for cooking applications and to analyse the performances in terms of thermal efficiency and emissions levels at different power and equivalence ratios.

The present thesis is divided into three phase developments namely first, second and third phase developments. In the first phase developments, existing conventional burner was modified by filling its distribution chamber with different porous media such as, stainless steel balls, pebbles and twisted stainless steel chips. The results presented for four important cases (with different combinations of the porous materials) showed a gradual improvement in the thermal efficiency. The CO and NO_x emissions found decreased with the increasing thermal efficiency. The thermal efficiencies reached to a maximum of 73% which is 8 percent higher than the conventional domestic cooking burner. The NO_x emissions are found to be lower than the range of conventional domestic cooking burner but the CO emissions are little higher than the lower limit of the domestic cooking burner. At the highest efficiency the power range is dropped down to a very narrow range due to the increased flame velocities than the air fuel mixture velocity making the burner prone to flash back.

During the second phase developments, the burner casing was fabricated with alumina powder using sodium silicate binder. Silicon carbide and alumina balls were used as combustion zone and preheating zone. The effect of burner geometry (wall thickness and diameter of the burner) on thermal efficiency was investigated at different powers and equivalence ratios. The diameters of the burners were increased from 60 mm to 100 mm in steps of 10 mm. They are named as B6, B7, B8, B9 and B10, where B stands for burner and the numerical numbers stands its diameter in cm. In order to reduce the heat loss from the burner, the thickness of the burner casing was increased from 10 mm to 40 mm for B8, B9 and B10. To study the temperature distribution in the burner, temperature at different positions has been recorded. The burners B8 and B9 were able to reach the maximum thermal efficiency of around 68%. Unlike, the effect of burner diameters on thermal efficiency, the same was not found to have any significant effect on the emissions. The CO emissions are

found decreasing with increasing equivalence ratio. Similarly, thermal efficiency was also found to decrease with increase in equivalence ratios, where the radiation output is higher. The NO_x emissions are found far below than the conventional burner range. The further modifications in B8 burner for proper temperature distribution increased the thermal efficiencies up to a maximum value of 72% which is 7% higher than the conventional burner. However, no distinguished change in the CO and NO_X emissions were observed. The burners B6, B7, B8 and B9 were able to run with equivalence ratio in the range of Φ = 0.3 to 0.5 and in power range of 0.6 to 2 kW. It is found that an increase in the burner diameter beyond a certain value (above 90 mm) reduces the thermal efficiency. The temperature distribution within the B6 burner confirms that the reaction zone was formed close to the interface of the preheating and combustion zones. It has been observed that, at 1.67 kW, the reaction zone moves downstream of the burner with the increase in the wattage. The flash back was eliminated within the operating conditions of the burner.

During the third phase of developments, yet another attempt for low emission and high thermal efficiency burner, a combinational burner was proposed and tested. In this burner, a porous matrix (PM) was placed at a distance (4 mm to 12 mm) above the PSB. The effect of distance between PSB and PM on the emissions characteristics was investigated. The CO emissions are observed lowest when the distance was 12 mm, beyond this distance the emissions are found to increase. The NO_x emissions are insensitive to power and equivalence ratio. The induced back radiation on the PSB from the PM limits the applicability of the burner to work in the range of 2 to 3 kW by inducing the flash back conditions. The first generation combinational burner showed a profound emission reduction in comparison of the existing porous surface burners.

Contents

List of Figures

List of Tables

Nomenclature

Symbols	**Units**	**comments**
ϕ	-	Volume fraction of fluid phases
Φ	-	Equivalence ratio
τ	m^{-1}	Extinction co-efficient
$\lambda_{II,\perp}$	W/m-K	Upper and lower bounds of effective thermal conductivity
$\lambda e,s,f$	W/(m-K)	Effective, solid and fluid thermal conductivities
T_1 *and* T_2	°C	Initial and final temperatures
S_L	m/s	Flame velocity
ρ	kg/m^3	Density
p	-	Porosity
pe	-	Peclet number
Nu	-	Nusselt Number
η_{th}	%	Thermal efficiency
$m_{W,p}$	kg	Mass of water and aluminium pan with lid and stirrer
l_c	mm	Characteristic length
L	mm	Specimen thickness

k	W/m-K	Thermal conductivity
d_m	m	Mean pore cavity diameter
$C_{W,V}$	kJ/kg-K	Specific heats of water and aluminium pan
CV	kJ	Calorific value

Abbrevations

CB	Conbinational burner
CFRC	Cyclic flow reversal combustion
CZ	Combustion zone
GoI	Government of India
LPG	Liquefied petroleum gas
INR	Indian rupees
ppi	pores per inch
ppcm	Pores per centimetre
PB	Porous burner
PBs	Porous burners
PM	Porous matrix
PMB	Porous medium burner
PMBs	Porous medium burners
PMC	Porous medium combustion
PRBs	Porous radiant burners
PRRB	Porous radiant re-circulated burner
PSB	Porous surface burner
PSC	Porous surface combustion
PZ	Preheating zone
RVC	Reticulated vitreous carbon
SAC	Super adiabatic combustion
SB	Swirl burners
SCH	Surface combustor heater
VOCs	Volatile organic compounds
WHO	World Health Organisation

Chapter 1

INTRODUCTION: PROBLEM AND AIM

In developing countries, majority of the energy requirements are still met with conventional combustion devices working on fossil fuels. However, the depleting fossil fuel reserves and the growing ecological imbalance due to pollutants originating from combustion have necessitated the need to look either for alternative sources of energy or to improve the efficiency of the existing combustion devices. Hence, a continued endeavour on improving performance of such devices has remained a paramount focus for the policy makers and researchers dealing with energy conservation and environmental pollution.

A conventional combustion device is characterized by a free flame, in which chemical reaction occurs in a small region of the combustion chamber, leading to a maximum energy release (high temperature) in that region. This gives rise to a very high temperature gradient across the combustion zone. This type of combustion takes place in the gaseous environment where convection is the predominant mode of heat transfer. Since gases have a very poor thermal conductivity and have low opacity, the contributions of conduction and radiation modes of heat transfer from the post flame to pre flame zone is negligible. Thus, the poor heat transport makes the conventional combustion devices less efficient and it gives rise to some other undesirable features such as low flammability limits, low power density (large size of combustor), weak power modulation, high level of pollutant emissions, etc. In order to overcome the above mentioned issues of the devices working on free flame combustion, attention has been focused on some innovative combustion technologies which are efficient and environment friendly for the past two decades. The domestic cooking gas burner is one

such device that goes well with this category of high emission levels, low thermal efficiency and power modulation.

In India and many other developing countries, the household cooking gas burners (characterized by free flame) use liquefied petroleum gas (LPG) as a most common fuel. LPG is synthesized by refining petroleum, and is usually derived from fossil fuel sources, being manufactured during the refining of crude oil, or extracted from oil or gas streams as they emerge from the ground. LPG has a high calorific value than kerosene and wood, and burns cleanly with no soot. As, the living standard of the people in India is improving, the number of LPG consumers is also increasing. The increase is very high in the urban household sector. In the year 2004, the dependency of Indian urban domestic sector on LPG fuel was about 48% and for the period of 2010 - 2011, the same had been projected to be about 90% [Antonette D'Sa and Narasimha Murthy, 2004]. The total domestic consumption of LPG in India is almost comparable with other petroleum products used in industrial applications. The measured (laboratory conditions) thermal efficiencies of the current LPG cooking burners available in the Indian market are in the range of 60-65% and at the same time the CO (90 mg/m^3 - 1050 mg/m^3) and NO_X (162 mg/m^3 - 216 mg/m^3) emissions levels are above the current standards of world health organization [Kandpal *et al.*, 1995] along with low thermal power modulation as discussed earlier. Considering the depletion of fossil fuels, energy conservation, environmental issues, and increase in demand on LPG in the near future, there is a need to explore the ways to further improve the thermal efficiency and the emission characteristics of the LPG cooking stoves.

There is also another dimension of the problem apart from the emissions and demand. In India LPG is highly subsidized from the government of India (GoI). In June 2003, the

unsubsidized price of the 14.5 kg domestic LPG cylinder was 470.00 INR and the subsidized price of the same was about 225.00 INR. The rest would be paid by GoI to the oil companies. Hence, GoI has to spend millions of rupees as subsidies in every year and which is rising with the increase in demand. In June 2003, however, the Ministry of Finance announced that the LPG and kerosene subsidies would be phased down in three years and eliminated by April 2006. The Ministry of Petroleum and Natural Gas was reported as favouring a five-year phase-down period to reduce the burden on the state oil companies from cost under-recovery as occurred in fiscal year 2002 - 03 which was not achieved till date due to the economic status of the common man in India [World Bank, 2003]. In order to cut down the increasing subsides, GoI initiated to support the research and development of the efficient burners for cooking applications.

The porous medium combustion (PMC) is one such technology that utilizes a novel concept of using a solid medium in the combustion zone for better heat transport from the burned to unburned portion of the air-fuel mixture. PMC technology has been known for decades but it has been developed to a stage for practical applications only in the recent past. The burners made of porous medium are found to have a better performance over conventional burners. This is attributed to better heat transport by conduction, convection and radiation. Since the porous matrix has high thermal conductivity and good radiative properties, the contributions of conduction and radiation in the PMC are significant. Besides, due to a large surface area of the porous matrix and high heat transfer coefficient, the convective heat transfer is also better than the free flame combustion. Thus, owing to better heat transport, the use of porous radiant burner (PRB) reduces some of the undesirable features associated with devices based on free flame combustion. The PMC is characterized by a high burning velocity, reduced temperature drop across the reaction zone, high radiant output, high peak flame temperature and reduced

enthalpy of flue gas. Unlike conventional burners, in a PRB, a low calorific fuel can also be combusted.

In general, based on the type of media used, the PMC is categorized into catalytic and inert. The former one utilizes a catalytic medium, which is coated on the solid matrix and participates in the combustion process; whereas the latter one remains inert but augments the heat transfer process. Further, depending upon whether the flame is stabilized over the surface or within the porous matrix, the porous radiant burners (PRBs) based on PMC can be classified as surface stabilized or matrix stabilized. In surface stabilized combustion, the flame stabilization and combustion takes place on the downstream surface of the porous matrix. Unlike surface stabilized combustion, in matrix stabilized combustion, the flame stabilizes and combustion takes place completely inside the porous matrix. The burners based on these are named as porous medium burner (PMB) and porous surface burner (PSB), respectively.

The matrix stabilized combustion possesses higher radiant efficiency. In addition, the matrix stabilized can be operated at higher firing rate 3 MW/m^2 whereas the firing rate in a surface stabilized combustor is limited to 400 kW/m^2 only. These two salient features of the matrix stabilized combustor have widened the scope of applicability of this category, and hence in recent times, much attention has been focused on matrix stabilized burners, rather than surface stabilized. However, its usage in cooking stoves has not been investigated so far. Hence, this thesis is devoted to investigate the applications of the porous burners particularly concentrating on domestic cooking stove. This thesis consists of six Chapters and the contents presented in each Chapter are discussed in the following sections.

In the second chapter, a brief historic view on porous medium combustion covering the main patent developments till date is presented. Then, the conventional domestic cooking burner, porous medium and surface combustion technologies are discussed in detail. This chapter also presents the state of the art on porous medium and surface combustion technologies. The state of the art mainly on PMC is sub-divided into experimental and numerical investigations, and applications of porous burners ranging from industry to domestic sector. The chapter ends with concluding remarks on the literature review and then objectives of the present thesis.

Chapter 3 deals with the first phase developments which show the possible applicability of the porous medium burner used in domestic cooking applications. The existing conventional domestic cooking burner was modified by filling its distribution chamber with different porous media such as, stainless steel balls, pebbles and twisted stainless steel chips. The results on emission and thermal efficiency at different power are discussed.

Chapter 4 deals with the second stage developments with the improved design of the burner casing and burner materials. The effects of burner dimensions on the thermal efficiency and emission characteristics are studied at different powers and equivalence ratios. The combustion behaviour within the burner is also studied using the temperature distribution at different positions of the burner.

Chapter 5 deals with the third stage of developments, which is yet another effort for low emission and high thermal efficiency cooking burner. In this chapter, a new combinational burner was investigated. The effect of distance between PSB and PM on the emissions characteristics was investigated along with the thermal efficiency. To understand the

combustion behaviour of the CB, the temperature distribution of the burner is studied. Conclusions and future work are presented in chapter 6.

Chapter 2

STATE OF THE ART

In this chapter a detailed survey on the early developments of porous medium combustion that lead to the establishment of the technology for application along with principle of operation is presented. The basic principle operation of the domestic cooking burner is also described. The experimental and numerical investigations on flame stability, emission characteristics, and radiation output of porous medium combustion carried out by different researchers are discussed. The results presented are specifically on the porous inert medium burners having single and double-layers. Research work carried out on the porous surface burners are discussed separately. The various applications of PB are discussed in detail from gas turbines to domestic heating systems. The objectives of the thesis are presented at the end of this chapter followed by the closure of the state of the art.

2.1 CONVENTIONAL DOMESTIC COOKING BURNER

All types of burners used in cooking stoves work on the principle of a Bunsen burner. The schematic of a typical burner of a conventional LPG domestic cooking stove is shown in *Fig. 2.1*. It consists of a fixed orifice for gas inlet, two ports for primary air supply, a venture-shaped mixing tube, and a burner head with ports (holes) drilled in it fitted on top of the mixing chamber. The narrow zone of the mixing tube is called as throat, which diverges into the hind part called its bell. The gas flow rate is controlled by a valve in the gas line. Positions of the two primary air ports relative to gas inlet port vary according to manufacturers. In some burners, they are located slightly downstream of the gas inlet port.

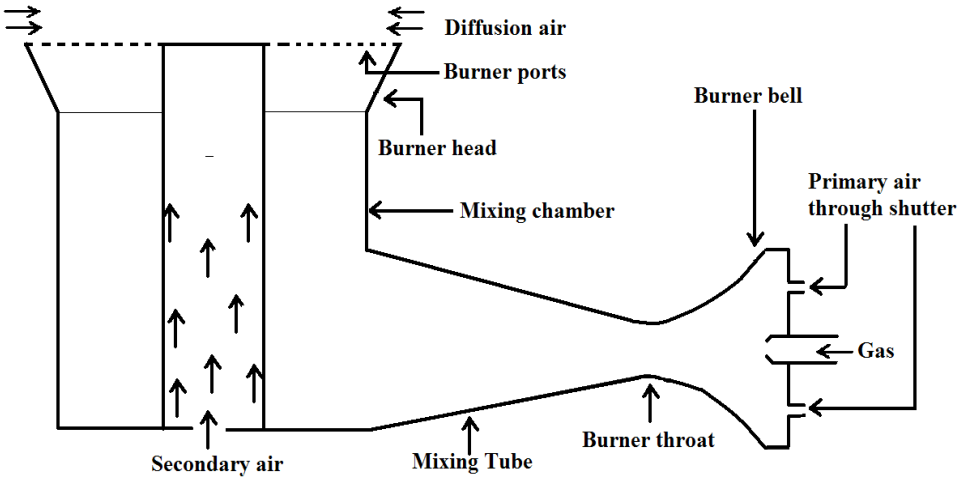

Fig. 2.1 Schematic of the conventional domestic cooking burner

Fig. 2.2 Photograph of the free flame in Conventional Domestic Cooking Stove Burner

The high velocity gas jet creates a low static pressure in the burner bell and this causes suction of primary air through the two primary air ports. Air and gas mixes in the mixing tube and through mixing chamber it comes out in the form of jets through the ports of the burner head. Combustion takes place on top of the burner head. The equivalence ratio of the mixture (air and LPG) hardly reaches to 1. The ports are closely located circumferentially and thus the

jet flames from the individual ports merge to form a single flame (*Fig. 2.2*). The secondary air is entrained to the combustion zone from the bottom of the mixing chamber and air also diffuses to the combustion zone from the circumferential area surrounding the flame. Thus, the combustion in the burner of a domestic LPG cooking stove is a partially premixed one. The combustion products are at a high temperature, so rise vertically away from the flame, transferring heat to the air close to the top of the flame. The heated air moving vertically away that draws in the cooler secondary air to the base of the flame.

The combustion in the burner of a domestic LPG cooking stove takes place in a gaseous environment and the flame stabilizes over the surface of the burner (*Fig. 2.2*). This combustion is known as free flame combustion. In free flame combustion, the reaction zone is very thin and because of which the temperature gradient across the flame is very high. Due to the above reasons the pollutant (CO and NO_X) formations in domestic LPG cooking stoves are above the current standards of the world health organization (WHO) [Kandpal *et al.*, 1995].

2.2 POLLUTANT FORMATION

The pollutant formed from the combustion process effects the environment and health in many ways. The pollutant formation happens in two ways: one is primary air pollutants which are emitted directly from the source and the other is secondary pollutants which are formed via the reactions involving primary pollutants in the atmosphere. The primary pollutants discussed in this section are carbon monoxide (CO), nitric oxide (NO) and nitrogen

dioxide (NO_2) because they dominate during the gas combustion process. The general effects and physical properties are presented in *Table 2.1*.

2.2.1 Carbon Monoxide

Carbon monoxide is the most abundant pollutant in the lower atmosphere. The physical properties and effects are presented in Table 2.1. The effects vary normal cough to death depending upon the exposure levels. The figure illustrating the different effects of CO exposure levels is given in *Fig. 2.1*.

Table 2.1 Some important physical properties and effects of the primary pollutants

Pollutant chemical name	Physical properties	Source created by humans	Natural sources	Effects on humans
CO	Colourless, odourless, flammable, toxic gas, slightly soluble in water	Combustion of fossil fuels	Atmospheric oxidation of methane and other biogenic hydrocarbons	Decreases the oxygen carrying capacity of blood. The other effects vary from headache, vomit, collapse and death depends on the levels of exposure starting from above 100 ppm to more than 600 ppm.
NO	Colourless, Odourless gas; non-flammable and slightly soluble in water; toxic	Combustion	Bacterial action; natural combustion processes; lightning	Damage respiratory air ways; can cause burns on the skin/eyes; low levels of exposure can cause cough, shortness of breath, tiredness and nausea
NO_2	Reddish-orange brown gas with sharp, pungent odour; toxic and highly corrosive; absorbs light over much of the visible spectrum	Combustion	---	Risk of respiratory symptoms such as acute bronchitis and cough and phlegm, particularly in children. Even though some studies have shown associations between NO_2 exposure and mortality

CO generally is the major species formed during the rich combustion, which is the case in IC engines that needs high power during the start up. For stoichiometric and slightly lean mixtures, CO is found in substantial quantities at typical combustion temperatures as a result of the dissociation of CO_2. Carbon monoxide concentrations rapidly fall with temperature [Turns, 2004]. According to Basu *et al.* [2000] 0.1 s of residence time is necessary for complete combustion. In furnaces, for example, where the residence time is measured in seconds, to reach conditions for complete combustion is not difficult. In IC engines the temperature rapidly falls and the residence time is not sufficiently long to approach conditions for complete combustion. The requirement of proper residence time is due to; the oxidation of fuel to CO is very fast; the oxidation of CO requires more time.

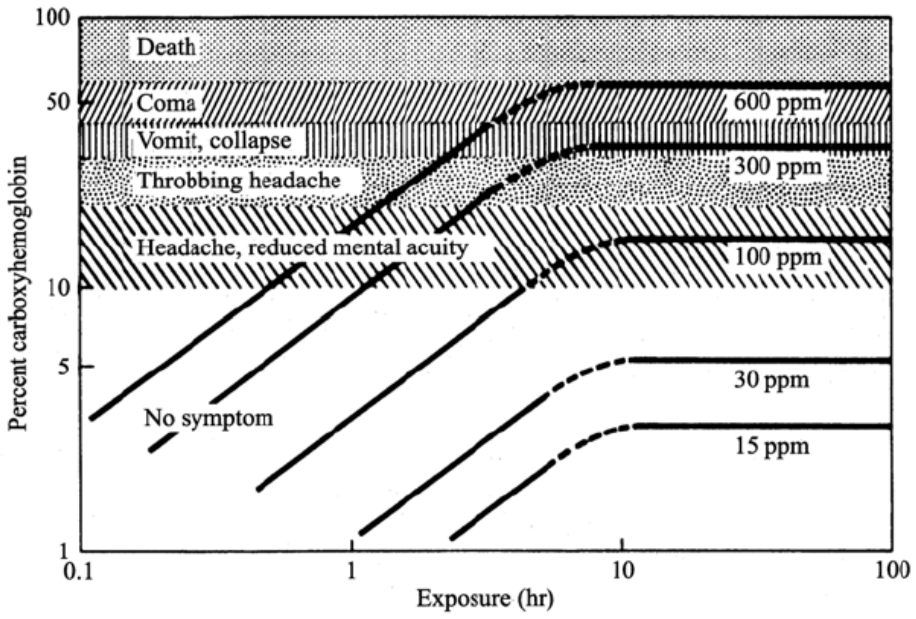

Fig. 2.3 Effects of different levels of CO exposure on humans [Avdic, 2004]

In order to decrease the CO formation concentrations in flue gases, the residence time must be as long as possible. Higher combustion temperatures are one more advantageous aspect of CO reduction. In addition, for medium lean air ratio numbers there is usually an optimal CO

concentration. At lower air ratio numbers the CO emission is higher and the CO equilibrium concentration is higher and the reaction velocity is lower, which is caused by the oxygen deficiency. For high air ratio numbers the oxidation velocity falls owing to the lower temperatures in the combustion zone. One should emphasize that the above considerations are valid only for pre-mixed combustion processes.

2.2.2 Nitrogen Oxides

Nitrogen oxides are also one of the important pollutants formed by humans mainly due to the combustion of fossil fuels. The major sources are automobiles and coal, oil and gas fired power plants. Both nitric oxide, NO, and nitrogen dioxide, NO_2, are produced in combustion, but NO is a major proportion. Both the emission species are frequently clubbed together with the title NO_x. Nitric oxide is formed both from atmospheric nitrogen, N_2, and from nitrogen contained in some fuels. The latter source depends on the fuel composition and is not important for fuels with low nitrogen contents but is a major source of NO_x in, e.g., coal combustion. Nitric oxide can be formed, however, when any fuel is burned in air because of the high-temperature oxidation of N_2.

Everybody is exposed to small amounts of nitrogen oxides in ambient air. Higher exposure may occur by burning wood, kerosene, near gas stoves or if one smokes. The effects are presented in *Table 2.1*. The important thing regarding NO medication is that there is no antidote for NO poisoning. The formation of NO can takes place in two ways which are discussed in the following sections.

Prompt NO formation

Nitric oxide can be formed from N_2 in the air through a mechanism distinct from the thermal mechanism. This other route, leading to what is termed *prompt* NO, occurs at low temperature, fuel-rich conditions and with short residence times. This mechanism was first identified by C. P. Fenimore, who found that NO concentration profiles in the post-flame gases did not extrapolate to zero at the burner surface. He did not find such behaviour in either CO or H_2 flames, which are not hydrocarbons. Fenimore concluded that the NO formed early in the flame was the result of the attack of a (high concentration) free hydrocarbon (CH) radical on N_2 making Nitrogen radical to react with oxygen to form NO. Because of the early formation of NO by this mechanism, relative to that formed by the Zeldovich mechanism, the NO thus formed is often referred to as *prompt* NO [Bowman, 1975]. Even in fuel - lean flames where the hydrocarbon radical attack of N_2 is unimportant, the non-equilibrium chemistry in the flame front can lead to prompt NO formation.

Thermal NO_x formation

The oxidation of atmospheric molecular N_2 at the high temperatures of combustion forms thermal NO_x. This means that thermal NO_x is formed during the combustion of all fuels in the regions of peak flame temperature ($\geq$ 1580°C). Because of the very short time scales involved in most combustion processes, thermal NOx formation must ultimately be considered as a kinetic process. In 1946, Zeldovich proposed a free radical chain mechanism for NO formation from air at high temperature [Seinfeld, 1986]. Due to the above mention high temperature, which is the temperature developed during a radical reaction step, the term *thermal NO* is named to this particular NO formation.

The strong dependence of the Zeldovich kinetics on temperature provides a major tool used in the control of NO formation in combustion systems. Any modifications of the combustion process that reduce the peak temperatures in the flame can be used to reduce NO_x emissions. Because of this temperature dependence, the NO formation rate varies strongly with equivalence ratio, with the highest when equivalence ratio is equal to 1. Reduction of the equivalence ratio is one possible method for NO_x control, but this method is substantially less effective in non-premixed combustion than simple theory might predict. Fuel-lean combustion reduces the flame temperature by diluting the combustion gases with excess air. If a material that does not participate in the combustion reactions is used as a diluent instead of air, the adiabatic temperature of stoichiometric combustion can be reduced and more effective control can be achieved. One common method is flue gas recirculation, in which the most readily available non-reactive gas, cooled combustion products, is mixed with the combustion air. This approach is used extensively in utility boilers and other large stationary combustors. Injection of other diluents such as water or steam can also be used to reduce the NO formation rates, but the penalty in reduced system efficiency may be larger.

Nitrogen dioxide

In the combustion zone, NO_2 levels are usually low, but exhaust levels can become significant (example gas turbines). Nitrogen dioxide is formed by the oxidation of NO, which is exothermic. Thus, the formation of NO_2 is thermodynamically favoured at low temperatures more precisely only when there is a very rapid cooling of combustion products in the presence of substantial O_2 concentrations which is not the case in domestic heating systems.

2.3 BRIEF HISTORY OF POROUS MEDIUM COMBUSTION (PMC)

The PMC is a two-century old technology. Its first research activity started in the beginning of the 19th century [Avdic, 2004]. However, due to non-commercialization, the interest in this technology faded away with time. The non-commercialization was due to the problems in flame stabilization associated with explosions and flash back, and so the burner's characterization could not be done and was left unexplored. There existed a large time gap between the early findings and the continued exploration for applications of the PMC. In recent years, owing to strict legislation on environmental protection and conservation of fuel, the interest in this technology has revived and many of its practical applications have been realized. The following paragraphs give a brief review of the PMC technology from its early development in the 19th century to till date with emphasis in the important findings/improvements of the technology and possible commercial applications.

2.3.1 Early developments

Sir Humphry Davy is the first to report a work relevant to PMC and more specifically the so called porous surface combustion [Avdic, 2004]. He made two important inventions. His first finding concluded that the combustion cannot occur in tubes below a certain radius. This minimum radius was named as "quenching radius". His second finding established the fact that even without a flame, a gas can be burnt below its ignition temperature. This was termed as "flameless combustion". These days, both the concepts are widely used in design and development of devices based on the PMC. The further developments and patents are clearly discussed by Avdic [2004] until before the end of 19th century.

Echigo [1984] reported one of the interesting developments in the area of the PMC, in 1984. He reported two major developments. The first one was related to the reduction of thermal NOx production and unburnt matters, such as CO and hydrocarbons. This was achieved through a homogenization of temperature in the combustion zone. The second one was related to enhancement of the combustion efficiency by a method wherein combustible mixture burnt in the porous matrix. In 1987, Fleming [1987] designed and patented a porous combustor and analysed the radiation energy generation process. He constructed a combustor that comprised of a porous plate with at least two discrete adjacent layers. The bottom layer was of lower thermal conductivity and acted as a preheat zone and the top layer had high thermal conductivity and emissivity which acted as a source for radiation. This design was found very effective in generation of radiant energy with improved energy efficiency, enhanced combustion intensity, and reduced emissions of noxious pollutants along with reduced flashback.

In 1991, Babkin *et al.* [1991] reported some important results related to flame propagation velocity in porous matrix. They measured the flame propagation velocity for methane-air and propane-air mixtures in four kinds of porous media. Their results established five steady-state regimes for gas combustion in an inert porous medium. They explained the phenomenon of flame quenching within the porous medium, which was important for defining combustion stability. They provided the criterion of Peclet number '*Pe*' that became the basis for flame stabilization. After this invention, later, many others [Sathe *et al.*, 1989a; Hsu *et al.*, 1993a; Mital *et al.*, 1997] clarified the stability regime for other fuels and investigated few other issues viz. effect of pre-heating, radiation output, flame propagation, etc. In recent times, a few newer designs of the PB have emerged [Tong *et al.*, 1990; Durst and Trimis, 2002; Jugjai

and Rungsimuntuchart, 2002; Wei *et al.*, 2002; Shinoda *et al.*, 2002] and some more possible applications have been identified. The same are reported in the later part of the thesis.

With the knowledge of the above early developments, Durst [1996a] and co-researchers patented a porous radiant burner with heat exchanger that can work at very low wattage (1-8 kW) with stable combustions and no flash back. This development was mainly aimed for European home heating systems. Their burner has increase in the pore size from the inlet to the outlet of the burner. This also allowed the burner to run at high inlet pressures.

Some of the recent patents in this area are as follows:

- A porous burner for gas turbine application which was built by Ellzey and William Jr. [2003].
- Then Volkert and peter [2006] patented a porous radiant burner for gas and air mixture.
- Bellucci *et al.* [2006] built a premixed burner with a swirl generator along with two perforated plates which are kept at a defined distance from one another in the inflow region of the combustion air in such a manner that the burner simultaneously allows damping of acoustic combustion chamber pulsations during operation.
- A pore-type burner with silicon–carbide porous body was built by Hoetger *et al.* [2006] which was configured for burning a fuel–air mixture and to generate a hot flue gas. The invention relates to a pore-type burner for burning a fuel/air mixture for the purpose of generating a hot flue gas. The burner includes a housing in which a pore material consisting of porous, high-temperature-resistant silicon carbide (SiC) is provided for combustion, in order to apply a hot stream of flue gas to a steam super heater.

2.4 PRINCIPLE OF POROUS MEDIUM COMBUSTION

The heat transfer mechanism in a PB is totally different from that in a conventional burner, which is characterized by a free flame as discussed in Section 2.1. The porous medium combustion PMC utilizes a novel concept of using a 3-D porous matrix in the combustion zone for better heat transport from the burned to unburned portion of the air-fuel mixture. *Fig. 2.4* shows the photgraphic view of the PMC. Since the porous matrix has high thermal conductivity and good radiative properties, the contributions of conduction and radiation in the PMC are significant. Besides, due to a large surface area of the porous matrix and high heat transfer coefficient, the convective heat transfer is also better than the free flame combustion. The better heat transport (through the combined modes of conduction, convection and radiation) results a homogeneous temperature distribution in the combustion zone. Depending on the flow velocity and thermo-physical properties of the porous material, the flame may stabilize either inside or on the surface of the porous matrix.

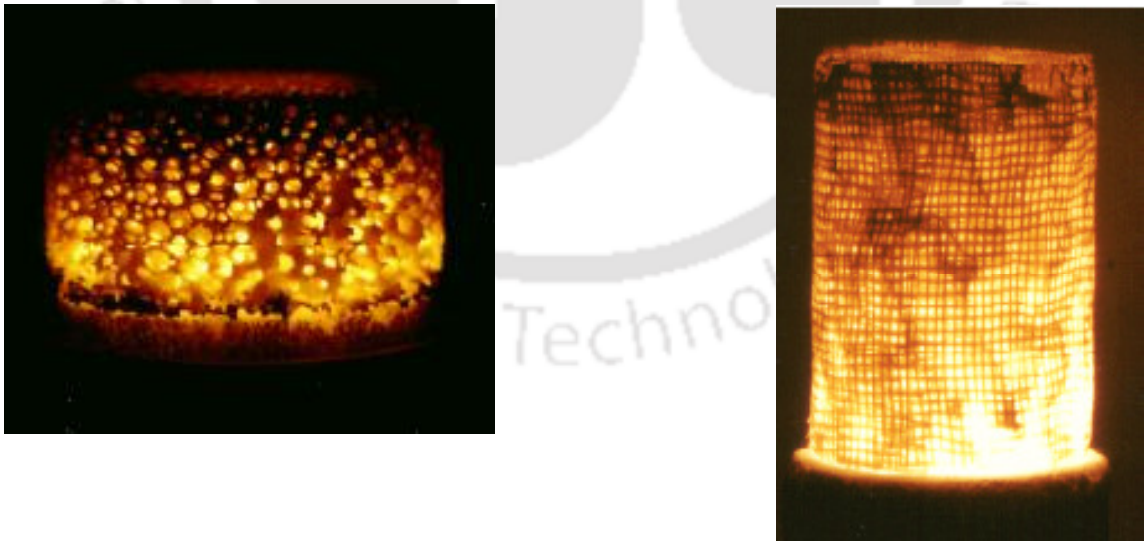

Fig. 2.4 Photographic view of porous medium combustion (flamesless combustion)[Durst and Trimis, 2002]

The PMC is characterized by a high burning velocity, reduced temperature drop across the reaction zone, high radiant output, high peak flame temperature and reduced enthalpy of flue gas. Unlike the conventional burners, in the porous burners, a low calorific fuel can also be combusted. *Fig. 2.5* shows the heat transfer mechanism of a single layer PB.

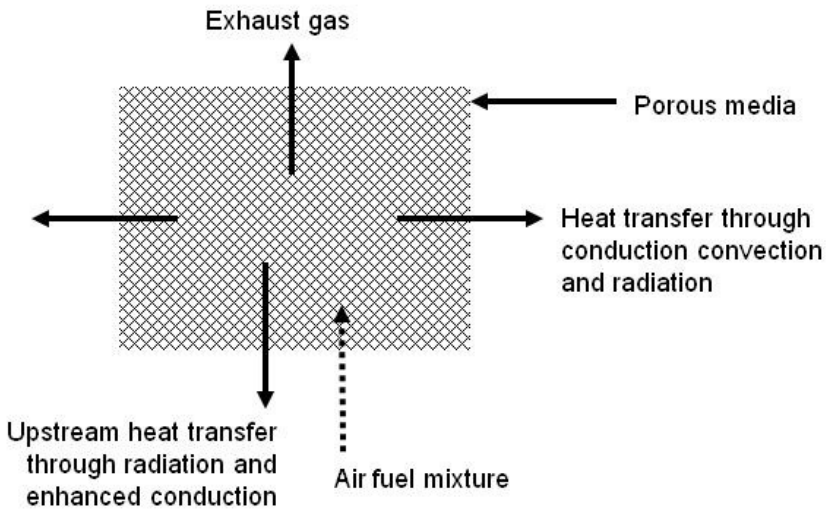

Fig. 2.5 Heat transfer mechanism in a single layer PB

In a single layer PB, air-fuel mixture enters the porous matrix from the upstream end and is ignited near the bottom surface. The flame front moves to downstream and covers the entire volume of the porous structure. The contact of the flame with the highly conducting and radiating solid material ensures better heat dissipation from the reaction zone. The heat dissipation depends on the material properties, more specifically on the porosity, which affects position of the reaction zone and the flame velocity. The burners based on PMC can further be classified based on the position of the flame stabilization. In general, based on the type of media used, the PMC is categorized into catalytic and inert. The former one utilizes a catalytic medium, which is coated on the solid matrix and participates in the combustion process; whereas the latter one remains inert but augments the heat transfer process. Further,

depending upon whether the flame is stabilized over the surface or within the porous matrix, the PMC can be classified as surface stabilized or matrix stabilized. In matrix stabilized combustion (Fig. 2.6.a), the flame stabilizes close to the inlet and combustion takes place completely inside the porous matrix. The gas temperature reaches its maximum value in the reaction zone and decreases in the downstream due to cooling. Unlike this, in surface stabilized combustion (Fig. 2.6.b), the flame stabilizes on the downstream surface of the porous matrix and the volumetric heat release becomes maximum there. *Fig. 2.7* illustrates the sections and subsections involved in PMC.

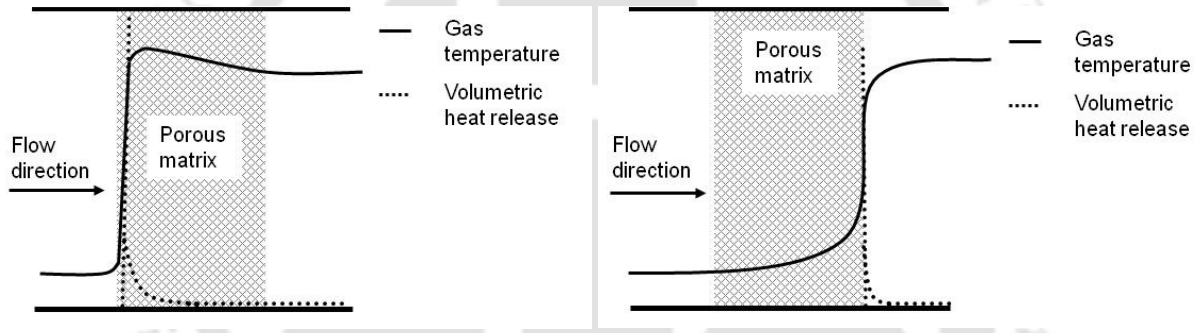

(a) *(b)*

Fig. 2.6 Schematic of (a) matrix stabilized and (b) surface stabilized PM

The dependency of the flame position on porosity has led to the concept of a double layered PB having different porosities [Kulkarni and Peck, 1996; Sathe, 1989a]. A double layered PB consists of a preheating zone (PZ) and a combustion zone (CZ) (*Fig. 2.8*). The PZ, which has a low porosity, prevents possibility of ignition and flame propagation thereby occurrence of flashback. The air-fuel mixture is preheated in this zone and it helps in improving the combustion efficiency and extension of flammability limit. Further, preheating improves the stability of the combustion regime too.

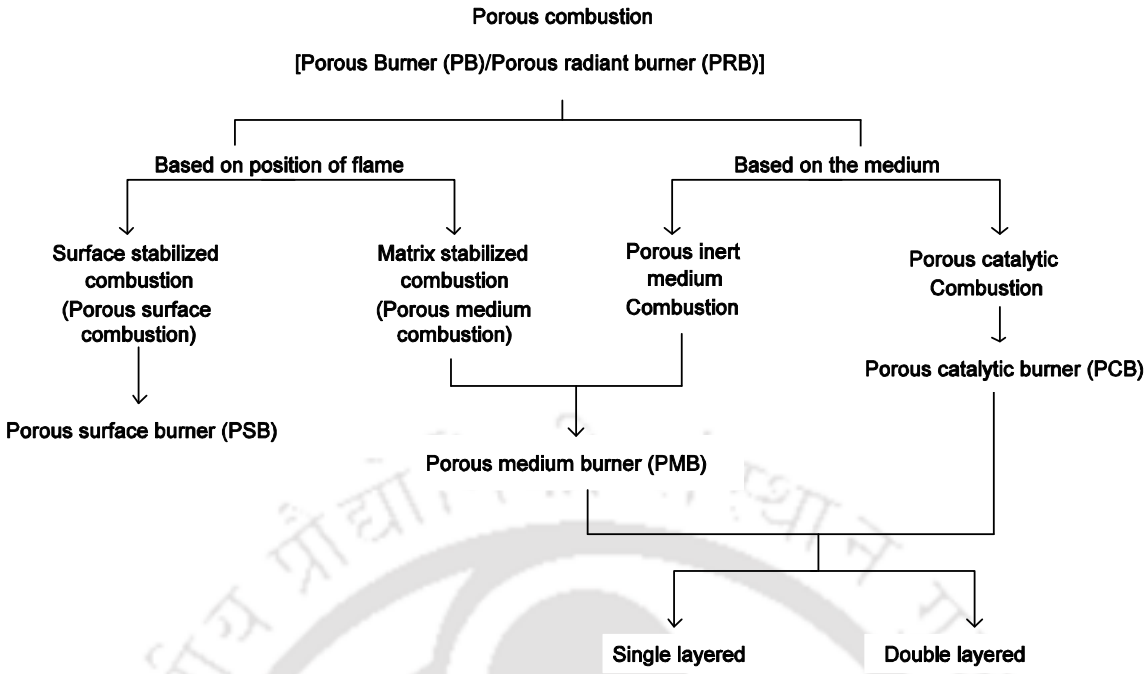

Fig. 2.7 The tree showing different kinds of porous burner

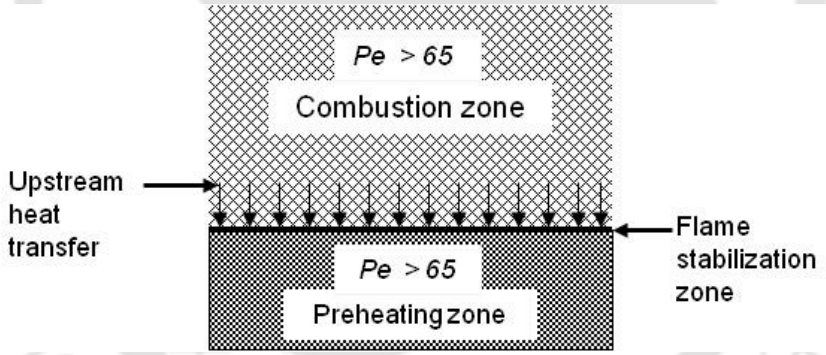

Fig. 2.8 Schematic of a double layered PB

In the CZ, due to high porosity, combustion takes place and flame propagates. In this, the reaction zone is widened and because of homogenization of temperature, the NOx formation is reduced. The interface of the two zones serves as a flame holder [Hsu *et al.*, 1993a and b] (*Fig. 2.8*). Babkin *et al.* [1991] provided the criterion for flame stabilization inside a PB as a function of Peclet number, *pe* (ratio of heat flow by transport to heat flow by conduction),

based on mean pore diameter. They proposed the following limiting condition for the flame propagation

$$Pe \geq 65$$

$$\text{where, } Pe = \frac{S_L d_m c_p \rho}{k}$$

where, S_L is the laminar flame velocity, d_m is the mean pore diameter, c_p is the specific heat, ρ is the density and k is the thermal conductivity of the gas.

For a proper operation, a double layered PB should be designed in such a way that the *Pe* for the pre-heating zone should be less than 65, and the same for combustion zone should be greater than or equal to 65. The optimization of porosities as well as the thermal conductivities of the two zones gives rise to a better heat utilization and temperature homogenization. Under certain conditions, the heat recirculation gives rise to a kind of flame called excess enthalpy flame.

2.5 EXCESS AND SUPER EXCESS ENTHALPY COMBUSTION

In 1971, Weinberg [1971] first introduced the concept of excess enthalpy. He reported that minimization of heat loss from a combustion device to the surrounding through heat recirculation from exhaust gases, generates a kind of flame called "excess enthalpy flame". The combustion, in which the excess enthalpy flame generates, is called "excess enthalpy combustion" or "super adiabatic combustion" (SAC). The typical characteristic of an excess enthalpy flame is that its peak temperature is higher than the corresponding adiabatic flame temperature.

Weinberg [1971] proposed several recuperative schemes, in which heat from exhaust could be extracted and used for pre-heating of incoming reactants. Among all the schemes, the one with internal heat recirculation seemed to be very promising as it led to the generation of excess enthalpy flame. He showed some of the benefits of excess enthalpy flame such as high combustion efficiency, thermodynamic efficiency, lower emission of pollutants, etc. Hardesty and Weinberg [1974] found that owing to a high heat feedback, for a given equivalence ratio, at high gas velocities, the peak temperature of the combustible mixture increased. At high gas velocities, the reaction zone also found to widen. After this finding, an enormous amount of works [Bernstein and Churchill, 1977; Choi and Churchill, 1979; Takeno *et al.*, 1979, 1980, 1983; Buckmaster and Takeno, 1981; Hashimoto *et al.* 1982; Kotani *et al.*, 1982, ,1984; Echigo *et al.*, 1987; Churchill, 1989; Min and Shin, 1991; Hsu, 1993a] have been devoted to demonstrate the practical benefits of heat recirculating PB. Among them, Echigo *et al.* [1987] found that owing to better heat recirculation from the burned to unburned air-fuel fuel mixture in the PMC, an excess enthalpy flame could be generated. They also concluded that, only after a sufficient preheating of inert medium and an optimum supply of excess air can led to the initiation of an excess enthalpy flame. *Fig. 2.9* illustrates the enthalpy comparison with and without heat recirculation.

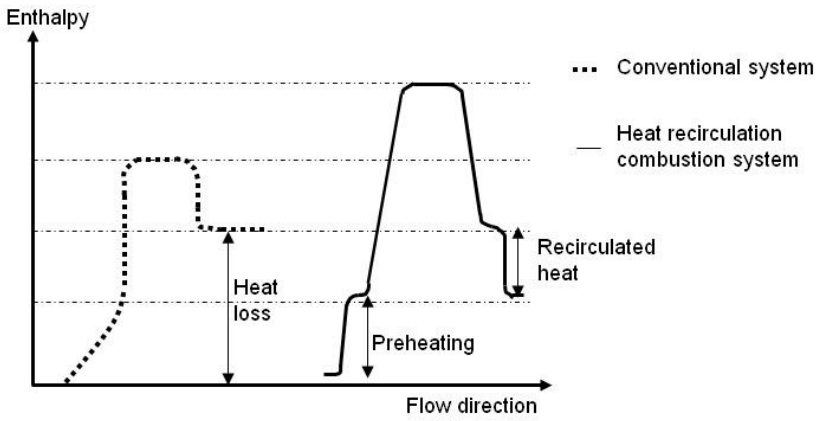

Fig. 2.9 Enthalpy comparison with and without heat recirculation

In PB, on account of high heat recirculation, the heat release rate increases with increase in mass flow rate above the laminar burning rate, Takeno and Sato [1979] found that with increase in flow rate, the porous matrix length required to produce an excess enthalpy flame also increased. Takeno *et al.* [1980] identified a critical mass flow rate above which the flame was not self-sustaining (flame blew off). They found the critical flow rate to be dependent on the type of combustion system; particularly the length of the porous matrix and the heat loses in the system. It was found that by doubling the solid length, the critical mass flow rate increased twice. They also showed that the flame was stable over a range of flow rates and below a certain value of equivalence ratio; it was not possible to maintain stable combustion.

In a theoretical study, Takeno and Hase [1983] explained the excess enthalpy in a gas-solid two-phase system by considering a model in which, conduction was accounted. However, they did not consider the effect of radiation and assumed constant solid-phase temperature along the flow direction. Hence, their analysis was applicable only for an extremely thin porous solid. Later, the same group of authors [Takeno and Murayama, 1986] demonstrated the importance of radiative heat transfer across the flame zone, as the maximum preheating of the unburned gas took place outside the thin flame zone. They measured flame velocities, which were as high as 18 times of the laminar flame speed for the same mixture. This was for the case in which external recirculation heat was accounted. They also estimated that for internal recirculation, the flame speed would increase by 4.2 times the corresponding laminar flame speed. They concluded that this increase in flame speed was due to a better heat recirculation.

The degree of excess enthalpy in the PMC can be further improved by using a reciprocating flow system [Hanamura *et al.* 1993; Zhdanok *et al.* 1993; Hoffmann *et al.* 1995]. In such a system, with the help of some non-returning valves, the combustible mixture is allowed to flow in a certain direction and after a certain time, the flow direction reverses. With this kind of arrangement, the amount of heat recirculation is increased and due to which the peak flame temperature becomes even higher than that for excess enthalpy flame. Hence, this type of combustion is called super excess enthalpy combustion. Zhdanok *et al.* [1993] analytically estimated the optimum period of reversal. The type of porous media (fine or course) was found to have a strong dependence on the performance of the PB. With fine porous media, the combustible limit extended and with coarse media, the performance was found to deteriorate [Hoffmann *et al.*, 1995].

2.6 PROPERTIES OF POROUS MEDIUM

Porous media can be made of packed beds of metal balls, foils, wires, ceramic foams, tiles, pebbles, etc. The research in the PMC started with metal balls. However, owing to high melting temperature, oxidation resistance and superior creep resistance, high permeability ($\approx 1.42 \times 10^{-7}$ m^2), high porosity (80 - 90%) ceramic foams have been found to yield better performance over metal balls. Hence, in recent times PRB made of ceramics has found wide applications than their metallic counterpart. *Fig. 2.10* shows some of the common porous ceramic materials. Attention is still focused on some new improved materials.

a. Al_2O_3 fibre structure

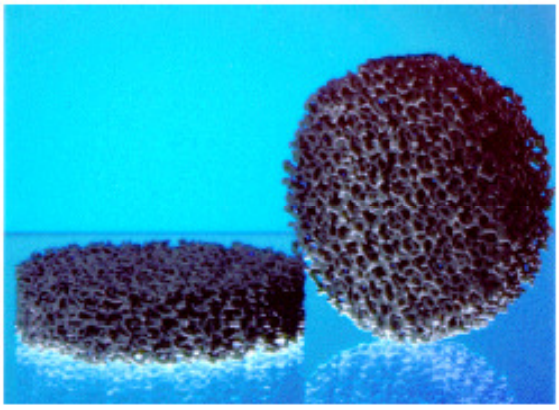

b. Ceramic Sic foams

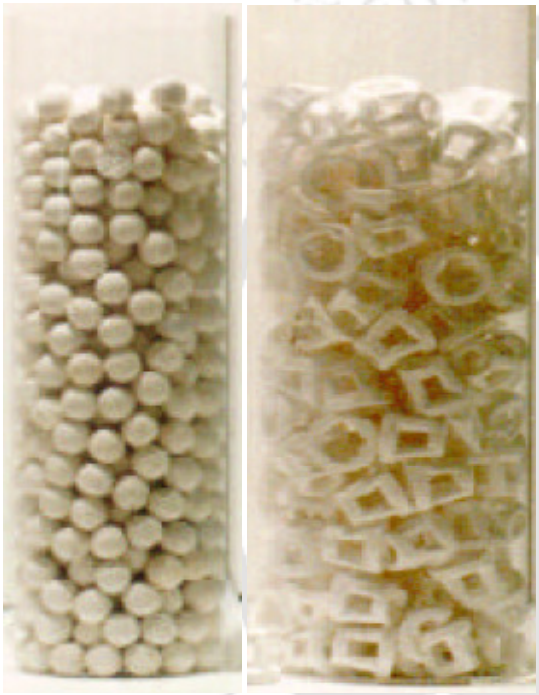

c. Packed beds from Al_2O_3 spheres and rings

d. Zirconium Oxide

Fig. 2.10 Some of the common porous ceramic materials [Durst and trimis, 2002]

The heat transfer performance of PB depends on thermo physical properties of the media used. Hence, the knowledge of thermo-physical and optical properties of the porous material such as heat transfer coefficient, porosity, heat capacity, thermal conductivity, emissivity, extinction coefficient, scattering albedo, anisotropy factor, etc. are very important. Further,

the durability of the material in terms of withstanding prolonged thermal and chemical stresses, and mechanical failures also require attention. At high temperatures, a porous material undergoes severe thermal and chemical stresses. Thus, the operation of a burner at an elevated temperature always leaves a chance to degrade the material. The temperature gradient in a double layered PB is even quite rigorous than a single layered PB. In a double layered PB, the upstream portion is normally at ambient temperature and depending upon operating parameters, somewhere in the downstream section of the second region (CZ), the peak temperature occurs. The typical temperature gradient in a PB remains in the range of 500-1000 K/cm [Goretta *et al.*, 1990]. In the last decade, several investigations were undertaken to establish desirable properties of materials that could be used in the PMC. In the following pages, the same are reviewed.

In recent times, several ceramics like alumina (Al_2O_3), zirconium oxide (ZrO_2), silicon carbide (SiC), silicon nitride (SiN), mullite, cordierite ($(Mg, Fe)_2Al_4Si_5O_{18}$), etc. have been identified as materials used in the PMC [Howell, 1996]. Hale and Bohn [1992] concluded that alumina has high scattering and extremely low absorption coefficients which can provide better heat transfer. Orenstein and Green [1992] investigated the thermal shock behaviour of alumina-mullite combination and they found that the thermal shock resistance was strongly dependent on pore size. Increase in pore size resulted in increase of thermal shock resistance.

Trimis and Durst [1996] tested different porous structures viz. ceramic pebbles, ceramic foams, metal foils and wires for use in the PMC. They reported that the heat transport properties of the porous medium depend on the form of the structure and the foam material. The foam structure (extruded holes or interconnected pores) influences conduction and radiation. Porosity and tortuosity of the structure affect convection and radiation. Mößbauer

et al. [1999] have investigated the suitability of silicon carbide foams, aluminium oxide fiber, zirconium oxide foams and carbon/silica structures for use in PMC. They suggested that for some applications, iron-chromium-aluminium alloys and nickel-base alloys could be used. Pickenacker *et al.* [1999] extended the study of Mößbauer *et al.* [1999] and moved one step further by describing the characteristic features of each ceramic materials considered. They summarized the data (*Table 2.2*) on thermal conductivity, emissivity, and thermal shock resistance.

Table 2.2 Ceramic material properties [Pickenacker et al., 1999]

Material	Max.allowable temperature in air	Thermal expansion coefficient, (20-1000°C)	Thermal conductivity (1000°C)	Total emissivity at 2000 K
Units	°C	10^{-6}/K	W/m-K	
Al_2O_3	1900	8	5-6	0.28
SiC	1600	4-5	20-50	0.9
ZrO_2	1800	10-13	2-4	0.31

Different porous materials are found to exhibit different characteristics. For instance, solid zirconia can withstand a temperature up to 1800°C, for Al_2O_3, the maximum limit of temperature is as high as 1900°C and for temperature resistant metal alloys, 1250°C is the ultimate limit. SiC withstands a temperature of 1600°C but shows outstanding characteristics with regard to thermal shock resistance, mechanical strength and thermal conductivity. On the other hand, Al_2O_3 fiber and C-SiC structures are characterized by a low conduction heat transport, a short start up phase, excellent radiative properties and a very good dispersion property. Metallic materials are found less suitable for the PMC since they are thermally unstable. Besides, metallic materials have a high thermal mass per unit volume, so that a PB

consisting of metallic materials responds with a great inertia. Fe-Cr-Al-alloys and nickel based alloys can also be used for some applications. But these materials can resist temperature up to 1400^{o}C only. The experiment with wire meshes showed poor conduction heat transport and dispersion properties, due to their high porosity. However, they have a short start up phase, excellent radiation heat transport, and excellent dispersion properties and a small pressure drop.

Sharafat *et al.* [2004] presented a short description of the different structures of ceramics foam porous media, manufactured from polymers, metals, glasses and ceramics. They reported that the ceramic foam comes in two different structures, viz. open and closed cells. For combustion applications, generally open cell ceramic foams are used. This open cell ceramic foam is manufactured by using three different methods: sponge replication, foaming agents and space holder methods. Typically, open cell ceramic foams exhibit high porosities (70-90%) with non uniform spherical-like cells connected to each other by ligaments and offer a unique combination of properties, such as low density, high surface area to volume ratio, high stiffness to weight ratio and high thermal shock resistance. The interconnected cells give rise to a tortuous path and the tortuosity is characterized in terms of pore diameter (d_p), or pore density (pores per inch - ppi). Typical pore diameters range between 0.01 to 2 mm. However, foams are also available in micrometer range. Delalic *et al.* [2004] have also suggested some materials for the PMC. Their findings are presented in *Table 2.3*

In the recent past, Weclas [2005] has reviewed some of the important parameters that need to be considered in selection of porous materials for IC engines. Eleverum *et al.* [2005] studied the durability of yttrium-stabilized zirconia. They found during transient phase, the burner suffered moderate strength degradation due to thermal gradients. The magnitude of strength

degradation was similar in both the 23.6 ppcm foam used in the upstream section and the 3.9 ppcm foam used in the downstream section. During the steady-state combustion operation, no degradation in material and its strength was observed.

Table 2.3 Properties of the some common ceramics used in the PMC [Delalic et al. 2006]

Material	Density	Thermal conductivity (20 - 100^{o}C)	Maximum operating temperature	Heat capacity (25 - 800^{o}C)
Units	kg/m^{3}	W/m-K	^{o}C	kJ/kg-K
SSiC	3.08-3.15	40 - 120	1400 - 1750	0.84
SiSiC	3.08-3.12	110 - 160	1380	0.84
HPSiC	3.16-3.20	80 - 145	1700	0.84

2.6.1 Thermal conductivity

The thermal conductivity and other properties of porous material vary greatly with the type of material and pore sizes. For example, the thermal conductivity of partially stabilized zirconia [Hsu and Howell, 1993d] is 13 times smaller than for that of cordierite [Fu, 1998b]. Since, heat recirculation depends on both conduction and radiation, the knowledge of effective thermal conductivity (accounting the combined effect of conduction and radiation) is an important parameter in the study of the PMC.

In the PMC, most of the ceramic structures have non-uniformly distributed pores with complex pore geometries. The reported models for prediction of the effective thermal conductivity are limited to small porosity ranges and simple pore geometry. This limitation is due to complexities associated with incorporation of actual pore geometry. However, using a probabilistic model, the effective thermal conductivity can be calculated more accurately. Zumbrunnen *et al.* [1986] considered a unit-cell probabilistic model. They observed that in

radiation dominated case, the effective thermal conductivity increased with increase in temperature difference across the porous solid and it was independent of thickness, this holds good when the thickness was large relative to pore size. Since this model considered the combined effect of radiation and conduction, the predicted results on effective thermal conductivity was not accurate.

Later, Fu *et al.* [1998b] developed a two-unit cell model using the thermal circuit method to predict the effective thermal conductivity of cellular ceramics. Their parametric calculations revealed that the effective thermal conductivity decreased with porosity since the conductivity of the solid is usually much larger than that of gas. This model was found to yield reasonable predictions of the effective thermal conductivity of the cellular ceramics. However, it was recommended to perform some additional experiments to measure the thermal conductivity of cellular ceramics at high and intermediate temperatures so that analytical results could be validated. Recently, Singh and Kasana [2004] developed an empirical formula and further developed a correlation for the estimation of effective thermal conductivity of highly porous aluminium and reticulated vitreous carbon (RVC) foams using air and water as fluid media. They proposed the following correlations:

$$\lambda_e = \lambda_{II}^{F} \lambda_{\perp}^{(1-F)} \qquad F \geq 0,\ 0 \leq F \leq 1 \tag{2.1}$$

$$F = C\left(0.3031 + 0.0623 \ln\left(\phi \frac{\lambda_s}{\lambda_f}\right)\right) \tag{2.2}$$

where, λ_e is the effective thermal conductivity, F is a correlation term, λ_{II} and $\lambda_{\perp}$ are the upper and lower bounds on the effective thermal conductivity of a two phase system, respectively, λ_s and λ_f are the thermal conductivity of solid and fluid phases, respectively,

and ϕ is the volume fraction of fluid phases. They found that the effective thermal conductivity was strongly dependent on porosity and the ratio of thermal conductivity of the constituents.

Hsu and Howell [1993d] measured the effective thermal conductivity of partially stabilized zirconia in the temperature range 290 to 890 K and pore sizes in the range 4 to 26 ppcm. Thermal conductivity was found to have negligible temperature dependence. They obtained the following correlation between pore diameter d (mm) and thermal conductivity, k (W/m-K):

$$k = 0.188 - 0.0175d, \qquad 0.3 < d < 1.5 \tag{2.3}$$

Barra *et al.* [2003] adopted a computational model reported by Hennke and Ellzey [1999] for double layered PB. The model treated the gas as 1-D reacting flow that interacted with solid matrix. The effect of solid and gas phase conduction, solid radiation, solid to gas heat transfer by convection and species diffusion were added in the model and the mass, energy and species conservation equations were solved. The results revealed that the upstream section of the burner should have low conductivity and for downstream, the conductivity should be higher.

2.6.2 Heat transfer coefficient

In porous media, especially for ceramic foam, it is very difficult to measure the surface area because of their tortuous nature. Hence, the heat transfer coefficient for these materials is usually presented in terms of volumetric heat transfer coefficient, i.e., the heat transfer per degree of temperature difference per unit volume of packed bed. The volumetric heat transfer

coefficient is primarily a function of pore diameter and geometry. Pore diameter affects volumetric heat transfer coefficient through surface area to volume ratio. A smaller pore diameter means larger surface area per unit volume and hence higher heat transfer coefficient and vice versa.

Lee and Howell [1991] numerically calculated the overall heat and mass transfer coefficients using a 2-D model to study the effects of radiation around a porous medium kept at some distance above the leading edge of the flat plate. With increase in the power density of the burner, radiative contribution to the total heat flux was found to be more. A similar trend was also observed with increase in heat transfer coefficient and the absorption coefficient.

Younis and Viskanta [1993] experimentally investigated the heat transfer coefficient by forced convection of air in porous ceramic foams (alumina and cordierite). An apparatus was designed to determine the volumetric heat transfer coefficient between the foam and a stream of air. Experiments were performed on foams having different mean pore diameters, and heat transfer coefficient correlations were obtained from each configuration tested. A strong dependence of volumetric heat transfer coefficient on mean pore diameter was observed. The volumetric heat transfer coefficient was found to decrease with increase in pore diameter. However, the average heat transfer coefficient was nearly constant over the time period during which the data were taken. Volumetric heat transfer coefficients were also determined for alumina and cordierite foams of same ppi from different manufacturers. It was observed that there was a considerable difference between the results for the two samples because of the difference in shape of the flow passage, mean pore diameter and porosity. For a mean pore diameter of 1.27 mm and for cordierite sample Nusselt number *(Nu)* versus Reynolds

number *(Re)* correlation viz. $Nu = 2.43\ Re^{0.42}$, $65 < Re < 457$ was obtained. With decrease in pore diameter the exponent of the *Re* was found to decrease. *Nu* obtained for the cordierite specimen was higher than those for alumina specimen for low *Re. B*ut at *Re = 345*, *Nu* for both specimens approached each other and became identical. They concluded that depending upon the material, length and pore diameter volumetric *Nu* correlations could take a variety of forms.

Fu *et al.* [1998a] measured the volumetric heat transfer coefficients between cellular ceramics and a stream of air using single blow transient experimental technique in conjunction with an inverse analysis. The specimen made of mullite, yttrium stabilized zirconia, SiC, cordierite (without coating) and cordierite with LS-2 coating were used. The value of ppcm ranged from 4 to 26 and the specimen thickness ranged from 6 to 12 mm. They obtained the following correlation between *Nu* and *Re.*

$$Nu_v = f(L/l_c)\,\mathrm{Re}^m \qquad (2.4)$$

where, Nu_v is the volumetric Nusselt number, L is the specimen thickness and l_c is the characteristic length.

The volumetric heat transfer coefficient was found to increase with a decrease in the ratio of specimen thickness to the mean pore diameter. Du *et al.* [2006] found the dependency of temperature profiles and burning speed of the gases on the volumetric convective heat transfer coefficient, extinction coefficient and specific heat of the porous media. Mishra *et al.* [2006] found an increase in the volumetric heat transfer coefficient for lower values of pore characteristic length.

2.6.3 Radiative properties

In the PMC, the amount of recycled heat from the post-flame zone to the pre-flame zone depends on the radiative properties such as absorption coefficient, scattering albedo and extinction coefficient of the solid material. The radiative properties are dependent on type of material and pore size [Hsu and Howell, 1993d; Mital *et al.*, 1997; Mishra *et al.*, 2006]. For partially stabilized zirconia, Hsu and Howell [1993d] provided the following correlation to show the dependence of the effective radiative extinction coefficient, τ (m^{-1}) on pore diameter, *d (mm)*;

$$\tau = 1340 - 1540d + 527d^2 \qquad (2.5)$$

The above correlation applies for pore sizes in the range 0.3 mm<d<1.5 mm. The data were collected for a temperatures range of 290-890 K. However, temperature dependence was not observed. Apart from this, they also presented a correlation for extinction coefficient τ $\left(m^{-1}\right)$ versus pore diameter and porosity, d (mm);

$$\boldsymbol{\tau = \left(\frac{3}{d}\right)(1 - p)} \qquad (2.6)$$

where, *p* is the porosity of the sample, which varied from 0.87 at large pore diameter to 0.84 at smallest diameter. This correlation is valid for d > 0.6 mm and it requires the assumption of isotropic scattering.

Hendricks and Howell [1994, 1996] measured the transmittance and reflectance of partially stabilized zirconia and silicon carbide having pore sizes of 4, 8 and 26 ppcm. They found that SiC retained its properties at all wavelength; however, partially stabilized zirconia showed a significant change, in the wavelength range 2500 - 3000 nm. The same group of authors also [Hendrics and Howell, 1996] found a modified correlation for extinction coefficient versus

pore diameter and porosity. They considered partially stabilized zirconia and silicon carbide and found the following correlation:

$$\tau = \left(\frac{44}{d}\right)(1 - p) \qquad (2.7)$$

Mishra *et al.* [2006] found the effect of extinction coefficient more prominent in case of large sized pore and for higher values of extinction coefficient, the peak temperature was higher.

2.7 COMBUSTION OF GASEOUS FUELS IN POROUS MEDIUM BURNERS

The research in the PMC involves both experimental and numerical investigations of combustion of gaseous fuels in different porous media. Experimental measurements in the PMC are difficult because the complex porous structure prohibits movement of mechanical or optical probes for any direct measurement of quantities of interest inside the porous matrix. Numerical modelling of the PMC too is complex and challenging, since it requires solution of coupled fluid flow, heat and mass transfer and chemical reactions in the porous matrix. Owing to dependency of solid and fluid properties on temperature and/or concentration, governing equations are non-linear and they pose difficulty in solution. Further, unavailability of precise thermo-physical and optical properties add to the limitations in numerical modeling. However, despite the above limitations, even with some simplifying assumptions, a good amount of numerical as well experimental works have been carried out to understand the physics of the PMC and to study the thermal performances of different PRBs.

In the recent past, many experimental and numerical studies have been conducted to analyse the combustion behaviour of gaseous air-fuel mixture in PRB. A few have thrown light on the structure of radiation controlled flame, flame stabilization and effects of various parameters

influencing flame propagation and emissions. The following paragraphs discuss some of the important experimental and numerical investigations.

2.7.1 Experimental investigations

Flame stabilization

Soete [1966] measured flame speeds and the rate of propagation of the reaction zone through packed beds of sand for methane/oxygen/nitrogen mixtures. They found that combustion in porous media was mainly controlled by the rate at which the reaction was accelerated by heat recirculation and retarded in the presence of solid wall (chain termination). He observed a decrease in the flame speed with the decrease in the grain size.

The flame in a PB is called radiation-controlled flame, as radiation dominates over the other two mode of heat transfer [Sathe *et al.*, 1989a]. The position of such a flame is dependent on various operating parameters such as physical and optical properties of the porous material, flow rate of the flowing fluid (air-fuel mixture), equivalence ratio, convective heat transfer coefficient between solid and fluid and thermal conductivity of solid. A balance between chemical reaction rate and two phase energy transfer rate through adjustments of porosity of the material, leads to stabilization of the flame within a porous medium. Babkin *et al.* [1991] and Dillon [1999] gave stabilization criteria of flame as a function of *pe*. The findings of Babkin *et al.* [1991] have already been discussed in Section 2.1.2. They evaluated *Pe* for hydrocarbon fuel. Dillon [1999] calculated *pe* for hydrogen. He found critical *pe* as 37 against 65 of hydrocarbon fuel [Babkin *et al.*, 1991]. He thought that the difference was probably due to different chemistry of the fuel used (hydrogen versus hydrocarbon) and the

absence of buoyancy effect, since the experimental combustion tube for his study was horizontal (this was vertical in Babkin *et al.*, 1991 experiments).

The stabilization of flame during the combustion is of great interest because an un-stabilized flame may lead to the condition of lift off/flash back or quench. Min and Shin [1991] in their investigations extended the flammability limits of propane-air mixture inside a honeycomb cordierite PB which was mainly due to the recirculation of heat to the incoming air-fuel mixture. At flow rates less than the normal burning velocity, flame moved to downstream of the burner which was considered due to the heat loss to the combustor. It was noticed that at higher flow rate and equivalence ratio, flame stabilized fully inside the combustor. Mital *et al.* [1997] studied the flame stabilization phenomena in a reticulated PB made of cordierite with a silicon-carbide based coating using methane as fuel. They observed the lift off limit between the equivalence ratio of 0.6 - 0.7 and the lean limit (complete extinguishment of the flame) between 0.5 and 0.6, depending on the firing rate. Below a firing rate of 300 kW/m^2, no flashback was observed. It was observed that at flash back condition, the measured laminar flame speed was 5 times greater than the corresponding adiabatic flame speed indicating the rise in flame speed with increase in equivalence ratio.

Flame speed is dependent on structure of the media used. Different media (with different porosity) induces different flow field and hence the flame speed varies. Babkin *et al.* [1991] measured the flame propagation speeds of premixed methane–air mixture. They used different types and shapes of porous media. They found the flame speeds were proportional to the cube of the laminar flame speed and to the square of the mean cell size of the porous media. Koester *et al.* [1994] studied methane-air combustion in a tube open at both ends. They found that the equivalence ratio determined the direction and rate of propagation of the

reaction zone within the tube. Korzhavin *et al.* [1997] made experimental and numerical investigations of flame propagation and the dynamics of combustion in the subsonic regime.

The gas phase combustion in porous media, especially at elevated pressures (88.5 - 433 kPa, higher than the atmospheric pressure) and in low velocity regime was studied by Sanmiguel *et al.* [2003]. At an elevated pressure, the width of the combustion front appeared to be small. The maximum temperatures at elevated pressures were lower than those observed for the same mixtures and fluxes at atmospheric pressure. As the operating pressure increased, the combustion front velocity was found to decrease. However, the observed burning velocity was 40 times higher than the velocity of the same mixture in an open space.

Cho *et al.* [2001] investigated the combustion characteristics of LPG and coke oven gas in a metallic fiber mat. They reported that depending on the combustion rate and excess air, the combustion of premixed fuel could occur in two modes viz. radiant mode and convective mode. In the radiant mode combustion takes place inside the mat, which heats to incandescence. This releases a considerable amount of energy by thermal radiation. In the convective mode a blue flame hovers above the surface of the permeable mat. The region between the fully radiant and blue flame modes is referred to as transient mode.

Thermal performance

The recirculation of heat in the PMC helps in better utilization of fuel and it also allows to burn gas/liquid fuels at very low equivalence ratios. In the following paragraphs, the literature, related to the power output, thermal efficiency, flammability limits and excess air ratios in the PBs are presented.

Xiong *et al.* [1995] examined the combustion stability and heat transfer rate in a PRB made of SiC and Al_2O_3. They found high combustion intensity up to 2.5 MW/m^2 and high heat transfer rate up to 310 kW/m^2. They examined the thermal efficiency of the combustor with SiC and Al_2O_3 and found higher with SiC at higher excess air. This was because the higher emissivity of SiC enhanced the radiation from the porous material to the tube surface. It was also found that in SiC PB, the flame could stabilize over a large range of excess air. On the other hand, at high excess air, Al_2O_3 was found to show lift off behaviour. They also concluded that there was a strong interaction between combustion, combined convective-radiative heat transfer and fluid dynamics within the burner.

Mohamad *et al.* [1994] modelled a combustor made of packed bed with embedded cooling tubes to study the effect of excess air on thermal efficiency. They found that with increase in excess air or activation energy, the flame gradually shifted to the downstream side of the burner causing a decrease in thermal efficiency. An opposite effect i.e. increase in thermal efficiency and decrease in pressure drop with increase in the particle diameter. Tomimura *et al.* [2004] proposed a new multi-layered gas to gas heat exchanger using porous media and investigated the heat transfer characteristics. For 2 - 5 layers and two types of walls (bare or finned), they conducted a series of experiments for inlet gas temperatures in the range 300 - 700°C and optical thickness in the range 0 - 15.4. The heat recovery section was found to play an effective role in lowering the outer wall temperature and increasing the total heat recovery rate. It was concluded that the optical thickness of about 8 was enough to obtain sufficient total heat recovery rate with finned walls

Hoffman *et al.* [1997] observed a stable combustion against an extremely low equivalence ratio (Φ = 0.026). The effects of flow velocity, half cycle and equivalence ratio on the

temperature profiles and CO and NO_x emissions were studied with a re-circulated PRB. They considered three burners made of cordierite ($2Al_2O_3.5SiO_2.2MgO$) of 87.5% porosity but with different ppi (6, 13 and 20) leading to different absorption coefficients and internal volumetric surface areas. They found an increase in the exhaust gas temperature along with the equivalence ratio. The velocity profile was found similar to temperature profiles. The half cycle was found to affect both temperature profile and combustion efficiency. The latter decreased with decrease in the half cycle. The combustible limit was found to improve for a medium having high porosity.

Shinoda *et al.* [1998] optimized the design of the burner using the criteria of fractional heat recirculation rate. They found that the fractional heat recirculation rate was almost constant as the equivalence ratio varied, but it was dependent on *Re* and aspect ratio of the burner. It was also seen that with increase in the number of passes of the burner, there was a minimal increase in fractional heat recirculation rate.

Mare *et al.* [2000] experimentally and numerically analysed the flame structure and extinction mechanisms in the combustion of propane-air and methane-air mixtures. They studied the effects of physical and geometrical properties of the solid porous matrix on the flammability limits for methane-air and propane-air mixtures. Separate solid and gas phase energy equations were used and they were coupled using convective heat transfer between the solid and gas phases. Despite the single step chemistry, a good quantitative agreement between the numerical and experimental results was obtained. They concluded that flammability limit was more sensitive to geometric properties of the porous medium than to

physical properties. Their results also confirmed that the flammability limits (*Table 2.4*) were independent of properties of the solid porous material.

Table 2.4 Comparison of experimental and numerical lean flammability limits for upward flame propagation in CH_4 - air and C_3H_8 - air mixtures in porous media [Mare et al., 2000]

Fuel	Flammability limits (%)							
	12.5 mm steel spheres		12.5 mm glass spheres		9.5 mm steel spheres		9.5 mm glass spheres	
	Exp.	Num.	Exp.	Num.	Exp.	Num.	Exp.	Num.
CH_4	6.30	8.38	6.52	8.38	7.38	-	7.93	-
C_3H_8	3.11	2.94	2.96	2.94	3.53	3.55	3.45	3.55

Exp. - Experimental; Num. - Numerical

The flammability limits, longitudinal temperature profiles of the burner in a two-stage gas turbine were found out experimentally and compared with the numerical results by Tanaka *et al.* [2001]. Taking different equivalence ratios, *Re*, diameter of the cylindrical body and keeping the height constant, the burner was optimized for heat recirculation rate and the thermal efficiency. Stable combustion was achieved for an equivalence ratio $\Phi = 0.2$ and a total volumetric flow rate of 14 lit/min ($Re \leq 953$). Both experimental and the numerical results for the temperature profiles were in good agreement. The peak heat recirculation rate was 14% when $\Phi = 0.2$ in case of numerical simulations but experiments showed the same as 11% at $\Phi = 0.6$. The effect of changing the geometry of the cylinder had no effect on recirculation rate. The heat circulation rate increased with decreasing *Re* ($Re < 100$) along with the changing geometry due to the prolonged heat exchange time of the flowing gas. But this was limited within 5% of the changing geometry and after that it did not have much effect. The maximum thermal efficiency was 60% at $\Phi = 0.1$ and 47% at $\Phi = 0.2$ in numerical and experimental study, respectively. The discrepancies were mainly due to

assumptions made in numerical analysis. It was also found that when *Re* was changed, the thermal efficiency varied inversely to the heat recirculation rate, particularly for *Re* > *100*, and it became possible to obtain the efficiency greater than 40%.

Shinoda *et al.* [2002] used the experimental burner of Tanaka *et al.* [2001] and evaluated the performance with methane-air mixture. Later, they compared the same with the low calorific value fuel. The experimental results showed that the peak heat recirculation rate of the burner with low calorific–fuel combustion was about one fourth of the value obtained for methane-air mixture. Similarly, the maximum thermal efficiency of low calorific fuel-air combustion was three fourth of methane-air combustion. The thermal efficiency for low calorific fuel was 45% and that for methane-air mixture it was 60%. Huang *et al.* [2002] experimentally studied the effect of preheating and other operating conditions on SAC and found that a stable combustion required a minimum equivalence ratio and for the initiation of SAC, the preheating of inert porous media must be high enough for stable combustion. With decreasing firing rate, the preheating rate was found to increase. With an increase in operational equivalence ratio, a stable combustion mode was found to exist.

Kamal and Mohamad [2005] investigated the effect of swirl on the combustion efficiency and radiation flux from a non-premixed flame PB by motorizing the burner with variable speed motor (vane rotary burner) and fuelled by natural gas. The radiation spectrum at the burner exit was measured and compared for different swirl numbers. The results showed an enhancement of radiation by 5.7 times with optimization of the gap between the flame base and the base of the porous medium. This improvement was attributed to superior air-fuel swirl mixing. The swirl improved the flame quality greatly as it became highly turbulent and spread more in the radial direction. CO and unburned hydrocarbon emissions were reduced

noticeably owing to higher mixing rate. NO_x emission decreased to a level below 10 ppm due to the improved heat transfer. Cookson and Floyd [2005] studied the performance characteristics of reticulated open metal foam (FeCrAlY) burner and compared it with ceramic tile burner. The pore size and the porosity of the porous emitter were 420 μm and 95%, respectively. The results revealed that for the same input, the metal foam burner operated at higher temperature than the conventional ceramic tile burner and was more efficient.

Scribano *et al.* [2006] designed a prototype PRB and examined the flame behaviour as a function of burner operating conditions such as *Re*, input thermal power, equivalence ratio and fuel to air momentum ratio. They found that all these parameters had significant effect on flame length, axial distribution of gas temperature and a uniformity of radiant tube temperature and pollutant emissions.

Radiation output/ efficiency

Radiation efficiency is the measure of radiation output at the exit of the burner to the input energy. Radiation output depends on various parameters like optical thickness, scattering albedo, extinction coefficient, and thermal conductivity of the solid medium, heat transfer coefficient between the gas and solid phase and size of the fibrous porous media. It is recognized as one of the most important parameters to evaluate the thermal performance parameters of PB. It is dependent on firing rate, equivalence ratio, flame support layer thickness, flame position, temperature distribution and porosity of the material.

Mital *et al.* [1997] measured the thermal efficiency with two different thicknesses of flame holder. It was found that, at a specific power and equivalence ratio, the thermal efficiency is higher in case of 3.2 mm than 6.5 mm. They pointed out the effects of other factors viz. flame position and resultant temperature distribution on radiation output. Barra and Ellzaey [2004] studied the effect of equivalence ratio and flame speed on radiation output. It was also found that the radiation output efficiency increases with decrease in equivalence ratio but the actual quantity of radiation was lower than at higher equivalence ratio. The flame speed decreases with the increase in equivalence ratio. The actual flame speed was at a low of 2 times the adiabatic flame speed due to the recirculation of heat to the downstream section of the burner because the total heat release rate at is very low at lower equivalence ratio. The results were in consistent with Khanna *et al.* [1994]

It has been found that for similar operating conditions, there is a wide variation (15 - 50%) in radiation efficiency reported by different researchers. This variation is attributed to the lack of a standard methodology. To partially overcome this problem, Mital *et al.* [1998] proposed a standard procedure. Later, this method was adopted by Leonardi *et al.* [2002] for measurement of combined (radiation plus convection) efficiencies for metal fiber (Fecralloy-Acotech, EN29001) burners. Experimental data were reported for a range of firing rates at three different equivalence ratios. It was found that the burner surface temperature and exit temperature increased with the firing rate and was higher for the double layered fiber pad than for a single layered pad. The radiation efficiencies measured for a double layered pad were about 5% higher than single layered pad. The radiation efficiency was found to increase with equivalence ratio and power.

Emissions

There is an exhaustive literature available on the emissions of PMB. Some of the most importants are discussed below. Goeckner *et al.* [1992] used the radiant tube burners with porous ceramic inserts with natural gas as fuel. NO_x was found to reduce by 30%. Temperature distribution along the burner axis was found uniform. Hoffman *et al.* [1997] made a detailed study of CO emissions and found it to be strongly dependent on the operating conditions along with the type of the porous media. They found an extremely low level of NO_x (1 ppm) in the operating range. Xiong *et al.* [1995] conducted an experimental study on 60 kW bench-scale porous matrix combustor heaters with two rows of water cooled tube coils. They reported ultra low emissions. NO_x and CO were less than 15 ppm and total hydrocarbon (THC) was less than 3 ppm

Mital *et al.* [1997] measured the emission indices of CO, HC and NO_x. They found the CO and HC pollution indices were relatively low, CO: 0.1 - 3.6 g/kg and HC: 0.1 - 1.2 g/kg. CO and HC emissions were found to decrease with decrease in equivalence ratio and increase in the firing rate. NO_x emission was found relatively low, 0.1 - 0.35 g/kg. It was found that the NO_x emissions had decreased with decrease in equivalence ratio, but increased with increase in the firing rate. The decrease in emission was attributed to higher energy release per unit area and to an increase in preheating at the higher firing rates. Suzukawa *et al.* [1997] developed an experimental burner for the industrial purpose and was able to reduce NO_x level by 50% compared to the conventional low NO_x burners.

Scribano *et al.* [2006] investigated the emission characteristics of self-recuperative radiant tube burner fuelled with natural gas in non-premixed mode. NO_x was found to reduce with

intense exhaust gas recirculation. They suggested a new design to recirculate exhaust gas to CZ and found 50% reduction in emissions for a wide range of power 12 - 18 kW and equivalence ratio of 0.5 - 0.8. CO emission was also found very low (<50 mg/Nm^3 at 3% O_2).

2.7.2 Numerical investigations

Flame stabilization

Like experimental studies, the stabilization phenomenon of flame within the porous medium has also been studied analytically and numerically by many researchers. For a given equivalence ratio and a range of flow rates, the flame can stabilize at different locations within a porous medium [Sathe *et al.*, 1989a; Hsu *et al.*, 1993a; Sathe *et al.*, 1989b]. Buckmaster and Takeno [1981] defined the conditions for blow-off and flashback. They found that the flame stabilization depended on some parameters like flow velocity, heat transfer coefficient and the thermal conductivity of the porous matrix. Their results also confirmed the dependency of combustion location and upstream internal heat transfer and vice versa. Chen *et al.* [1987] studied the effect of thermal conductivity, volumetric heat transfer coefficient and exit boundary conditions on temperature and flame speeds in the 1-D porous medium without considering the effect of radiation. The flame speed was found to reduce when the volumetric heat transfer coefficient reduced below 10^7 W/m^3-K and a significant difference between the solid and gas temperatures were observed. The temperature profile was not affected when the thermal conductivity was varied from its value for air to that of pure zirconia. A little effect was found on temperature profiles. However, due to increased preheating of gas through the upstream conduction from the flame front, a significant effect on the flame speed was observed.

Yoshizawa *et al.* [1988] applied a 1-D two-phase model with single-step kinetics and analysed the effect of radiation on the structure and behaviour of the premixed flame in the porous medium. They found that the temperature profiles and burning velocities were highly dependent on radiative properties, especially absorption coefficient of the porous medium. The burning velocity, flame thickness and gas phase temperature were highest when the reaction zone was close to the centre of the porous medium. An increase in absorption coefficient caused not only an increase in the optical thickness of the reaction zone, but also an increase in the surface area of particles leading to an increasing role of the inter-phase heat transfer and an accompanying decrease of the maximum temperature and burning velocity, and increased thickness of the reaction zone. The temperature and flame speed increased with the increase in the thickness of the medium along with decreasing reaction zone thickness keeping absorption coefficient constant. Yoshizawa *et al.* [1988] and Sathe *et al.* [1989b, 1990a] found that with increase in porosity, the flame velocity increased owing to increased conduction and radiation.

Sathe *et al.* [1989a] studied the flame behaviour of methane, in the equivalence ratio range of 0.55 - 0.6. They found the flame speed as 120 mm/s and the flame width to be 2.5 mm. From their study, they concluded that depending upon the firing rate; flame could be stabilized at two different regions. One at the interface of the two porous zones (PZ and CZ, refer to *Fig. 2.8*), and second one at the region before the exit plane of the combustion zone. However, the best radiant output could be obtained if the flame was located near the burner centre. They also reported that near the edge of the porous matrix, the flame speed variation was controlled by conduction, whereas radiation became a contributing factor for flame propagation in the interior. Later, the stabilization of flame at two different locations was confirmed by Hsu *et al.* [1993a].

Hanamura and Echigo [1991] studied the detailed temperature profiles, reaction rates and energy balance of methane air combustion in the equivalence ratio range Φ = 0.55 - 0.66. With increase in equivalence ratio, the flame position was to found to locate near the porous plate. The flame blew off at an equivalence ratio Φ = 0.66, It was found that with decrease in mass flow rates, the flame moved upstream of the PB and the temperature of the porous zone was increased. Kendall *et al.* [1992] also investigated the flash back phenomena in two different types of porous media viz. reticulated ceramic foam and packed ceramic fiber. The packed ceramic fiber was found to be least prone to the flashback as its inner surface temperature was low and the reticulated ceramic foam was found the most prone to flashback, as it conducted heat more effectively to upstream.

Sahraoui and Kaviany [1994] found that the flame speed was strongly affected by the geometry of the porous medium. With decrease in pore size, the flame speed was found to increase. Their conclusion was based on the result of their 2-D direct simulation of the PB consisting of either discrete or connected square cross-section element and using single step chemistry. The same group formulated one more model using volume averaged properties. With that model, they were able to predict the flame speed, but not the local super-adiabatic temperatures in the gas phase. Escobedo and Viljoen [1994] used a 1-D model with single-step chemistry and found that for a given equivalence ratio, with increase in the heat transfer coefficient, the range of stable flow rates of fuel-air mixture increased. Kulkarni and Peck [1996] studied the effect of extinction coefficient in a double-layered burner and they found that increase in upstream extinction coefficient resulted in decrease in effective flame speed.

Zhdanok *et al.* [1998] numerically studied the flame localization inside an axis-symmetric cylindrical and spherical PB. The main advantage with these configurations was natural

stabilization of combustion front in the medium due to decrease in the filtration speed and the heat loss from the flame across the radius. They also found dependency of heat losses at the outer boundary of the burner on the fuel flow rate, heat content of the mixture and the external radius. Combustion front localization showed a dependency on the ignition radius. The burner was found to have a narrow combustion region in case of low calorific value fuels and at limited flow ranges.

To stimulate the flow in a 3-D porous structure, Yamamoto *et al.* [2005] used the Lattice Boltzman method. They solved distribution functions for flow, temperature and concentration fields and compared them with the empirical correlations. Both were in good agreement. The porous structure considered was Ni-Cr metal obtained by the 3-D computer tomography technique. Their objective was to improve the design of diesel particulate filter for diesel powered vehicles. An inhomogeneous flow was observed in regions where local temperatures were high. The information was considered to be vital for better design of diesel particulate filter. The simulation was also helpful in better understanding the soot combustion.

In all the above numerical simulations, the reaction zone thickness was assumed negligible. With two-temperature approximation, Bubnovich and Toledo [2007] analytically studied the thickness of the reaction zone. They provided analytical solutions for three different zones: PZ, reaction zone and the zone occupied by combustion products (CZ). The thickness of the reaction zone was found to be 9.156 mm. They compared their analytic results with those of the numerical simulation and a good agreement was found.

Thermal performance

Yoshida *et al.* [1990] analysed transient characteristics of combined conduction, convection and radiation heat transfer in a homogenous porous medium. They validated their results with experiments. With decrease in gas velocity, the time constant of the system was found to increase and it varied widely in the porous medium. The transient response was much faster at the entrance of the porous medium than at its exit. As a result, the net radiative heat-flux at the entrance of the porous medium reached steady state fast. Hsu *et al.* [1993b] numerically studied premixed methane-air combustion in a double layered PB. The burner consisted of two cylinders of the same length and diameter but with different pore sizes stacked together and insulated around the circumference. The simulations were performed for equivalence ratio in the range, Φ = 0.1 - 0.43. The predicted lean limits were lower than the limit for a free laminar flame. The maximum flame speed occurred close to the exit plane.

To predict the thermal efficiency, flame location, temperature distribution and pressure drop, Mohammad *et al.* [1994] used a 2-D model for matrix stabilized PMC with single-step kinetics. They predicted the possible amount of excess air, firing rate, pore size, geometry, for a range of design and operating parameters and system configurations. They compared their numerical results with available experimental data and found $\pm$15% variation. Hayashi *et al.* [2004] proposed a 3-D modeling of a double layered porous media. Their model was valid to operate in the range of 5 - 20 kW and considered a mixture of air and fuel (a blend of fuel-oil and vegetable oil) for domestic heating. The range of equivalence ratio was 1 - 1.8. They applied a single-step mechanism for describing combustion in the porous media and n-heptanes were considered to model the actual fuel. Their work mainly aimed at a better understanding of the PMC to develop efficient household combustion systems. For most of the operating conditions, the flame was found to stabilize at the interface of the two layers.

But the exceptions were found at the low power and excess air conditions for which it was suggested to reduce the pore size of the bottom perforated plate.

A comparison of gas phase reactions using single-step and multi-step kinetics was made by Hsu *et al.* [1993b, 1991b, 1991a]. It was observed that the consideration of single-step kinetics in the PMC modelling provided similar results as that with the multi-step kinetics for lean mixture. In case of models with single-step chemistry, the reduced accuracy in predicting the reacting flow was counterbalanced by lower levels of uncertainties in the heat transfer coefficient, turbulence, etc. than the model with multi-step kinetics. Hsu *et al.* [1993c] developed a 1-D model wherein they considered both the single step and multi-step chemical kinetics. They concluded that it is essential to use multi-step kinetics only if accurate predictions of temperature distribution, energy release rates are desired. Their model was able to predict CO emissions accurately and over predicted NO.

The previous investigations [Weinberg, 1971; Sathe *et al.*, 1989a; Xiong, 1991] provided the qualitative information about the heat recirculation and the conduction and radiation modes of heat transfer in the PMC. However, there was no quantitative information. Using 1-D transient formulation with complete chemistry of methane combustion, Barra and Ellzey [2004] numerically quantified heat recirculation, radiation efficiency, solid conduction, and solid-solid radiation and flame speeds at different stable conditions. For better understanding, for equivalence ratio in the range 0.55 - 0.9, the above parameters were non-dimensionalised. High heat recirculation efficiency (ratio of solid-gas convection in preheating zone to firing rate) was observed for a high flame speed ratios (ratio of effective flame speed to laminar flame speed) at lower equivalence ratio. Solid conduction as well as solid-solid radiation was found to be important for heat recirculation efficiency. The radiation efficiency for preheating

at high equivalence ratio was more than conduction efficiency at low equivalence ratios. The non-dimensional exit temperature was almost constant at equivalence ratio Φ = 0.9. The radiation efficiency was higher at lower equivalence ratio but the magnitude of radiation was less when compared at higher equivalence ratios. The variation in the length of the burner had no effect on the amount of heat recirculation as well as on conduction and radiation.

Leonardi *et al.* [2003] and Chen [1987] made an extensive investigation to study the effects of the volumetric heat transfer coefficient, solid matrix emittance, effective thermal conductivity, extinction and scattering coefficients as well as firing conditions on the thermal performance of the PB.

Radiation output/Radiation efficiency

Many have recognized the importance of radiation in the PMC. An initial contribution towards the development of mathematical model accounting radiation is attributed to Echigo *et al.* [1986]. Due to unavailability of the exact thermo-physical and transport properties, they made simplified assumptions and used arbitrary property values along with single-step kinetics. They did not consider any reaction at the exit of the porous medium. Later Echigo and his co-researchers [Echigo, 1991; Yoshizawa *et al.*, 1988; Echigo *et al.*, 1986] studied the exchange of energy within a highly porous medium due to conduction, convection and radiation. In early experimental and numerical works, Echigo *et al.* [1982, 1986] found that the heat re-circulated in the upstream direction through the metal mesh screen was approximately 60°C higher than the downstream. Upstream temperature was found to increase with increasing the optical thickness. The effect of radiation was noticed due to high temperature drop across the screen. They also reported that the lean flammability limits was

extendable in the experimental burner made of porous ceramic plate enclosed in a permeable cylinder of stainless steel mesh. However, they did measure the radiation efficiency. Tong and Sathe [1988] performed a parametric study for a fibrous porous medium and considered the effect of absorption, emission and isotropic scattering. Solid conduction and scattering of radiation were observed to have a significant influence on radiation output, while the gas conduction had a negligible effect on burner's performance.

Tong *et al.* [1987] also discussed dependency of the size of the porous fiber on radiation output. They performed 1-D analysis of porous PRBs having sub-micron size fiber of silica and alumina. They found that with reduction in fiber diameter, the single scattering albedo was reduced and this led to increase in radiation output. They also found a rapid increase in radiation output when the diameter of the fiber decreased below 1 mm. At a temperature of 1000°C, for a fiber of approximately 0.2 mm, the radiation output was found to increase to 65% and 109% for silica and alumina, respectively as against the reference case of 0.5 mm fiber diameter. The same group of authors [Tong and Li, 1995] numerically showed that the radiation output increased with optical thickness, for low conductive and low scattering albedo materials. A similar study was undertaken by Andersen [1992] and Baek [1989]. They studied the effect of fiber size of porous ceramic on radiative output. It was found that fiber diameter of less than 1.0 mm produced significantly higher radiant output. For a temperature of 1500°C, the output increased by 72% for the silica and 150% for alumina materials. Yoshizawa *et al.* [1988] pointed out the relevance of the absorption coefficient and total optical thickness in calculating temperature profiles, radiant energy density and the position of the flame within the PB. They found that with decrease in absorption coefficient, the maximum temperature increased, the size of the reaction zone decreased and its position shifted upstream. An optically thick porous layer maximized radiant output and a highly

scattering porous media ensured more homogenous solid temperature distribution [Chen *et al.*, 1988; Shinoda, 2002; Kulkarni and Peck 1996].

Sathe *et al.* [1990b] investigated the radiation efficiency of the porous PB and found the same in the range of 26 - 40% when the flame stabilized in the upstream half of the porous medium. Sathe *et al.* [1989, 1990a] concluded that the best radiation efficiency was achieved if the flame stabilized at the centre of the burner having an optical thickness of about 10 and low scattering albedo, low solid thermal conductivity and high heat transfer coefficient. The results were in good agreement with the experimental results of Sathe *et al.* [1990a], which used lithium-aluminium-silicate foams with methane as fuel. At the lean mixture conditions, with shifting of flame to the surface, Leonardi *et al.* [2003] found a drastic drop in the radiation efficiency of the burner.

Singh *et al.* [1991] observed that low scattering albedo improved radiation efficiency due to high absorption. They concluded that for better performance, one should choose a porous material which possesses neither a very high nor a very low scattering albedo. Lim [1997] concluded that increasing the scattering albedo in the post-flame region of a two layer PB resulted in an increase of the gas and solid temperature in the post flame zone. However, increasing scattering albedo at the pre-heating zone resulted in lowering the peak- and post-flame temperature. Malico and Pereira [2001] performed a study on the influence of radiative properties on flame speed, temperature distribution etc. They found that increase in extinction coefficient resulted in a higher post-flame temperature gradient, increased heat transfer to pre-flame zone and a reduced peak temperature.

Kulkarni and Peck [1996] made a numerical study on a 5 cm long double layered PB. They determined the effect of porosity, length, extinction coefficient and albedo on radiant output from the burner. They concluded that for maximization of radiation output, the upstream layer of PB should have lower porosity, higher scattering albedo, shorter length and higher optical thickness than the downstream section. Further, the downstream section should be non-scattering. For the downstream section, they found the optimum extinction coefficient ranged 1 - 2 cm^{-1}. They concluded that the optimization of extinction coefficient was important because large extinction coefficient (large pore diameter) resulted in insufficient radiation to pre-heat the mixture. Similarly, smaller extinction coefficient (large pore diameter) resulted in spreading of radiation over a large distance. Barra *et al.* [2003] also studied the effect of material properties on stable operating range of the double layered burner. In their model, they kept the scattering albedo constant and varied the extinction coefficient. The optimized extinction coefficient for the downstream section was found to be 2.6 cm^{-1}.

To overcome the limitations of the 1-D models, Sahraoui and Kaviany [1994] considered the 2-D direct numerical simulation using single-step kinetics without radiation. They considered combustion in a porous medium consisting of discrete or connected square cylinders arranged in-line or staggered. The same was compared with the model based on volume averaged properties. The results showed that the direct numerical simulations predicted the flame speeds more accurately.

Tong and Li [1995] made a theoretical study to examine the effect of the fiber coatings on the radiation output. The burners made of coated silica fibers were considered along with the coatings of silicon carbide, graphite and platinum. It was found that silicon carbide coatings

resulted in minimal enhancement. Both graphite and platinum coatings provided significant enhancement in the emittance by a factor of three and six at the mean temperature of 1000 K and 1500 K, respectively.

Hackert *et al.* [1999] examined a honeycomb geometry consisting of many small parallel plates. Their model gave quantitative temperature distribution, flame velocity and interfacial heat transfer. Nevertheless, it could not predict detailed effects of process in the flame. In their study, they found that with an increase in wall emissivity, the burning rate and radiation output increased.

Talukdar *et al.* [2004] analysed heat transfer in a 2-D rectangular PB taking into account the effect of radiation effect. The non-local thermal equilibrium between gas and solid phases was considered. It was found that the radiant output decreased if the emissivity of the top and the bottom boundaries of the burner increased. They further observed that in the transient state, with the passage of time until the steady state, when the solid temperature became very high, both radiative and convective fluxes increased.

For the purpose of uniform heating, consideration of directional radiative behaviour of heating devices is important. To study the parameters affecting the directional radiative behaviour, Li *et al.* [2005] developed a model for a gas fired porous PB having a bundle of reflecting tubes. The energy equations were solved by the finite volume method and the radiative source terms were computed using the Monte Carlo method. They found a need for a trade-off between the radiation efficiency and uniform radiative heating of the object.

Emissions

Bouma and Goey [1995] studied combustion of a lean premixed methane air mixture stabilized in a ceramic foam burner. The combustion model was formulated using 15 species, including the chemistry of NO_x formation. It was shown that in radiant mode operation, the flue gas temperature was considerably low and hence the emissions of CO and NO_x were found lower compared to blue flame mode. Hsu and Matthews [1993c] did a numerical study to predict concentrations of different constituents of the exhaust gas and compared the same with the experimental data. At low equivalence ratio, due to low flame temperature, NO_x concentration was found low.

To study the emissions from a 2-D PB with integrated heat exchanger, Malico *et al.* [2000] incorporated the detailed kinetic mechanism in their previous model [Malico and Pereira, 1999]. The results were compared with the experimental data reported by Durst and Trimis [1996b]. It was found that CO emissions were under predicted and NO emissions were over predicted, especially for richer mixture. This observation was similar to Hsu and Matthews [1993c]. Their results also revealed that with increase in solid conductivity and heat transfer coefficient between solids and fluids, the peak temperature was lowered and hence the NO emission was also low. However, an increase in the extinction coefficient did not show an obvious effect on NO emissions.

Brenner *et al.* [2000] used pseudo-homogeneous heat transfer and flow model for the porous material to study the combustion behaviour and also the predictability of the code. Al_2O_3 and SiC lamella were considered as porous medium. The model was found difficult in simulating the conditions of flame stabilization between the combustion and preheating zones where

most of the NO_x formed. Hence the NOx prediction was not accurate. Their results showed a better radiant output and low CO emissions in the case of SiC.

2.8 APPLICATIONS OF POROUS MEDIUM BURNER

Owing to several advantages, applications of the PBs are widespread. They are used both in industrial and in domestic sectors. Gas fired PBs are used in a number of manufacturing processes such as paper drying, paper finishing, powder and paint curing, baking, textile drying, polymer processing, etc. They are also used in household air and water heating system, IC engines (pre-heaters of vehicles), gas turbine combustion chamber, steam generator and electricity generation. Some of the important applications of the PB are discussed in the following sections.

2.8.1 Domestic Applications

Jugjai and Rungsimuntuchart [2002] implemented the idea of the PMC in a LPG cooking stove for improved efficiency. In doing so, they proposed a new concept named as semi-confined porous radiant re-circulated burner (PRRB) where the primary air was preheated to higher temperatures than conventional burner (CB). They combined the PRRB with the available CB and swirl burners (SB) to study the improvements in efficiencies and emissions. With the former, they could achieve 12% higher thermal efficiency than the 30% for the CB, and with the latter, it was just double the CB. This led to an energy saving of around 50%. The NO_x and CO emissions were found significantly low in the PRRB (SB) than PRRB (CB). The calculated thermal efficiencies for the model PRRB (SB) and the experimental results were in good agreement. However, they did not put the porous material in the combustion path and hence could not harness the true benefit of the PMC technology.

Qui and Hayden [2006] designed and fabricated a PB made of fiber felt along with a recuperator using natural gas. The main objective was to study the performance of the existing gas-fired lanterns equipped with porous medium. The different modes of combustion in the fiber felt, performance at various operating conditions and the effect of heat recuperation were studied. Flame stabilized in the porous ceramic fiber felt was found to be strongly dependent on the firing rate and excess air ratio. The stable flame was obtained in the range 16 - 54.5 W/cm^2. The effect of recuperation was also considerable. The light output was measured and it was found to increase with combustion air temperature (*Table 2.5*).

Table 2.5 Light output and lighting efficiency of the light-PB [Qui and Hayden, 2006]

Gas heat input (W)	Combustion air Temperature (°C)	Light output (Lumens)	Lighting Efficiency (Lumens/W)
2593	24	1608	0.62
2593	300	2360	0.91
2548	465	3934	1.54
2593	550	4855	1.87
2548	586	4982	1.96

2.8.2 Gas turbines and Boilers

Tanaka *et al.* [2001] explored the possible application of the PB in the combustor of the second stage of the chemical gas turbines developed by Arai *et al.* [1999]. The aim of their investigation was to utilize the unused chemical energy of the exhaust in the second stage combustor equipped with porous medium, so that the flammability limits would widen and thermal efficiency be improved. For this, they optimized the burner in terms of chemical, fluid mechanical and geometrical parameters using thermal efficiency and heat recirculation rate as the criteria. From their results, they concluded that use of the porous medium in the chemical gas turbine would be a good choice.

Delalic *et al.* [2004] successfully used porous media heat exchangers as an integral component in the low temperature (condensate) boilers. The results showed a better heat exchange efficiency and combustion stability. The thermal efficiency was found to be higher than 95% for both 5 kW and 9 kW burners at different excess air-ratios. It was possible due to the fact that a part of the latent heat of the water condensation from exhaust gas was transferred to water in the heat exchanger. NO_X and CO_2 emissions were low due to improved energy efficiency. The system was found to be applicable for central heating system also.

2.8.3 Fuel cell and Hydrogen Production

Hydrogen production in ultra rich combustion of methane and hydrogen sulfide was investigated by Bingue *et al.* [2002, 2004]. The maximum conversion rate obtained was 60%. Mjaaness *et al.* [2005] experimentally investigated the possible use of the PMC as a reformer in the fuel cell. They used PBs of two types: double layered alumina foam and double layered alumina beads to convert methanol, methane, octane and automotive grade petrol for the generation of hydrogen which is used in the fuel cell. The experiments showed that the alumina beads had long lifetime than foams and the conversion efficiency of the burner was also high.

In the recent past, Raviraj and Janrt [2006] did an experimental study with an aim of achieving higher conversion efficiency along with the parameters affecting the conversion efficiency. They could achieve 65% net conversion efficiency for a particular equivalence ratio and inlet velocity of the methane. For better conversion efficiency, they suggested low specific heat and low thermal conductivity porous media.

2.8.4 Furnaces, Process and IC engines

The convection to radiation converter made of porous ceramic has been identified as an effective means to enhance heat transfer in burners, combustors, industrial furnaces and high temperature plug flow systems. With an objective of heat transfer enhancement, Zhang *et al.* [1997] proposed a novel application of PB in a partially bypass flow system. They assumed hydro-dynamically fully developed and thermally developing laminar flow inside a circular duct incorporated with porous core in which heat was transferred from high temperature gaseous medium to a heat absorbing wall. The numerical results showed that the use of porous medium was very effective to enhance both convective to radiative heat transfers. The system was found suitable for a gas medium having a weak emittance, lower wall temperature and low velocity.

Liu and Hsieh [2004] conducted experiments in the PBs using the LPG under steady-state and transient conditions. In their experiments, they introduced cooling tubes in the post flame zone to recover the maximum heat used to preheat the incoming air–fuel mixture unlike conventional PMC. The heating of working fluid passing through the cooling tubes has found many applications such as in water and air heaters, boilers and chemical processes. A particular phenomenon called metastable combustion (having single flame speed at a particular equivalence ratio) was observed due to the changes of heat balance in the burner. It was also observed that the metastable combustion ceased during transient state and drove the flame out of the packed bed. The CO and NO_x emissions were also reported for the particular burner.

Kesting *et al.* [1999] developed a high temperature staged Oxy-fuel PB. The main aim was to succeed in keeping the temperatures of the radiation burner below the known material limits (< 1800°C), although pure oxy-fuel combustion was realized, which normally yields to very high temperatures (> 2800°C). They found that the burner could be operated at nearly stochiometric condition without reaching very high combustion temperature. This was made possible by adjusting the radiant surface of the burner in such a way that the necessary heat could be transferred by radiation. With continuous staged combustion, the radiation output was controlled and a better heat recirculation was achieved. The radiation efficiency of the burner was found higher and the temperature within the CZ was homogenous. The emission was low and hence it was identified as ultra low emission burner. The burner is mainly aimed at glass melting furnaces, surface treatment, and metal treatment.

Mo¨ßbauer *et al.* (2001) designed and tested a compact ultra low emission steam engine based on PMC technology for automotive application. The prototype showed a possible application of PMB to the current car engines along with the steam generator which can offer advantages over the state-of-the art existing technologies. Durst and Weclas [2001] first applied PB technology to the diesel engines. Weclas [2005] explored the application of the PMC in IC engines and he found improvements in many respect. The main benefit was the reduction of NOx and elimination of soot. The combustion was found homogeneous and flameless. The media was found effective to control gas flow, fuel injection and its spatial distribution, vaporization, homogenization, ignition and combustion. The investigations showed encouraging results.

2.8.5 Combined Heat and Power Generation and Miscellaneous applications

The idea of combined heat and power with the PMB was put forward by Echigo *et al.* [1993, 1994, and 1995] and a system was developed by Hunt *et al.* [1994, 1995] for hybrid electrical vehicles. PMB is also taking its place in thermo-photovoltaic power generation [Qui and Hayden, 2007]. The usage of PMB in combination with solar water heaters for home and commercial heating was studied by Avdic [2004]. In the near future the PMB will be the most prospective ingredient for combined heat and power generation. Very recently, few researchers have focused on micro and meso-scale applications of PMC technology [Marbach and Agrawal, 2006; Marbach *et al.*, 2007; Li *et al.*, 2008; Sadasivuni and Agrawal, 2009; Kamijo *et al.,* 2009]. Dobrego *et al.* [2005, 2006, and 2007] made a remarkable contribution by eliminating highly polluting volatile organic compounds (VOCs) such as formaldehyde, benzole, asphenol, acetone etc; through oxidation in PMB.

2.9 POROUS SURFACE COMBUSTION

As discussed earlier the flame is stabilised on the surface of the porous matrix not more than 1 mm. The hot gases from the combustion heats up the porous matrix and then the surface starts radiating. The initial work in this direction was first done by Bone [1912], Lucke [1913], and Hays [1937]. The first notable numerical contribution in this direction is by Hanmura and Echigo [1991]. They explained the detailed behaviour of the flames in the surface burners with respect to time for understanding the stabilization mechanism along with the three critical limits for blow-off, flash back and extinction correlated to the flame velocity, flame structure and thermal radiation propagation.

Williams *et al.* [1992] conducted the experimental investigations on surface combustion with methane and air premixed mixtures within and near the downstream of the porous matrix. The maximum rate of heat release was found at or above the surface of the porous matrix. The major contributor in the formation of NO_x was prompt NO. Itaya *et al.* [1992] and Nakamura *et al.* [1993] observed a steady flame in methane air combustion over a porous ceramic plate in an open atmosphere. The ceramic plate was found to act as a flame holder. Nakamura *et al.*[1993] studied the methane–air premixed combustion on the surface of the combustions and found that the maximum height the flame should be stabilized is 1 mm for better balance between the velocity of the combustion and gas flow to avoid flash back. The temperature on the surface was found proportional to the thickness of the porous matrix because the air-fuel mixture will have enough time to preheat to high temperatures. The peak surface temperature reaches at a particular thermal load and after that the flame gradually detaches from the surface and the surface temperature starts decreased. Itaya *et al.* [1994] also made study on surface combustion of methane and air on a porous ceramic plate in a cylindrical furnace. They found extension of lean flammability limit and higher temperature of ceramic plate owing to the higher thermal radiation from the furnace wall.

Bouma *et al.* [1995] and Bouma and Goey [1999] studied the porous surface combustion experimentally and numerically. The formation of major CO and NO were studied in detail. The levels of both the emissions above the porous matrix surface at different heights were illustrated. Both the experimental and numerical results were in good agreement. To predict the CO emission more accurately, the authors suggested having gas radiation in the modelling. It was found that, prompt NO as well as thermal NO was important for the prediction of the total NO. Lammers and Goey [2004] studied the effect of gas radiation

experimentally and numerically on the surface temperature decrease on the porous surface burner and inturn the emissions.

Jugjai and Sawananon [2004] studied a surface combustor heater (SCH) coupled with a heat exchanger, with a new concept of cyclic flow reversal combustion (CFRC) for residential and commercial complexes, steam super heaters and thermal fluid heaters of industrial applications. The authors claimed that, the proposed SCH with CFRC concept could provide the basis for development of state-of-the-art technology for new versions and more advanced thermal systems, such as highly efficient ultra-low-pollutant-emission boilers, for efficient utilization of energy. Both interior and surface combustion processes using silicon carbide-coated, carbon - carbon composite porous media were investigated by Marbach and Agrawal [2005], and Nemoda *et al.* [2004]. Results affirmed PMC as an effective method to extend the blow-off limit in lean premixed combustion. Recently, Marbach *et al.* [2007] presented a numerical study of heat recirculation in an annulus around a surface combustor made of silicon carbide-coated carbon foam. The proposed model was validated for methane combustion in chamber volume of 0.364 cm^3 and overall system volume of 1.5 cm^3. Experiments were conducted for reactant flow velocities varying from 0.25 - 1.0 m/s in the equivalence ratio range of 0.50 - 0.80. Results showed an excellent agreement between measured and computed temperature profiles at different reactant flow rates. The proposed combustion system design achieved a significant reduction in the heat loss as compared to the baseline design tested experimentally.

2.10 CONCLUDING REMARKS

Owing to some undesirable features such as thin reaction zone, sharp temperature gradient, large sized combustor, low power density, low power modulation range, low efficiency and high level of pollutant emissions associated with combustion devices based on free flame technology, the need for combustion inside an inert porous medium which addresses the above problems was discussed. A brief history of research and developments in the PMC was provided. The basic principle of heat transfer mechanism in the PMC was explained. The concept of excess and super excess enthalpy combustion was brought out and their practical benefits were discussed. It has been found that till date, the actual conditions governing the excess enthalpy flame generation have not been clearly specified. This leaves a scope to further study the actual parameters affecting it and hence, research is still underway to have a better understanding of the complete phenomena.

The thermo physical and radiative properties of different porous materials which used in construction of porous burner were presented. The materials have been found to have a significant bearing on the performance of the PB. It was found that both metallic and ceramic foams could be used in construction of PB. However, owing to an overall better heat transport properties and superior creep and corrosion resistance, ceramic foams are preferred. Since for different applications, the materials requirements are different, research for appropriate materials is still continuing.

The results of various studies on flame stabilization phenomena within single as well as double layered PBs were reported. It was found that the flame was found to stabilize even at low equivalence ratio due to heat recirculation. Flame stabilized at the centre of the single

layered and at the interface of a double layered PB provided better performance. The flame speed was found higher than the laminar flame speed that helped in enhancing the degree of preheating of the incoming air-fuel mixture. However, the flame stabilization phenomenon for low calorific fuel is yet to be investigated.

In the PMC, due to pressure diffusion, a self-sustaining combustion wave is generated. However, to understand the physics behind this pressure driven combustion wave, the studies offered by different researchers were limited. Similarly, for measurement of turbulence intensity, which is influenced by porosity, the effort put forward was also very less. Hence, there is a considerable scope in evaluation of effect of anisotropic porosity on turbulence.

A good amount of work has been carried out to investigate the thermal performance of the PB made of different materials having different power outputs, different firing rates, equivalence ratios, and optical properties. Because of better heat recirculation, the lean flammability limit was found to be extended for all types of fuels. For a double layered PB, it has been found that the porosity of the PZ should be lower than that of the CZ. Even PB having three or more layers with different porosities has started.

Radiation greatly influences the thermal performance of the PB. The radiation output has been found to depend on various parameters like equivalence ratio, firing rate, flame support layer thickness, porosity and aspect ratio which in turn influence combustion and thermal efficiencies. In the absence of a standard procedure, a wide variation (15 - 50%) in radiation efficiency has been found. A doubled layered PB showed higher radiation efficiency than the single layered PB. The radiative output was found to increase with optically thick, low

conductive and low scattering albedo material. For a double layered PB, it was concluded that for increased radiation output, the upstream layer of PB should have lower porosity, higher scattering albedo, shorter length and higher optical thickness than the downstream section. Radiative contributions have been investigated by considering spectrally blind porous matrix and effect of anisotropy has not been considered. For an accurate analysis, these two aspects need to be addressed in the radiation modelling of the PMC.

In the PMB, because of heat recirculation, the CZ temperature is lowered and the combustion is nearly complete with sufficient residence time. Reduced temperature has been found to be one of the most effective means to control thermal NO_x and because of nearly complete combustion, CO level is considerably low. Mathematical models to estimate NO_x and CO emissions for different cases are limited and the available ones have assumed simplified cases. Further research considering complete chemistry of NO_x formation is required.

Researchers explored many areas of application for PMB. Depending upon the applications, researcher reported the thermal efficiency ranging from 60 to 80%. The power range for these burners is 5 - 60 kW. There is no work reported on the application of PMB for cooking application, which requires a power range of 0.5 - 2 kW.

In case of PSC, the literature is very meagre but can give an insight for proper understanding of the combustion behavior and pollutant formation. The applications also need to be explored. The differences in PMB and PSB are the later has high emissions, low power density in comparison with the earlier.

2.11 OBJECTIVES OF THE PRESENT WORK

In view of the above conclusions made on the available literatures, the following objectives are considered for present study.

- To ascertain the applicability of the porous burner for domestic cooking applications in the low power range of 0.5 - 2 kW.
- To investigate the effects of the equivalence ratio, power and burner diameter on the thermal efficiency and emissions of the burner.
- To study the effects of equivalence ratio and power on the flame position and temperature distribution within the burner.
- To explore the possibility of using any other new burner for domestic cooking applications.

Chapter 3

FIRST PHASE DEVELOPMENTS

In this chapter, the performance investigations of the domestic LPG cooking stove using the porous media like metal balls, pebbles and metal chips in the mixing chamber without its burner head is discussed. A brief discussion about the experimental set up and procedure are presented. The thermal efficiency and emission characteristics of the burner at different powers (Appendix-I) are also presented.

3.1 EXPERIMENTAL SET UP AND MATERIALS

In the conventional burners, the combustion takes place over the surface of the burner which is exactly above the head of the burner. *Fig. 3.1* shows the different types of burner heads available in the Indian market for conventional LPG cooking stoves. To achieve combustion in a porous matrix, the head was removed from the burner and filled with the porous materials in the mixing chamber as illustrated in *Fig. 3.2*. The air was supplied though natural draft same as in conventional burner. The base and the side of the mixing chamber were insulated using ceramic wool to minimize the heat losses. *Table 3.1* summarizes the four combinations of porous media that formed two zones of the PMB as discussed in Section 2.3.

The four combinations as given in *Table 3.1* were arrived on the basis of the desired height and color of the flame. The objective was to achieve matrix stabilised combustion. In order to stabilise the flame within the porous burner several trails were made with different thickness

of the porous materials. The thicknesses of Zone 1 (CZ) and Zone 2 (PZ) were kept around 18-20 mm and 12-15 mm, respectively for proper combustion with in the porous media.

a. Nikitsa Burner

b. Regular Burner

c. Side Flame Burner

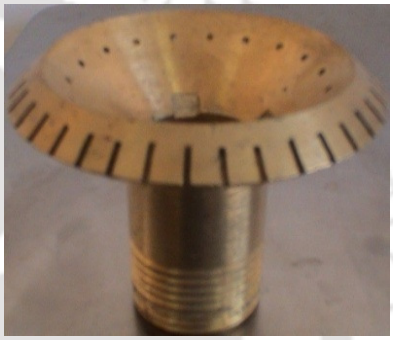

d. Sun-flame Burner

e. BPL Burner

f. Super Flame Burner

g. Aluminium Base Burner

Fig. 3.1 Conventional burners available in the market chosen for comparison (only burner heads are shown)

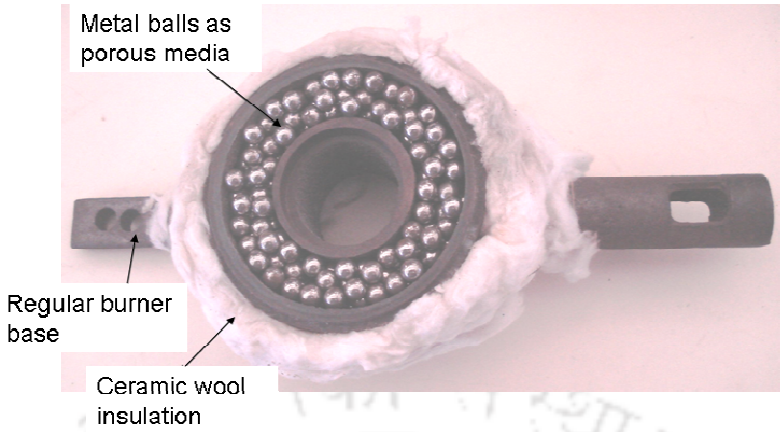

Fig. 3.2 Insulated mixing tube of a conventional burner filled with metal balls as porous media

Table 3.1 Two sections of porous burner with different combinations of CZ and PZ

Porous media	Zone 1	Zone 2
1. Ball - Ball	3 mm diameter Metal balls	Metal balls of diameter 8 mm
2. Pebble - Ball	3 - 4 mm average diameter pebbles	Metal balls of diameter 8 mm
3. Pebble - Ball with insulation and reduced height	3 - 4 mm average Diameter pebbles	Metal balls of diameter 8 mm
4. Pebble and metal chips insulation with the reduced height between the burner surface and the bottom surface of the vessel.	3 - 4 mm average diameter	Metal chips

3.2 EXPERIMENTAL PROCEDURE

In India, Bureau of Indian Standards sets guidelines for testing the thermal efficiencies for all types of cooking stoves. For LPG cooking stoves, the thermal efficiencies are determined according to Indian Standards (IS) 4246:2002. Following the guidelines of IS 4246:2002, thermal efficiencies of cooking stoves in the present work were estimated by conducting the water boiling test and the procedure followed is briefly described.

A 5 kg LPG cylinder was connected to a regulator and then with a pressure gauge in between to the burner. To purge air and to establish the required gas pressure, LPG at a pressure of 30 *mbar* was allowed to pass through the burner for a few minutes. Only one burner of the cooking stove was tested at a time. The diameter and height of the aluminum pan used for water boiling test was selected according to the range of gas flow rate used in the experiment. The pan mass along with its lid and the mass of water used in the pan was noted. The weighing balance used has a resolution of 1 gm (make: Sartorious) Temperature T_1 of water was noted and recorded as long as it remained constant. The cylinder was disconnected and its weight m_1 was noted and then again the cylinder was connected to the line. The gas supply was turned on and it was ignited. Water was heated up to 80^{o}C and for uniformity in temperature; stirring was started and continued until the end of the test when the temperature T_2 of water reached 90 ± 1°C. Then the burner was put off. The cylinder was disconnected and its new weight m_2 was noted. The difference in the weight, m_2 - m_1 (= m_f) estimates the mass of gas used to heat water from T_1 to T_2. The weighing balance used has a resolution of 0.1 *g* (make: TULA, India).

The percentage of thermal efficiency, η_{th}, of the stove was calculated based on the following formula:

$$\eta_{th} = \frac{(m_W \times C_W + m_p \times C_p)(T_2 - T_1)}{m_f \times CV} \qquad (3.1)$$

where, m_W is the mass of water, C_w and C_p are specific heat capacity of water and aluminium pan respectively, m_p is the mass of pan along with the lid and stirrer and m_f is the mass of the fuel. The calorific value of the fuel, CV = 45636.12 kJ/kg**,** specific heat of water and aluminium are C_p = 0.8959 kJ/kg-K and C_W = 4.1826 kJ/kg-K, respectively. For every burner,

experiments were repeated at least three times and average of the three values was taken as the final efficiency. The same procedure was also followed when porous media was used. The uncertainty analysis was carried out by considering the inaccuracies in the mass and temperature measurements. A maximum value of uncertainty in the thermal efficiency calculation was found to be ± 2.8%. The detailed uncertainty analysis is presented in Appendix- III. To compare the thermal efficiencies and emissions of the burners with porous media with those of the conventional LPG cooking stoves, a market survey was carried out to get the various types of burners used in conventional domestic cooking stoves. Seven types of burners were selected from the Indian market. Burner heads of the same are shown in *Fig. 3.1*. The thermal efficiencies of the seven types of conventional burners selected from the Indian market were in the range 60 - 65%. The typical measured efficiency curve of a conventional domestic cooking burner is shown in *Fig. 3.3*. The burners shown in *Fig. 3.1* follow the same trends, i.e. thermal efficiency found to decrease with increase in wattage (increases heat loss to the surroundings) as shown in *Fig. 3.3*.

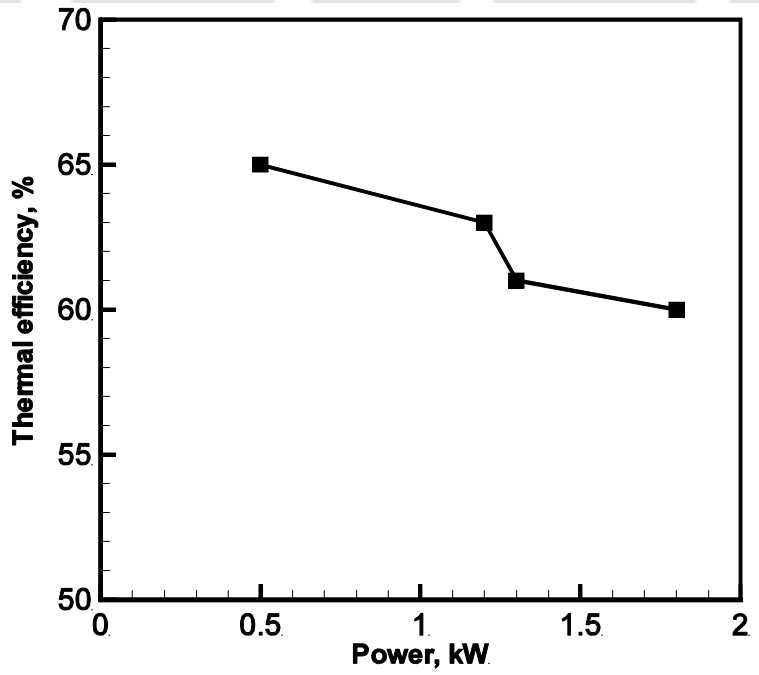

Fig. 3.3 Typical efficiency graph of the conventional domestic cooking burner

The flue gas sampling was done according to the IS: 4246. A hood shown in the below *Fig. 3.4* was fabricated according to the dimensions mentioned in the IS: 4246. The hood was placed above the burner along with the vessel and the portable flue gas analyser probe was place in the first sampling hole. The main purpose of the hood is to isolate the flue gases from the atmospheric air to avoid any influence on the former by the later. A portable flue gas analyser is used (TESTO 350XL, maker: TESTO, Germany) for recording CO and NO_x emissions. The detailed specifications of the instrumentation/equipments used in the experiments are given in Appendix - IV.

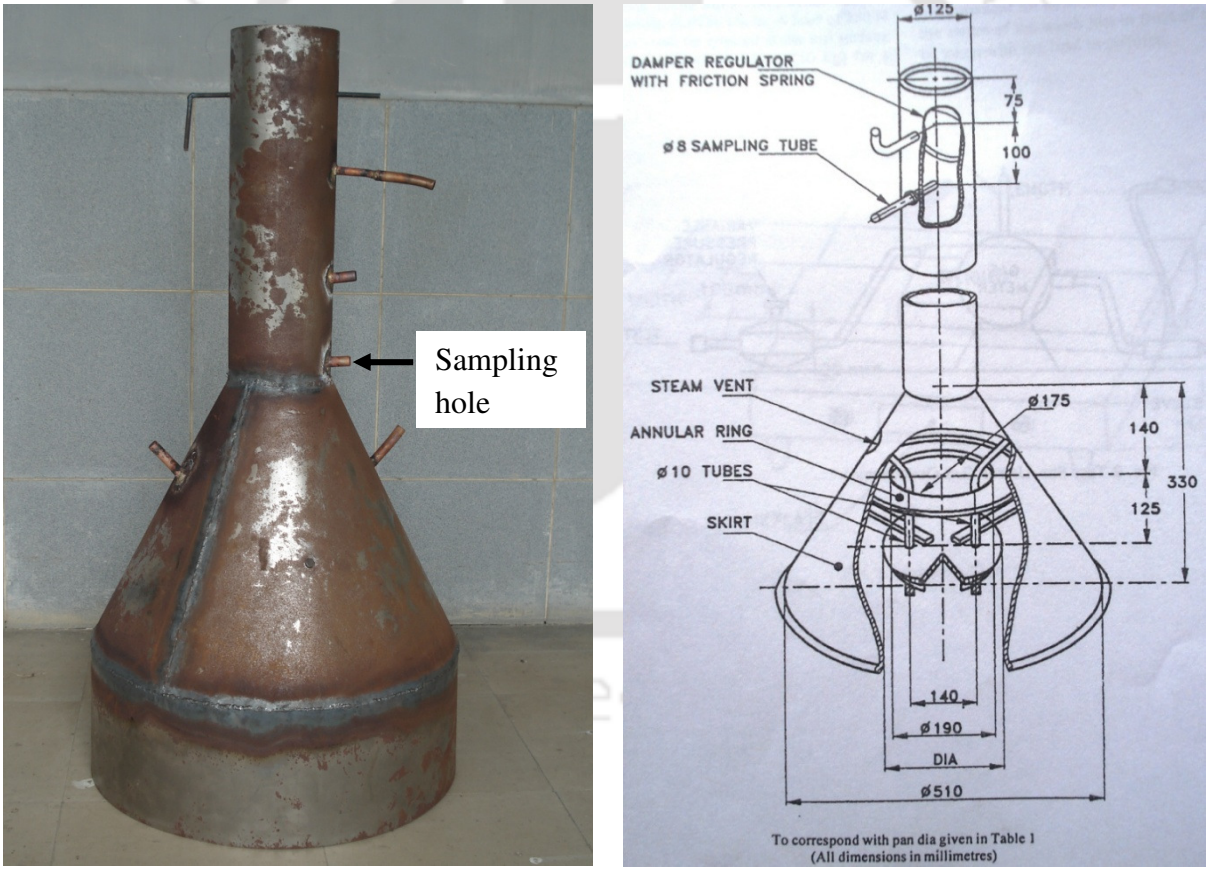

a. Hood for flue gas sampling

b. Schematic of the hoof for flues gas sampling (imported from IS: 4246)

Fig. 3.4 Photo and schematic of the hood for flues gas sampling

The typical CO and NO_x emission levels of the domestic cooking burner in the range of equivalence ratio 0.9-1.0 are illustrated in *Fig. 3.5*. Both the CO and NO_x emissions rise with the power and the maximum values observed were around 1050 mg/m^3 and 216 mg/m^3, respectively, which are much higher than the recommended values [Kandpal *et al.*, 2002] of World Health Organisation (WHO).

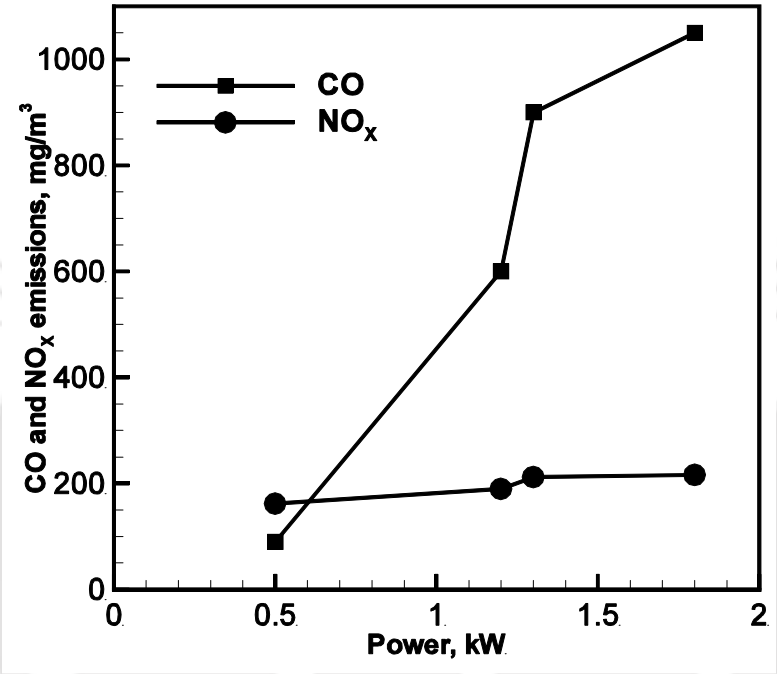

Fig. 3.5 Typical emissions graph for a conventional domestic cooking stove

3.3 RESULTS AND DISCUSSIONS

Thermal efficiency and emission testes were carried out by using different porous media in the mixing chamber of the conventional LPG cooking stove.

3.3.1 Thermal efficiency

Case 1: *3 mm and 8 mm metal balls:*

In this case, the 3 mm metal balls formed the PZ and 8 mm balls formed the CZ and no insulation was provided around the burner. The flame height was reduced to 2/5th of the

conventional burner and a complete blue flame was also achieved. The flame in this case stabilized just above the surface. The soot formation was observed in the preheat region indicating undesirable combustion phenomenon. The reason for undesirable combustion in the preheat zone was due to high thermal conductivity and emissivity of the metal balls. The thermal efficiency in this case was found to 68%, which is 3% higher than the conventional burners. Though there was an improvement in the thermal efficiency, a blue flame of reduced height was still observed.

Case 2: *Pebbles and 8 mm metal balls:*

The relative thicknesses of CZ and PZ were retained for the rest of the Cases 2 to 4 with different porous media. To avoid the undesirable combustion in the PZ, metal balls were substituted with pebbles (average diameter of 3 mm). Because of low thermal conductivity and emissivity of pebbles, combustion was not observed in PZ. The thermal efficiency of about 69% was observed. The temperatures of the surrounding atmosphere, the stove metal body and the floor just below the stove were found to be more than the previous case. This rise in temperature is due to the combustion of LPG in the mixing chamber which results in the reduction of flame height to about $3/5^{th}$ of the conventional stove. In this case also no insulation was provided to the burner.

Case 3: *Pebbles and metal balls with insulation on the mixing chamber:*

To avoid the heat loss, ceramic wool insulation of thickness 40 mm was provided along the sides and the base of the mixing chamber. Further, to minimize radiation heat loss in the downstream, distance between the top surface of the mixing chamber and bottom surface of the pan was reduced from 20 mm to 10 mm. With these modifications, thermal efficiency was found to increase up to 72%. However, similar to the previous two Cases, fully matrix

stabilized combustion was not observed and one can see flames over the surface of the porous media as shown in *Fig. 3.6*.

Fig. 3.6 Combustion in the porous medium of metal balls

Case 4: *Pebbles and metal chips with insulation on the mixing chamber:*

To avoid the difficulty in filling the metal chips into the gap as in previous case (*Fig. 3.6*), the central portion of the mixing chamber was removed. This arrangement provides a required pressure drop to stabilize the flame within the porous medium and also to distribute the heat combustion uniformly. The metal balls in the CZ of the mixing chamber were replaced with mild steel chips (average thickness 0.5 mm and 50 - 80 mm length) to reduce the thermal mass. As expected, with the change in the geometry and metal chip matrix, unlike the previous cases of metal balls, the burner was found to become red hot and no flame was observed outside the chip matrix. The thermal efficiency in this case was found to be 73%. In this Case, the radiative heat generation was felt comparably higher than all the above cases along with the increase in the temperature of the mixing chamber which was attributed by the fact that the wall of the mixing chamber became red hot.

The thermal efficiencies of the burners with mixing chamber filled with porous media as described in Cases 1 to 3 were found in the range of 68% - 72%. The replacement of metal balls in the CZ by mild steel chips (Case 4) increased the thermal efficiency further to 73%. These results are summarized in *Table 3.2*. It is observed that with the use of metal chips in the CZ and providing insulation over the mixing chamber, thermal efficiency can be improved by 8% higher than the maximum value achievable with conventional stoves. In the present tests, the thermal efficiency and the emissions for all the cases were measured at the lowest and at the highest operating power limits of the burner due to the very low power difference.

Fig. 3.7 Combustion in porous medium metal chips

Table 3.2 Comparison of thermal efficiencies of different experimental porous burner with conventional burners

Sr. No.	Burner model	Operating limits of burner in Power (kW)	Thermal efficiency (%)
1.	Conventional Burners available in the Indian market	0.5 - 1.8	60 - 65
2.	Metal balls and gravel (Cases 1 - 3 of Section 3.1)	≈1.3 - 1.8	68 - 72
3.	Metal chips (Case 4 of Section 2)	≈1.5 - 1.8	73

The results showed that at higher thermal efficiencies the power range became narrow and below this, the burner was prone to flash back. This was mainly due to the low stream velocities of the air-fuel than the flame speed. In the Cases of 1 - 3, the flame speeds were lower than the Case 4 because the flame was on the surface of the burner and there was less recirculation of heat from the CZ to the PZ. In Case 4, as the combustion starts occurring inside the porous matrix, the flame speed found to higher than previous cases and then narrowed down to the higher side of the air fuel flow rate where the flame velocity is lower than the gas air mixture velocity.

3.3.2 Exhaust gas analysis

Emissions resulting from combustion are an important environmental factor. In Table 3.3, CO and NO_x emissions are summarized for the three cases considered in *Table 3.2* of Section 3.1. In porous media combustion, CO and NO_x emission levels have been found less than the free flame combustion.

Table 3.3 comparison of emissions and emissions of conventional burner embedded with different configuration porous media

Sr. No.	Burner model	Operating limits of the burner in Power (kW)	NO_x (mg/m^3)	CO (mg/m^3)
1.	Conventional burners	0.5 - 1.8	162 - 216	90 - 1050
2.	Conventional burners filled with metal balls and gravels (Cases 1 - 3 of Table 1)	≈1.3 - 1.8	108 - 135	150 - 270
3.	Conventional burners filled with Metal chips (Case 4 of Table 1)	≈1.5 - 1.8	81	180

In case of Cases 1 - 3, the CO emissions levels were found to increase with power (*Table 3.3*). The raise in the CO levels was due to the less residence time and also the equivalence

ratio hardly reached to 1, where the air was entrained in the fuel stream by natural convection. The NO_x levels did not follow any specific trend but were fluctuating in the operating power range (*Table 3.3*). It was believed that the fluctuation might be due to hot and cold spots on the surface of the porous media. However, the NO_x levels had been reduced well below the lower limit of the conventional burner. In Case 4, the NO_x levels become stable in the very narrow power range due to the effect of radiative cooling of the flame. In case of CO emissions it can be due to the proper distribution of air-fuel mixture and temperature in the CZ.

Chapter 4

SECOND PHASE DEVELOPMENTS

This Chapter presents the performance investigations of the newly developed porous medium burners (PMB) at different powers and equivalence ratios (Appendix - II). The burner casings with different diameters such as 60, 70, 80, 90, and 100 mm at two different thicknesses 10 mm and 40 mm were fabricated. Silicon carbide foams and alumina balls were used in combustion and preheating zones, respectively. The thermal efficiencies and emission characteristics of different PMBs were estimated in the possible operating range of different equivalence ratios and powers by varying the geometrical parameters as discussed in the following sections.

4.1 EXPERIMENTAL PROCEDURE AND TEST SET-UP

A schematic and photograph of the experimental set-up used for testing the performance of PMB's are shown in *Fig. 4.1* and *Fig. 4.2*, respectively. The fuel flow rate and air flow rates were monitored using rotameters with control valves. The power can be varied with the fuel rotameter and the corresponding equivalence ratio can be changed using the air flow meter. The rotameters were pre-calibrated by the manufacturer for the specific gases. Air and LPG were supplied at 30 mbar and 600 mbar, respectively. In the following paragraphs design and fabrication details of the PMBs are discussed.

4.1.1 Materials and specifications

The PMB's were developed based on two layered PMC as discussed in Section 2.3. Combustion zone was formed with SiC porous matrix. The preheating zone was filled with

alumina (Al_2O_3) balls of 5 mm diameter (supplier: Mica Industries, Mumbai, India). The specifications of the porous matrix throughout the experiments were kept constant at 10 ppi with porosity of 0.9. The thickness opted for the CZ was 15 mm and 20 mm for the study.

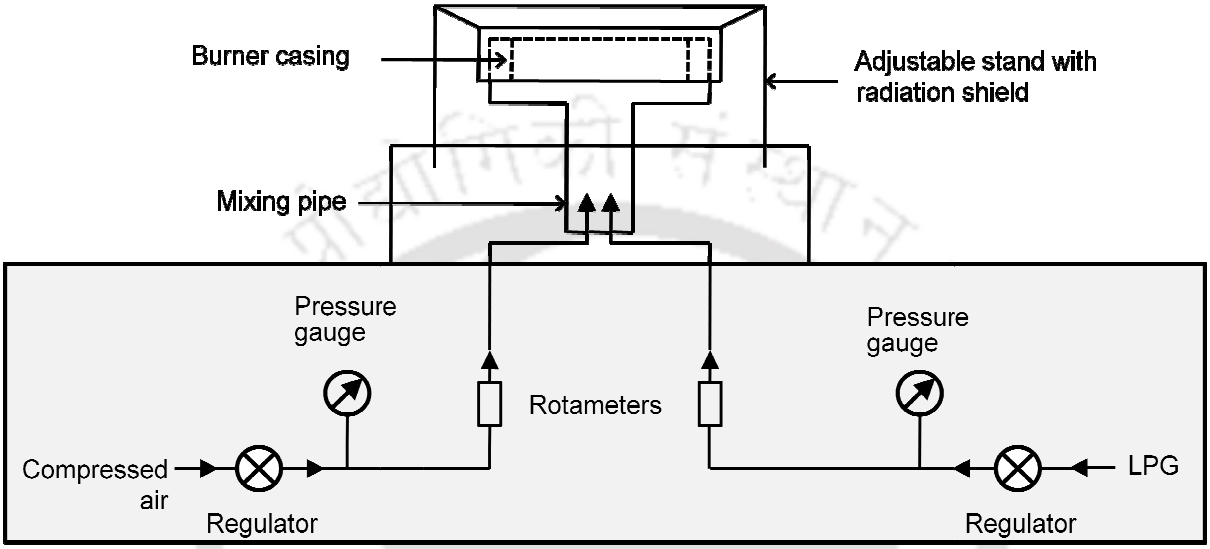

Fig. 4.1 Schematic of the experimental set up

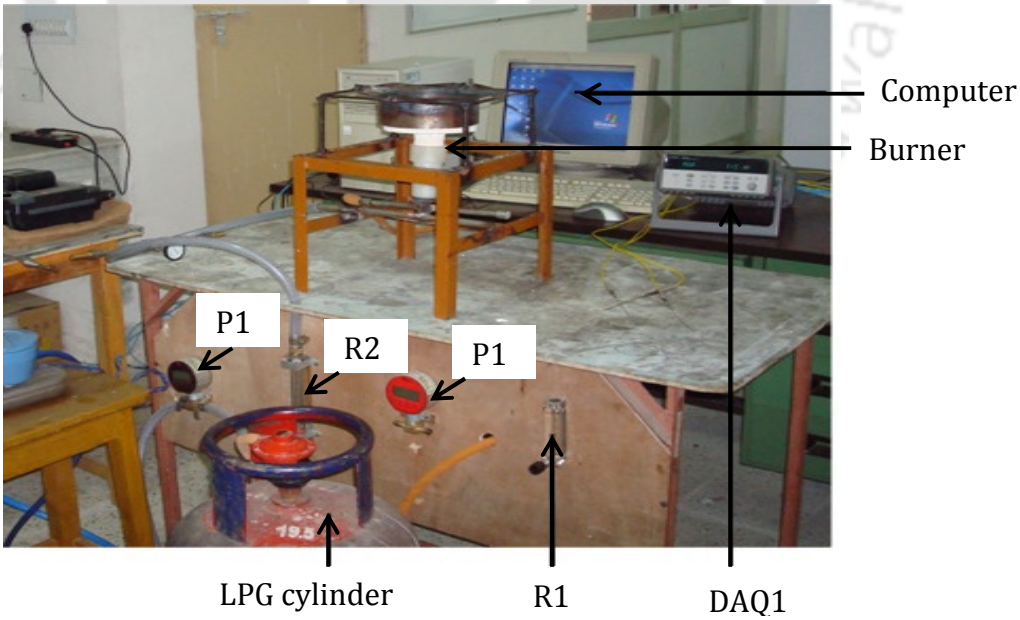

Fig. 4.2 Photographic view of the experimental set up (P1&P2-pressure gauges for LPG and air; R1 & R2-Rotameters for LPG and air)

4.1.2 Burner casing and mixing tube

The burner casing was fabricated at IIT Guwahati using alumina powder (mixture of coarse and fine) and sodium silicate binder. The mixture was rammed into proper moulds and then allowed to remove water vapour at low temperatures around 150 °C slowly to avoid any cracks in the sample. Then the samples were removed from the moulds and sintered at high temperature up to 1200 ºC for strength and to withstand the thermal stresses. Different parts of the burner are shown in *Fig. 4.3* and the schematic of the burner is illustrated in *Fig. 4.4*. Different specifications and names of the various PMBs are given in *Table 4.1*. The diameter of the burner was increased from 60 mm to 100 mm in steps of 10 mm. Burners were named as B6, B7, B8, B9, and B10, where B stands for the burners and the numerical number stands for its diameter in cm. The wall thickness of B6 and B7 burners was kept at 10 mm and for B8, B9 and B10; it was increased to 40 mm.

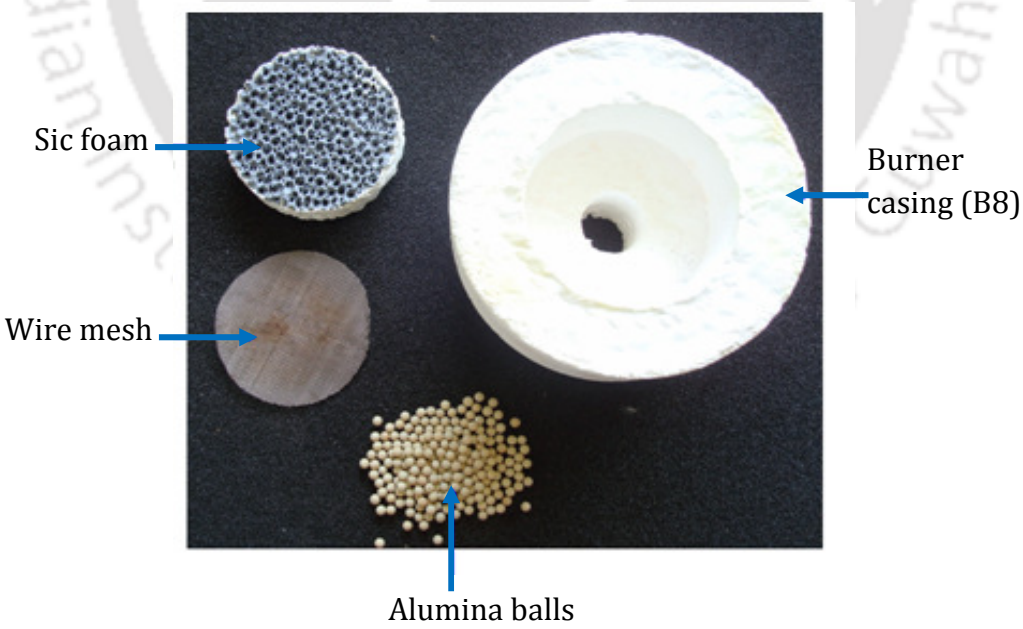

Fig. 4.3 Photograph showing the basic materials used in the burner

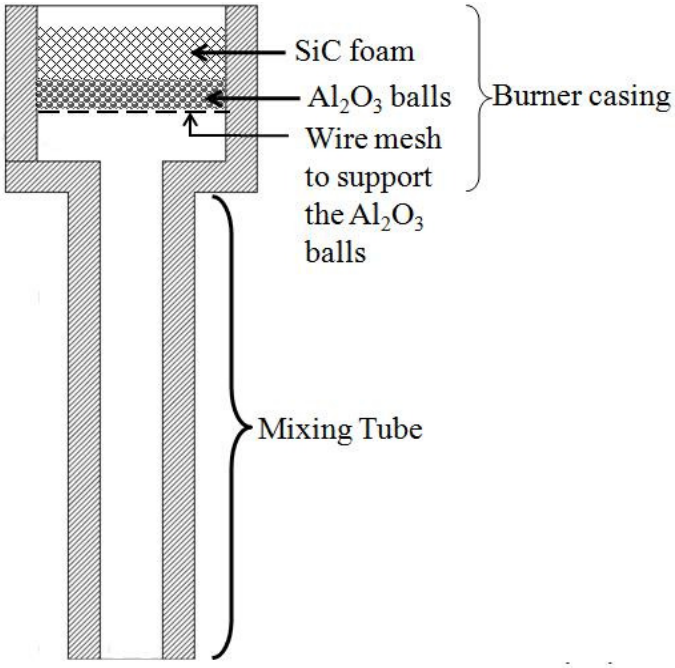

Fig. 4.4 Schematic of the porous burner

Table 4.1 Specifications and nomenclature of different experimental burners

Specifications, cm	**Burner type**				
	B6	**B7**	**B8**	**B9**	**B10**
Burner casing inside diameter	6	7	8	9	10
Burner casing height	5	5	5	5	5
Mixing tube inside diameter	2	2	2	2	2
Mixing tube length	11	11	11	11	11
Wall thickness	1	1	4	4	4
Thickness of combustion zone	1.5	1.5	2	2	2
Thickness of preheating zone	1.2 - 1.5	1.2 - 1.5	1.2 - 1.5	1.2 - 1.5	1.2 - 1.5

4.1.3 Temperature measurement

The temperature at different locations within the burner was recorded using the specially made metal sheathed K - type thermocouples. Two types of thermocouples; one has grounded junction, for CZ, and the other with exposed junction, for PZ illustrated in *Fig. 4.5* and *Fig.*

4.6, respectively were used. The output of the thermocouples was acquired directly to the personal computer through a data acquisition unit (DAQ1), which converts the thermocouple electrical output and into corresponding temperature. All thermocouples are calibrated using standard procedures.

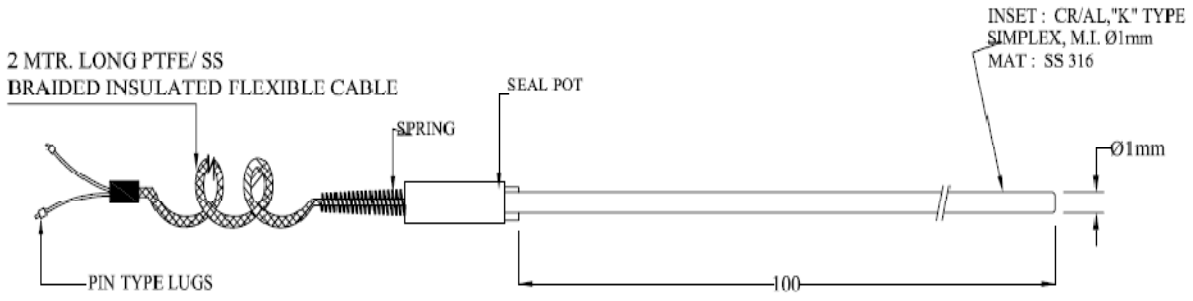

Fig. 4.5 Specifications of the metal sheathed grounded K- type thermocouple (all dimensions are in mm)

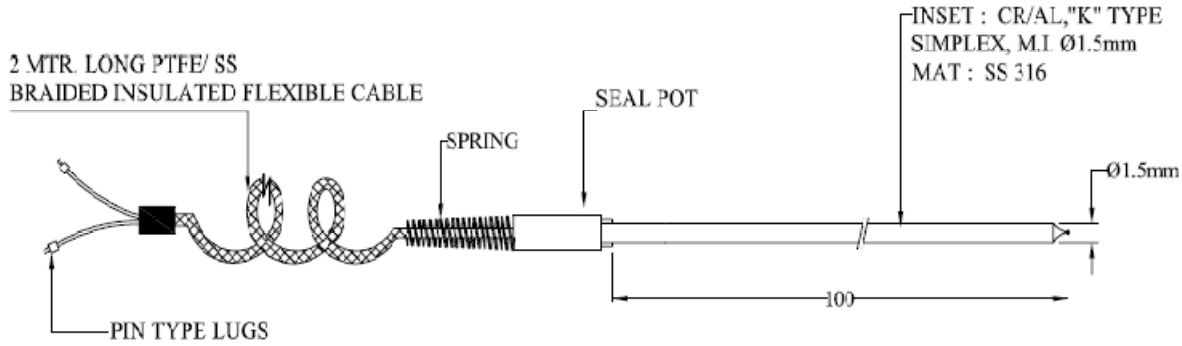

Fig. 4.6 Specifications of the metal sheathed exposed K- type thermocouple (all dimensions are in mm)

The positions of the thermocouples along with their nomenclature are shown in the *Fig. 4.7*. In the nomenclature, 'T' stands for temperature, the second letter stands for the position in the burner (C - combustion zone, I - interface of two zones, P - preheating zone and D - down the wire mesh) and the numerical number stands for the serial numbers of the thermocouples.

In fact to ensure the uniformity of temperature in the burner another four thermocouples were placed on the same plane opposite to that of shown in *Fig. 4.7*.

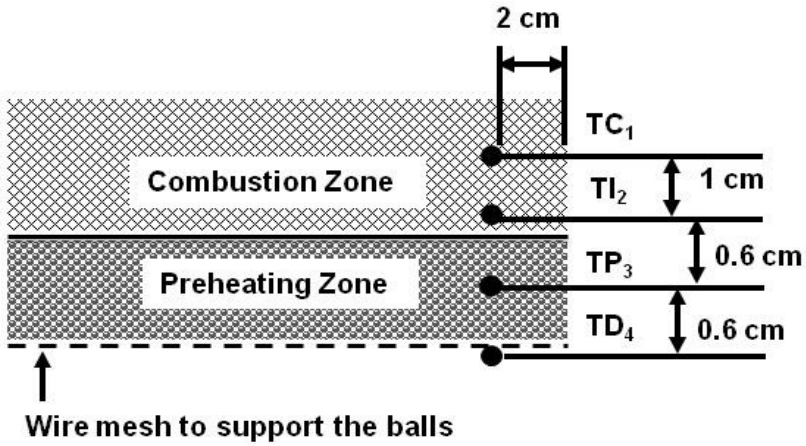

Fig. 4.7 Position of thermocouples within the burner B6

4.1.4 Start up procedure

The start up of the burner should be followed in a specified manner. Initially the burner was started at high equivalence ratio for a specified wattage and then gradually increased the air flow rate to achieve a specified equivalence ratio. Once the burner stabilizes, then the equivalence ratio can be increased or decreased for that particular wattage.

As per the domestic cooking demand, the experiments were conducted at different power ranges (0.5 to 2 kW) and equivalence ratios. The ratio of air furl ratio (AFR) at stochiometric condition to actual AFR is equivalence ratio (Φ). The formula for the same is given by:

$$\Phi = AFR_{Stioch} / AFR_{actual} \qquad (4.1)$$

The equivalence ratio (Φ) is a measure of how far the actual mixture is from the stoichiometry. Φ = 1.0 means the mixture is at stoichiometry. For rich mixtures Φ is greater than 1 and lean mixtures Φ is less than 1.

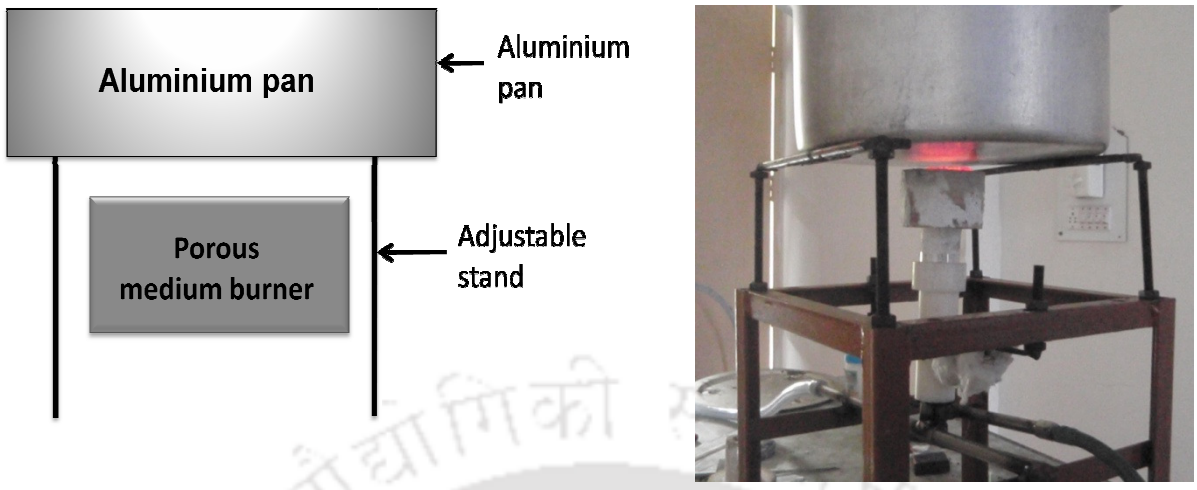

(a) (b)

Fig. 4.8 Schematic and photo showing the arrangement of aluminium pan above PMB for B6 and B7 burners

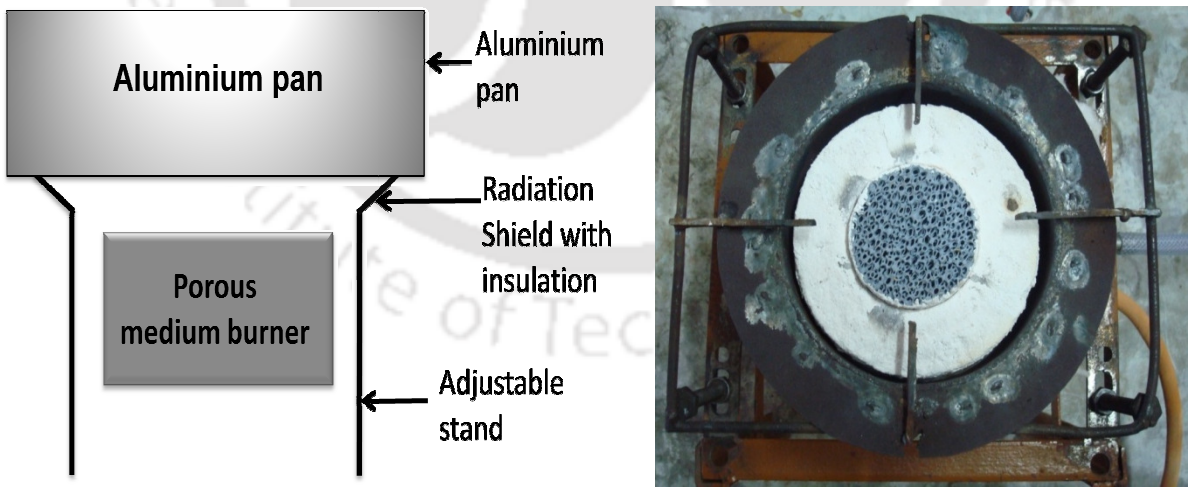

(a) (b)

Fig. 4.9 Schematic and photo showing the arrangement of aluminium pan above PMB for B8 and B9 burners

The CO and NO_x emissions were measured using the TESTO 350 XL portable flue gas analyser. The sampling was done as suggested in the Bureau of Indian standard, IS: 4246:2002. The thermal efficiencies of the LPG cooking stoves were determined according to Indian Standards (IS) 4246:2002. The procedure is discussed already in Section 3.1. The aluminum pan used for water boiling test was having the dimensions of 270 mm diameter and 140 mm height. The arrangement of the aluminum pan above the burner for the burner B6 and B7 is illustrated in *Fig. 4.8*. For the rest of the burners (B8 to B10), the arrangement is shown in *Fig. 4.9*. The uncertainty analysis was carried out by considering the inaccuracies in the mass and temperature measurements. A maximum value of uncertainty in thermal efficiency calculation was found to be ± 2.8%.

4.2 RESULTS AND DISCUSSIONS

In this section, emission characteristics and thermal efficiencies of PMBs at different power and equivalence ratios are discussed. Temperature variations at different locations of the burner are presented.

4.2.1 Temperature Distribution

Fig. 4.10 shows the temperature distribution within the burner at 1.11 kW and $\Phi = 0.54$. It is observed that the temperature at point TI_2 is higher than the other regions of the burner, i.e., the reaction zone was situated at the interface of PZ and CZ. *Fig. 4.11* shows that the temperatures at TD_4 measured for different powers and equivalence ratios were well below 100 °C and in the PZ (TP_3), the measured temperature was around 600 °C which was almost constant at all conditions. Thus there was no continuous rise in the preheating temperature of

the incoming air-fuel mixture with the increase in power. This assures the no flash back condition as the burner runs nearly with constant flame velocity.

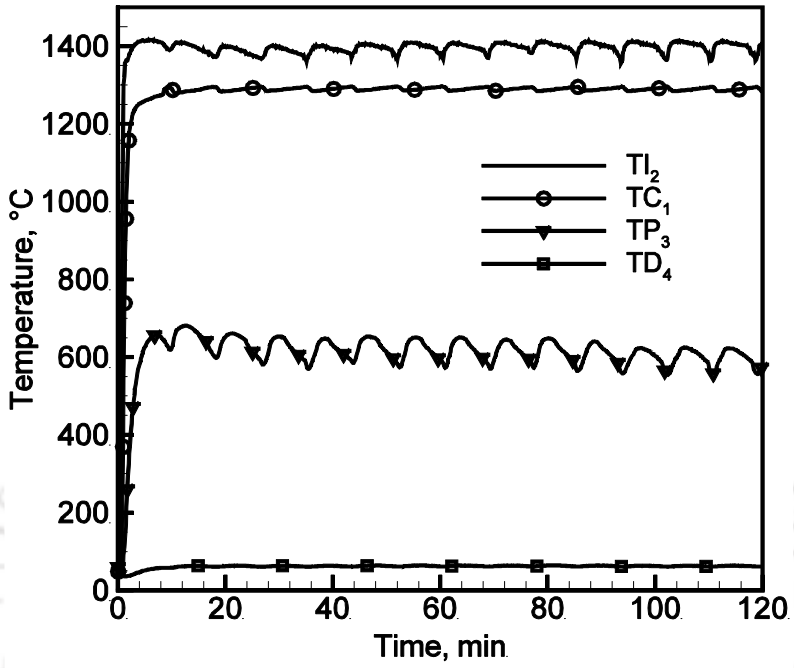

Fig. 4.10 Temperature distribution of B6 burner showing the position of reaction zone at 1.11 kW and Φ = 0.54

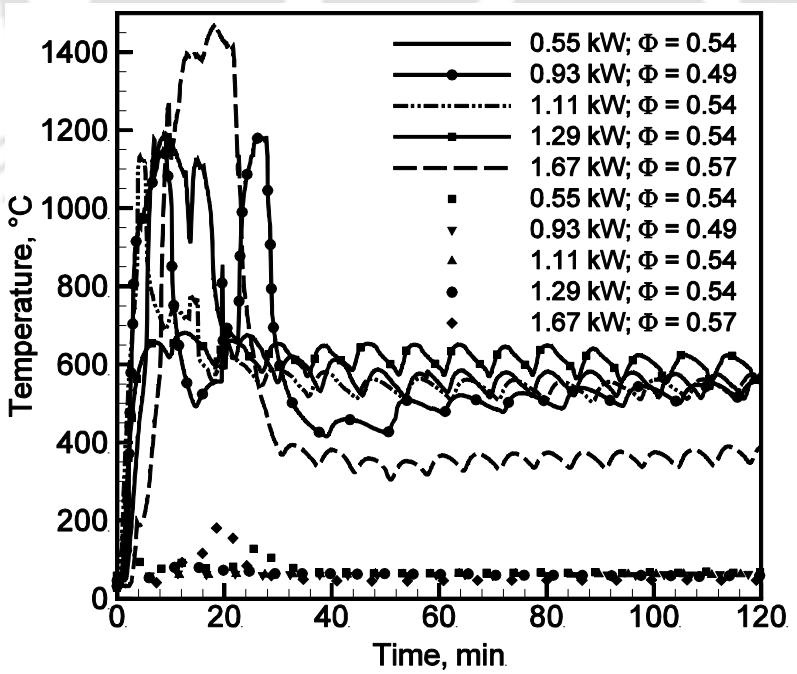

Fig. 4.11 Temperature distribution showing no flash back conditions of B6 burner (lines: TP_3 symbols: TD_4)

It is well known that the continuous increase in temperature of the incoming air fuel mixture raises the flame velocity gradually and makes the burner prone to flash back condition once the flame velocity reaches beyond the flow velocity of the incoming air fuel mixture [Takeno and Murayama 1986; Mital *et al.*, 1997 Koester *et al.,* 1994]. Thus, the constant temperature in the PZ assures the no flash back condition. This happens only when the heat from the preheating zone is completely carried away by the incoming air fuel mixture which attribute to the proper air fuel mixture distribution and the optimised thickness of the preheating zone. The temperature in PZ was few degrees above and below the ignition temperature of the LPG (580 °C). This preheating helps in reducing the NO_x by avoiding a sudden rise in the temperature and also assures the enough radiation effect from the CZ.

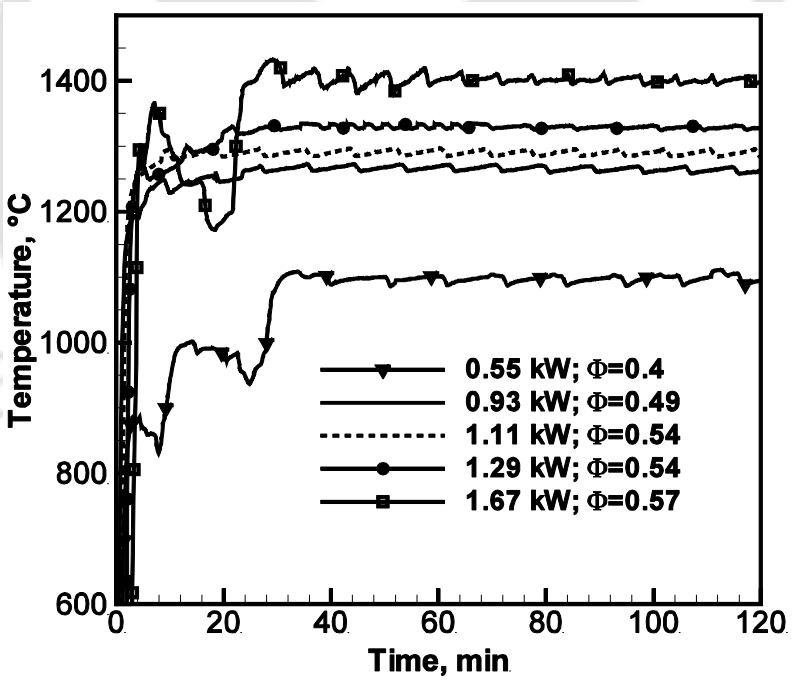

Fig. 4.12 Temperature distribution of B6 burner at TC_1 for different equivalence ratios and wattages

The movement of reaction zone from the interface to the downstream of the burner was observed when the wattage was increased to 1.67 kW. From *Fig. 4.12*, it was observed that at

1.67 kW and Φ = 0.57, the temperature of TC_1 was higher than all other wattages. At the same time, TI_2 was recorded lower than TC_1 (*Fig. 4.13*) which was unlike in the case of other wattages. This is mainly due to the movement of the reaction zone towards the downstream of the burner which was observed by other researchers also [Sathe *et al.*, 1990; Leonardi *et al.*, 2003].

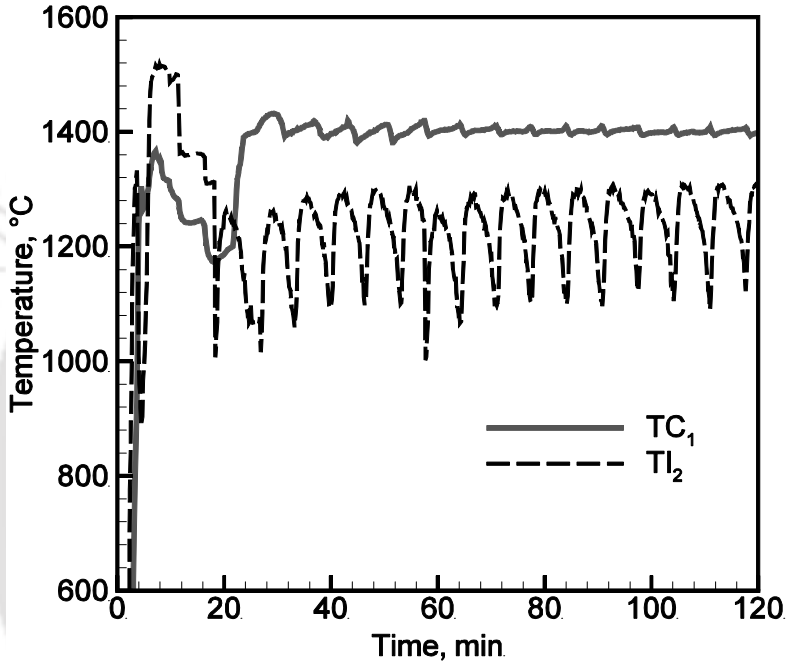

Fig. 4.13 Temperature distribution of B6 burner at 1.67 kW

The same was also attributed to the fact that the temperature in the PZ was started to reduce from 1.67 kW as shown in the *Fig. 4.11*. From *Fig. 4.12*, considering the sequential temperature distribution at point TC_1, the process of flame stabilization takes about 10 - 30 minutes for the range of 0.93 - 1.67 kW. The cyclic behavior at TI_2 in *Fig. 4.13* can be interpreted as the temperature variations due to the movement of the reaction zone not too far from the previous position. Nevertheless this behavior is not progressed to the downstream (TC_1) of the burner. This kind of cyclic behavior was not seen at TC_1 below 1.67 kW.

To study the temperature uniformity on the surface of the PMB, temperatures were recorded at different radial positions on the surface of the porous matrix. The position and nomenclature of the thermocouples are shown in *Fig. 4.14*. *Fig. 4.15* shows the temperature profiles recorded at different power and equivalence ratios on the surface of the burner. It was observed that the temperatures measured at various locations of PMB surface were almost uniform indicating the existence of uniform combustion. At the lowest power, the difference was little high due to very low flow rates which did not allow a uniform distribution of heat.

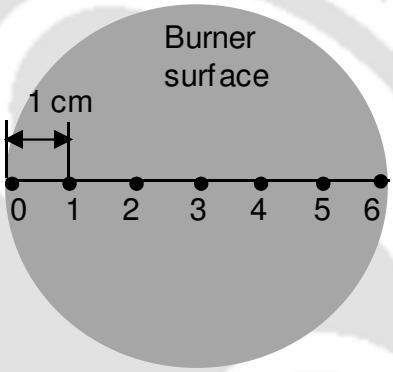

Fig. 4.14 Position of thermocouples on the surface of B6 PMB

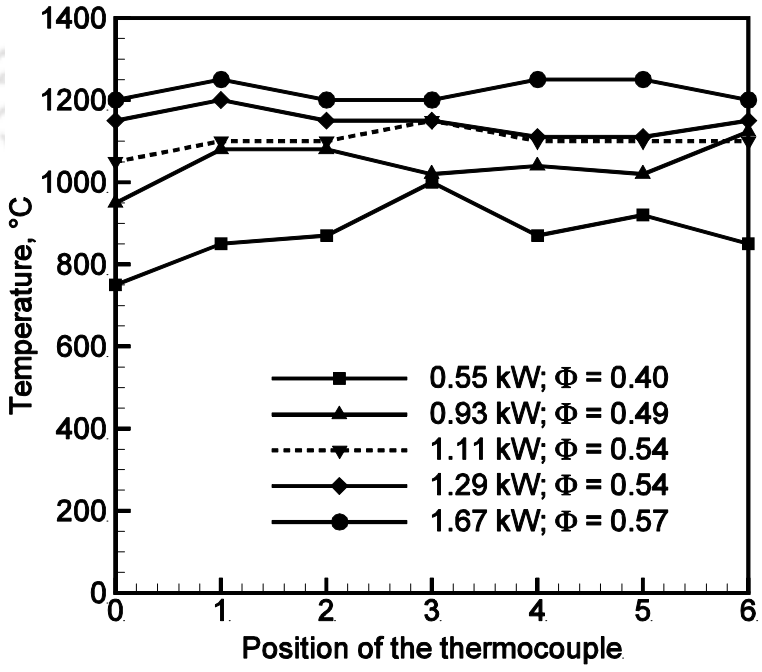

Fig. 4.15 Temperature profile on the surface of B6 PMB

The temperature distribution within and above the burner gave a depiction of the combustion behavior and the heat distribution within and on the surface of the burner. Similar thickness of CZ and PZ of the B6 burner is maintained for the rest of the burners, i.e., for B7, B8, B9 and B10. In the following paragraphs, results of the effects of the burner dimensions on the emission characteristics and thermal efficiency of different PMBs at different power and equivalence ratios are presented.

4.2.2 Emission characteristics

The measured values of CO and NO_x emissions of the domestic cooking burner are in the range of 90 - 1050 mg/m^3 and 162 - 216 mg/m^3, respectively. *Fig. 4.16* shows the effects of the equivalence ratio and power on the CO and NO_x emissions for B6 burner. It is observed that the NO_x emissions were varied from 0 - 30 mg/m^3 which are well below the range of conventional cooking burner (162 - 216 mg/m^3). However, the CO emissions were marginally higher than lower CO emission limits of the conventional burner (90 mg/m^3). In the case of B7, the CO emissions reached below the lower limit of the domestic burner (shown in *Fig. 4.17*). But in the case of B8 burner, as illustrated in *Fig. 4.18*, the CO emissions are found to be high in comparison with B6 and B7 burners. Further, it is observed from *Fig. 4.19* that the emission levels of B9 burner were in the range of B6 and B7 burners. Higher CO levels of B8 burner is due to large gap between the porous matrix and the burner casing inside wall which lead to the escape of the un-burnt fuel, and thereby, resulting in higher CO emissions. A gap between the porous matrix and the burner casing inside wall is unavoidable due to the complexity involved in making the SiC foam in perfect round shape. Due to the same reason, unlike the conventional burner, the CO emissions of all the PMBs are found to increase with the decrease in the equivalence ratio. This observation is also

attributed to the fact that the burners are operating near the temperature range of 1100 - 1400 °C where the CO and NO_X emissions are minimum [Durst *et al.,* 2002].

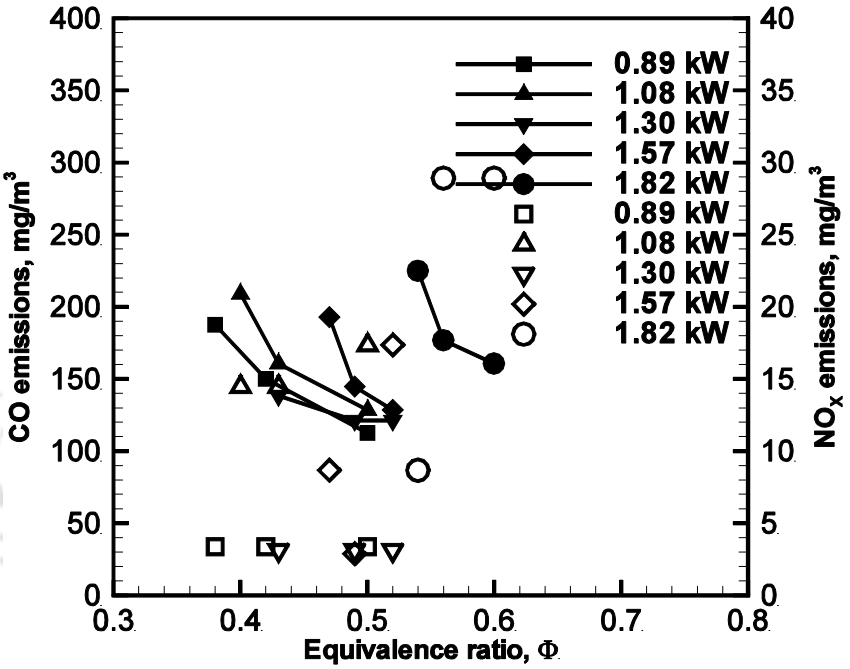

Fig. 4.16 Effect of equivalence ratio on emissions characteristics at different wattages of B6 burner (solid lines: CO emissions and symbols: NO_X emissions)

The above points conclude that the gap between the porous burner and the inside wall of the burner casing is the primary source of high CO emissions in comparison with the lower limit of the conventional burner. In the case of B10 burner, the distribution of the fuel air mixture itself became difficult and this caused the formation of visible hot spots on the burner surface which in turn lead to a steep rise in the CO and NO_x emissions. From Figs 4.16 to 4.19, it is observed that the effect of equivalence ratio on thermal efficiency and emission characteristics is prominent than that of power.

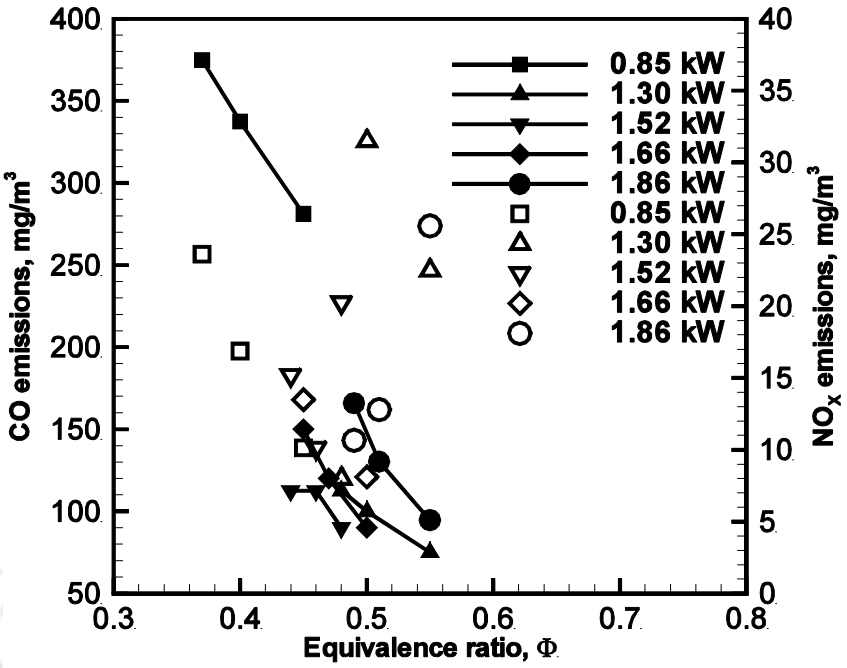

Fig. 4.17 Effect of equivalence ratio on emissions characteristics at different wattages of B7 burner (solid lines: CO emissions and symbols: NO_X emissions)

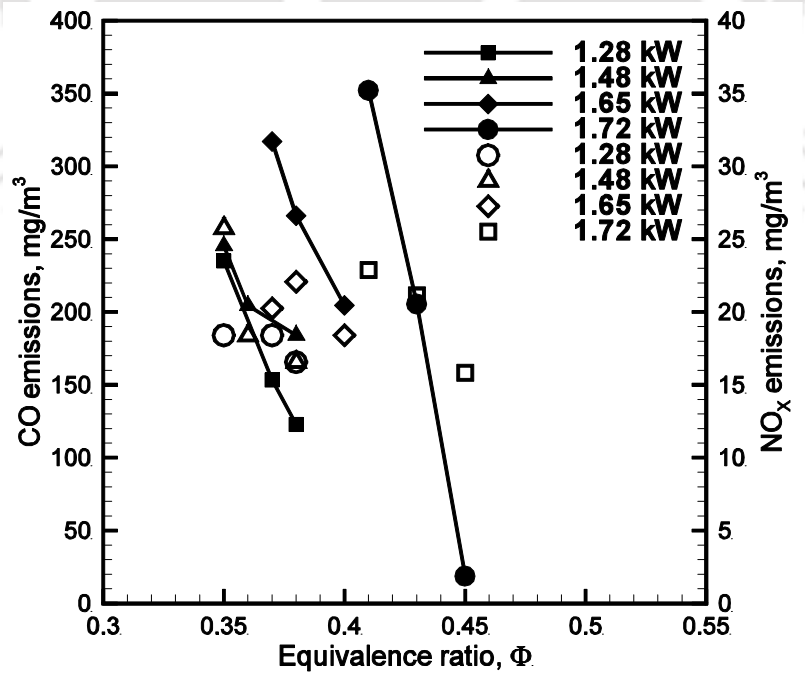

Fig. 4.18 Effect of equivalence ratio on emissions characteristics at different wattages of B8 burner (solid lines: CO emissions and symbols: NO_X emissions)

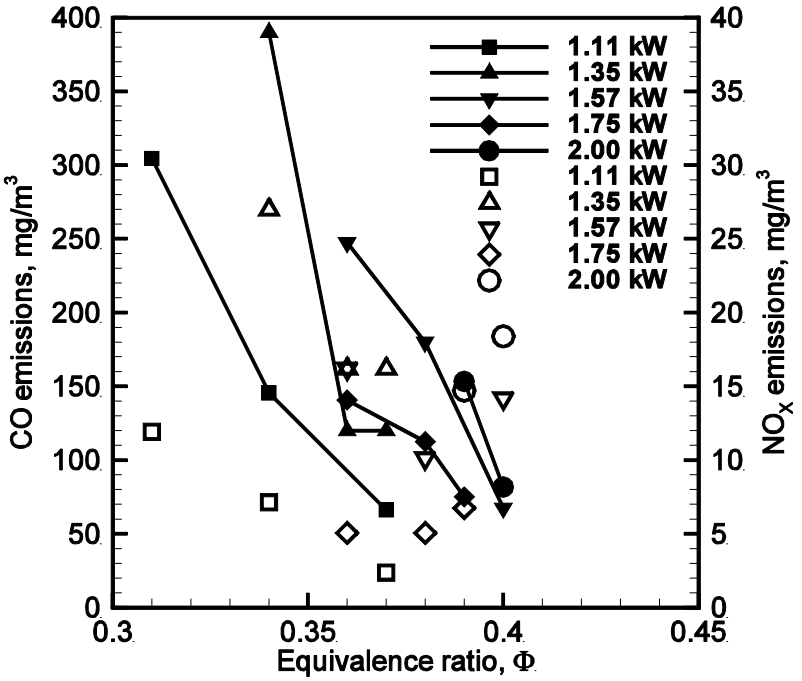

Fig. 4.19 Effect of equivalence ratio on emissions characteristics at different wattages of B9 burner (solid lines: CO emissions and symbols: NO_X emissions)

4.2.3 Thermal efficiency characteristics

The measured thermal efficiencies of the domestic cooking burners were in the range of 60 - 65%. It is observed from *Fig. 4.20* and *Fig. 4.21* that the thermal efficiencies of B6 and B7 burners, respectively, were approached close to the domestic cooking burner. In case of B8 and B9 burners, illustrated in *Fig. 4.22* and *Fig. 4.23,* respectively, the thermal efficiency reached 68% which is 3% higher than the conventional cooking burner. The increase in thermal efficiency is mainly due to the increase in effective heating area of the aluminum pan and also due to the arrangement of aluminum pan above the surface of the burner. For B8 and B9, the arrangement of the aluminum pan above the burner was modified as illustrated in *Fig. 4.9*. The radiation shield traps the radiation heat and directs to the vessel. It is also observed that the increase of burner diameter beyond 90 mm results in lowering the thermal efficiency due to higher heat loss (*Fig. 4.23*). Hence, one can conclude that there exists an optimum

burner diameter beyond which the increase of diameter will not help in achieving the higher thermal efficiencies.

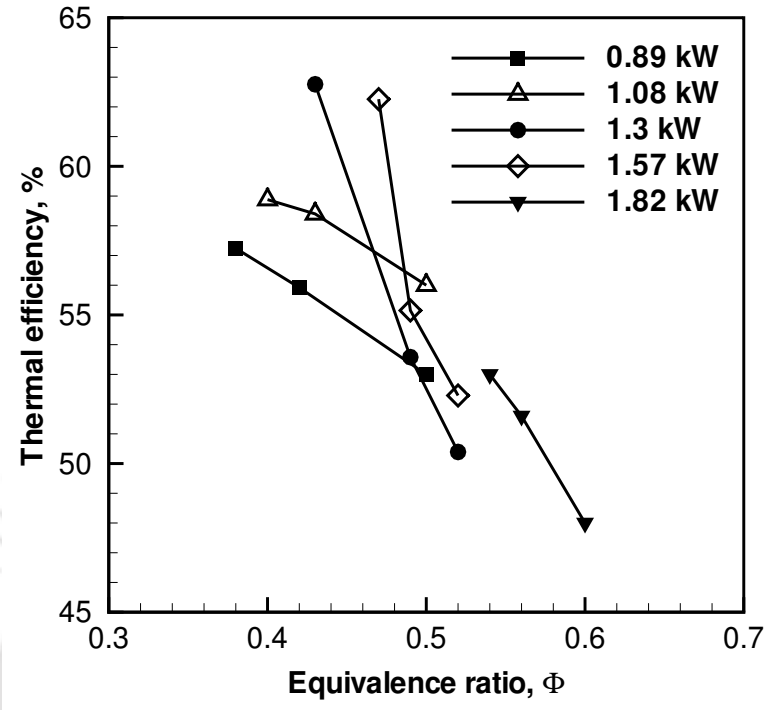

Fig. 4.20 Effect of equivalence ratio on thermal efficiency characteristics at different wattages of B6 burner

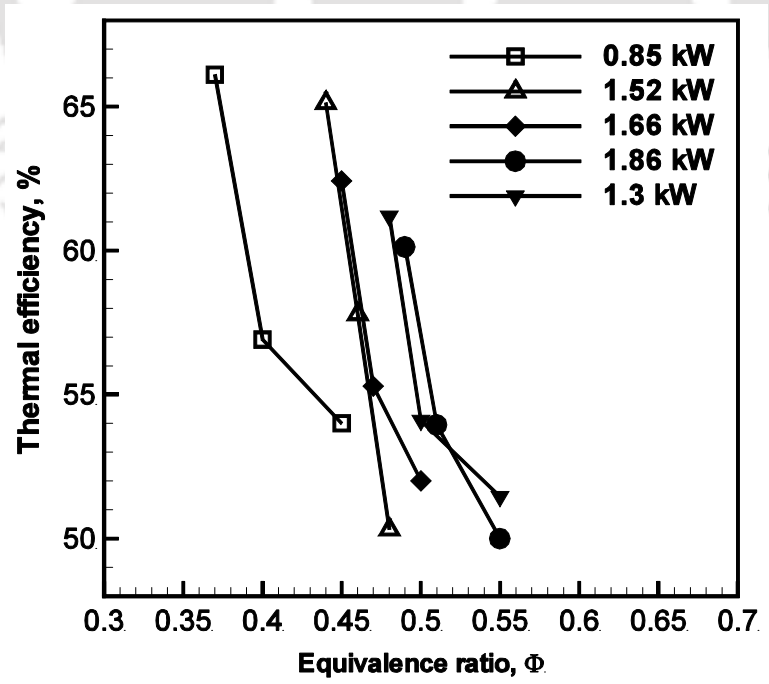

Fig. 4.21 Effect of equivalence ratio on thermal efficiency characteristics at different wattages of B7 burner

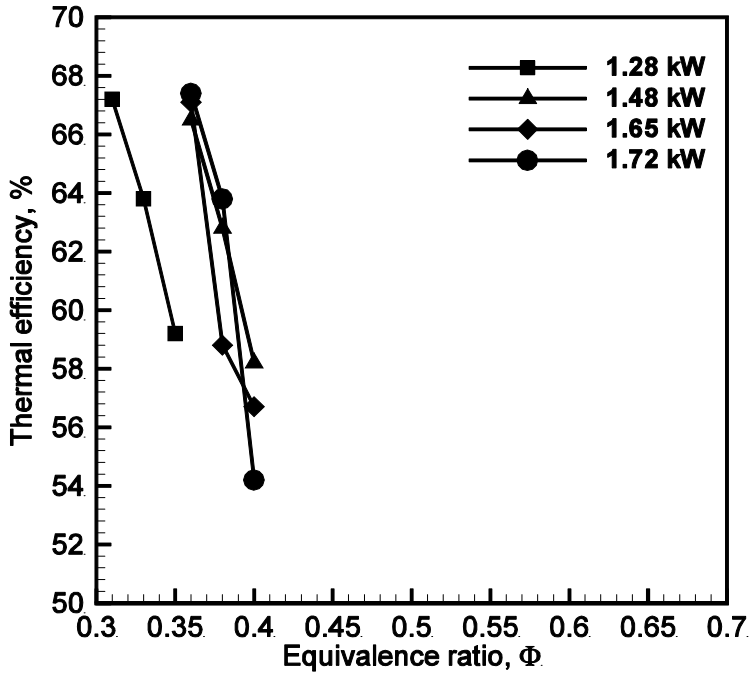

Fig. 4.22 Effect of equivalence ratio on thermal efficiency characteristics at different wattages of B8 burner

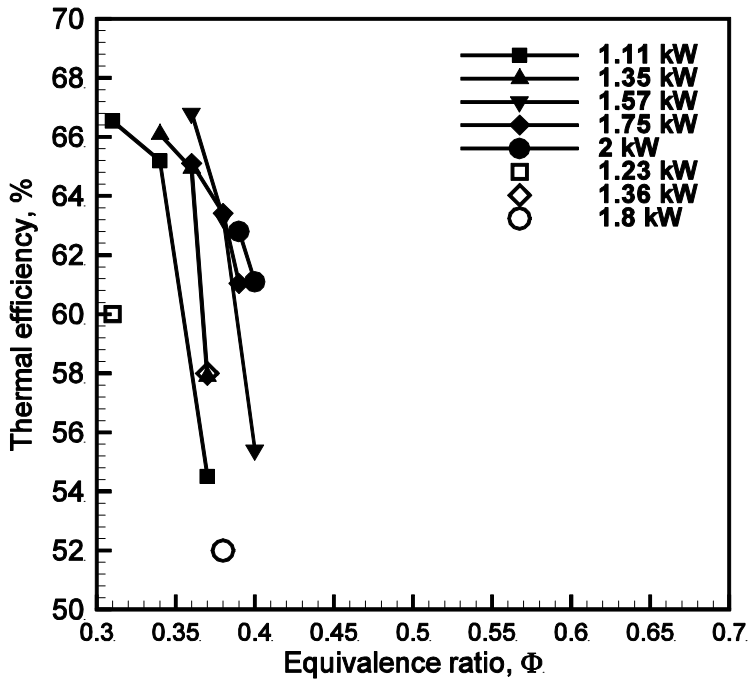

Fig. 4.23 Effect of equivalence ratio on thermal efficiency characteristics at different wattages of B9and B10 burners (lines: B9; symbols without filling: B10)

From the experimental investigations, it was observed that at any given wattage, thermal efficiencies of all the burners were found to decrease with the increase in the equivalence ratio. The reason for lower thermal efficiencies at higher equivalence ratios are due to the increase in radiation output [Leonardi *et al.*, 2003; Barra and Ellezy, 2004] which in turn increases the radiation heat loss. The higher radiation output is not always desirable and depends on the application. It is expected that still a higher value of thermal efficiency may be achieved if the radiation heat loss can be minimized by providing a proper radiation shield around the burner. It is always better to have a radiation heat trap capability on the vessel side used for cooking.

4.2.4 Effect of air fuel distribution

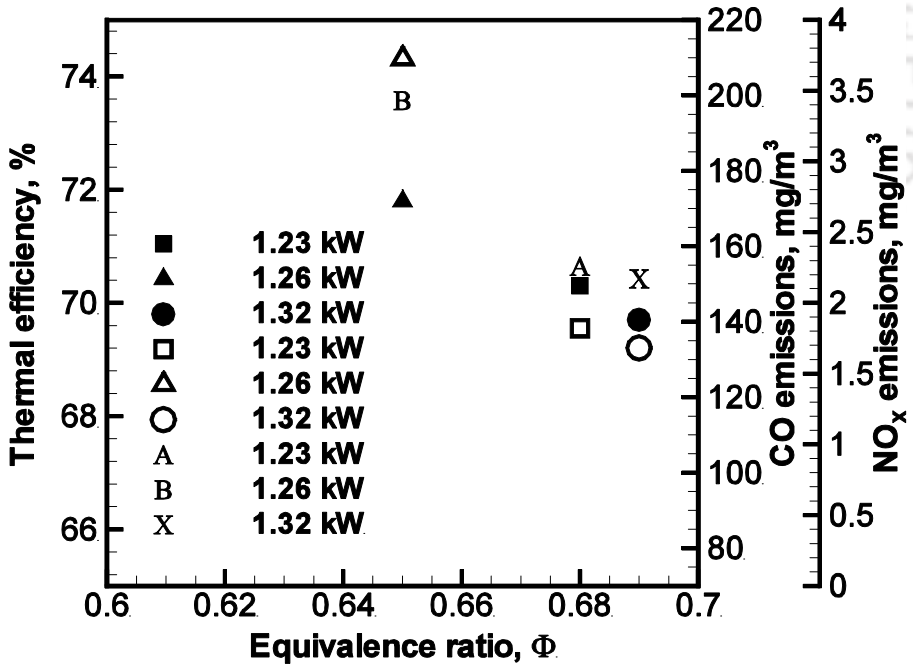

Fig. 4.24 Effect of equivalence ratio on thermal efficiency, and CO and NOX emissions (symbols with fillings: thermal efficiency; symbols without fillings: CO emissions and alphabetical: NO_X emissions)

Based on the above experimental results, B8 burner is considered as an optimised burner for further study. In the process of making the temperature more uniform on the burner surface, the mass flow rate of the air fuel mixture was reduced in the middle of the burner by providing two extra layers of wire mesh below the existing one which can increase the resistance to the flow of air fuel mixture. The diameters of the wire meshes were kept at 20 mm and 40 mm. The measured thermal efficiency and emissions characteristics are shown in *Fig. 4.24*. The CO emissions and thermal efficiency of the B8 increased with decrease in equivalence ratio. The CO emissions were still on the higher side of the lower limit of the conventional domestic burner. However, the thermal efficiency rose up to 72% which is 7% higher than the conventional domestic burner. Apart from the higher thermal efficiency, the burner was able to run at high equivalence ratios. To understand the actual behaviour of the burner the current data is insufficient and further experiments need to be carried out.

Chapter 5

THIRD PHASE DEVELOPMENTS

This Chapter presents the performance investigations of a newly developed combinational burner (CB - combination of porous surface and porous medium burner). In this case, a porous matrix (PM) was placed at a distance from the surface of porous surface burner (PSB). The effect of the distance between the PM and the PSB on emissions is presented at different equivalence ratios and powers. The thermal efficiency along with the temperature distribution at different possible operating range of power and equivalence ratio is also discussed.

5.1 INTRODUCTION

There are only two main porous radiant burner technologies currently available viz; PMC and PSC. The concepts of PMC and PSC are explained in Section 2.3. The pore sizes of PMB's are relatively large (2 - 3 mm), which makes it possible for the flame to propagate and stabilize within the porous medium. The main advantages of this type of burner are: high radiant efficiency, low emissions and high power density. However, in this type, the flame stabilization is little difficult as the adiabatic burning velocity may increase by a factor in the order of 10 relative to the free burning velocity due to an increase in upstream energy transport [Bouma and De Goey, 1999]. The radiation output from these burners is around 50% and in the previous case, it reaches to a maximum of 25%. The combustion process in a PSB is more stable than the combustion within a porous medium [Bouma and De Goey, 1999]. The decreasing thermal efficiency due to the increasing radiation output (high radiant heat loss) is already explained in Section 4.2.3. The PSB [Bouma and Goey, 1999] cannot be

applied directly for domestic application due to the high emission levels. The basic aspects of the PMB and PSB are compared in *Table 5.1*.

Hence, an effort has been made to develop a new burner featuring medium power radiant output and low emissions for domestic cooking applications. The newly developed burner has been named as a "*combinational burner*". The experiments on this burner were performed at FMP Technology GmbH, Erlangen, Germany under the supervision of Prof. Dr. Dr. h. c. F. Durst.

Table 5.1 Comparison of a PMB and a PSB

Burner type	Power Density	Lowest possible emissions, ppm		Equivalence ratio, Φ	Low calorific fuel
		CO	NO_x		
PMB	Very high (≈3MW/m^2)	2	0.1	0.01	Applicable
PSB	Low (≈400kW/m^2)	25	1	0.9	---

5.2 EXPERIMENTAL PROCEDURE AND SET-UP

An experimental set-up developed to study the performance of a CB is shown in Fig. 5.1.a. Fig 5.1.b shows the photographic view of the same. Propane was used as a fuel due to the availability. Its calorific value (46364.62 kJ/kg) is almost equivalent to the LPG (45636.12 kJ/kg). In the experimental set up, propane was supplied (make: PROGAS) through the mass flow meter (make: AALBORG, Germany) to the burner. Air was supplied through the mass flow controller (MFC), manufactured by BÜRKERT, Germany. For the specific gas, both the flow measurement devices were pre-calibrated by the manufacturers. Both propane and air was introduced in the mixing tube to ensure a better mixing of the air fuel mixture before combustion. The flow rates were displayed on the computer through data acquisition unit. Air flow rate was controlled through the computer while the fuel flow was adjusted manually.

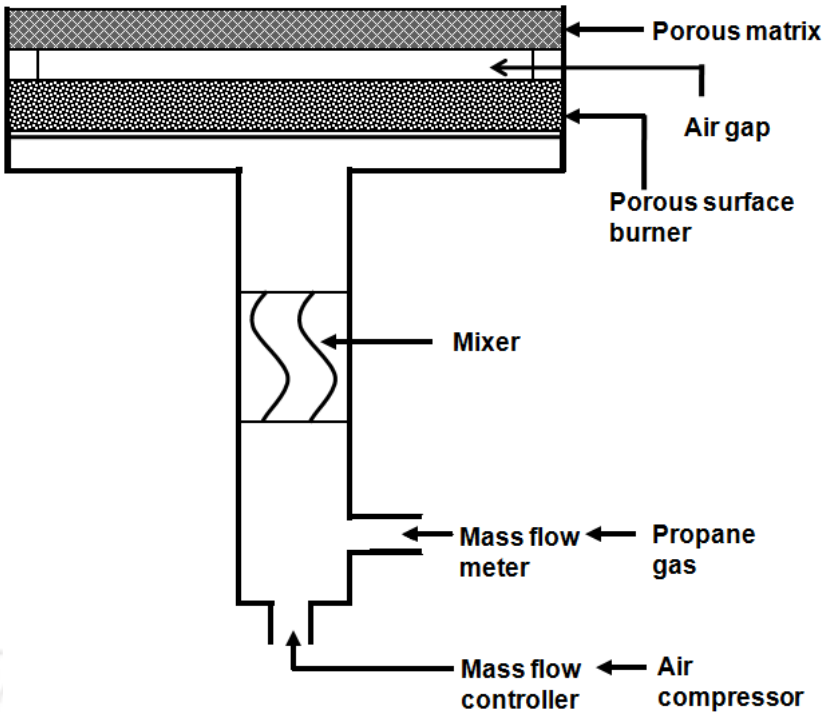

a. Schematic diagram of the combinational burner experimental set up

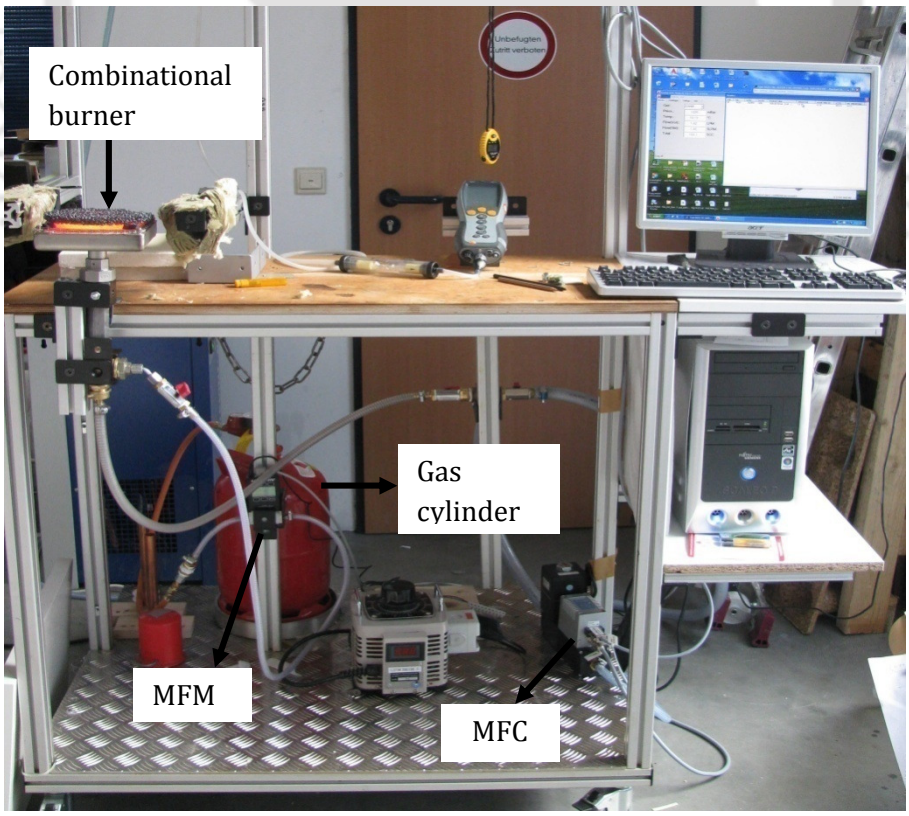

b. Photographic view of the experimental set up

Fig. 5.1 Schematic diagram and Photographic view of the CB experimental set up

5.2.1 PSB and Materials

The dimension of the PSB used was 145×145 mm^2 with pores of 0.5 mm diameter. This burner was produced by ECO Ceramics, Netherlands. The PM used above the surface burner was made of silicon carbide of 10 ppi with a pore size of 5 mm.

5.2.2 Temperature and emissions measurement

Temperatures were measured in the centre of the burner at different heights using metal sheathed K- type thermocouples. The positions of the thermocouples are shown in Fig. 5.2. The temperature distributions within the burner for power range of 2 - 3kW were presented at the three different equivalence ratios of 0.83, 0.76 and 0.71. The CO and NO_x emissions were measured using the TESTO 330 portable flue gas analyser. The sampling was done at a height of 50 cm from the burner with a metal sheet ring around the burner to avoid any intrusion of atmospheric air. The height of 50 cm was considered as the breathing height of a person from the domestic cooking burner in a squatting posture [Kandpal *et al.*, 1995]. The thermal efficiency of the burner was estimated by conducting the water boiling test as described in section 3.1.

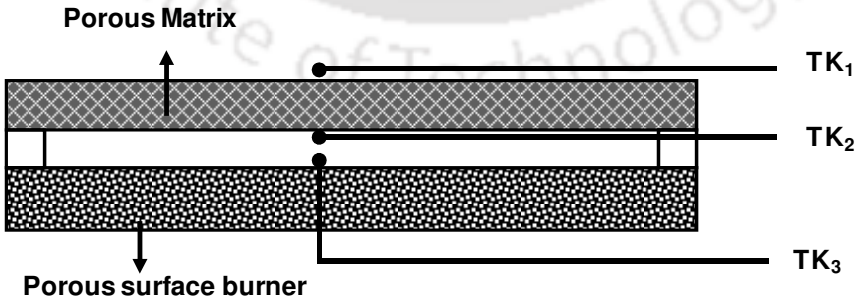

Fig. 5.2 Position of the thermocouples in CB for recording the temperature distribution

5.3 RESULTS AND DISCUSSIONS

In this Section, the emission characteristics and thermal efficiencies of the burner at different equivalence ratios and powers are discussed along with the temperature distribution of the burner.

5.3.1 Emission characteristics

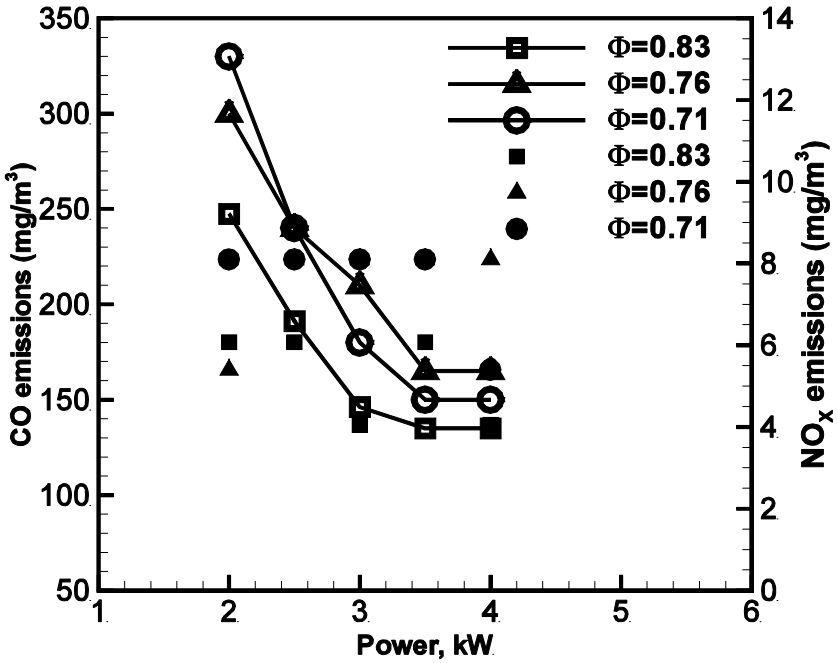

Fig. 5.3 Emissions levels from the surface burner (solid lines: CO; symbols: NO_X)

Initially, the porous surface burner was tested without any porous matrix. The results of the emissions are presented in *Fig. 5.3*. The CO emission levels of the PSB for low power were high and hence, these burners are not recommended in the present form for domestic applications. Unlike the PSB [Bouma and De Goey, 1999], the experimental porous surface burner's (newly developed) CO emissions increase with decrease in wattage. This is mainly due to the improper temperature distribution (formation of cold spots) over the large surface

area (145x145mm^2). Even if the temperature distribution is good enough, the emissions will raise with wattage drastically. However, the higher emissions levels will be expected beyond the applicable limits of the domestic applications [Bouma and De Goey, 1999]. In case of Bouma and Goey [1999], the increase in emissions is mainly due to the less residence time of the combustion gases.

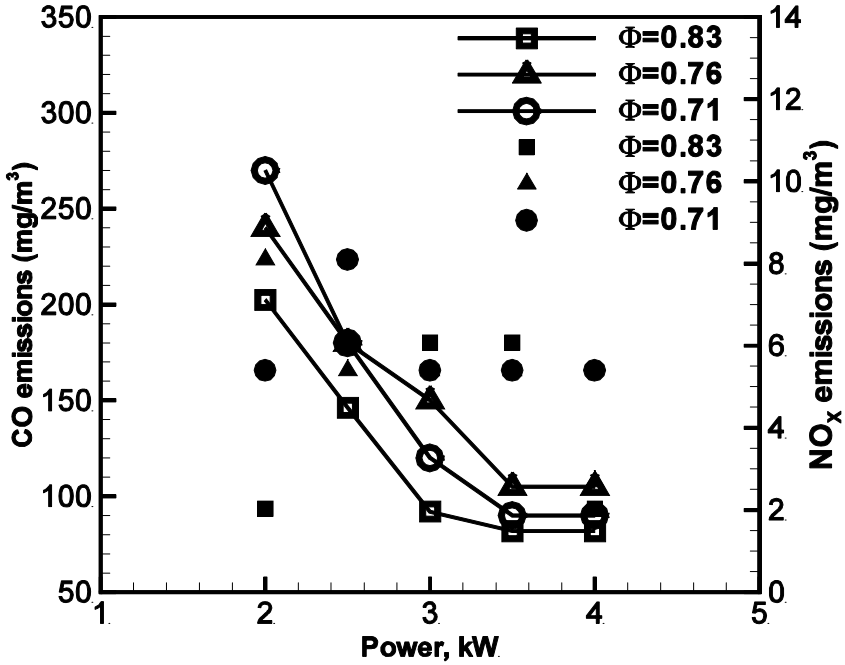

Fig. 5.4 Emissions from the Combinational burner when the PM is at 4mm distance

During the experimental studies, the porous matrix was placed at a distance of 4 mm above the surface burner, and then the emission readings were taken. The results are plotted in *Fig. 5.4*. As it is evident from *Figs. 5.3* and *5.4*, on the introduction of porous matrix in the system, the CO emissions levels were found to reduce. This was due to the fact that the PM allowed for proper second stage combustion with increased residence time required for the CO oxidation. In this case, the CO emission levels just reached the lower limit of the conventional domestic burner.

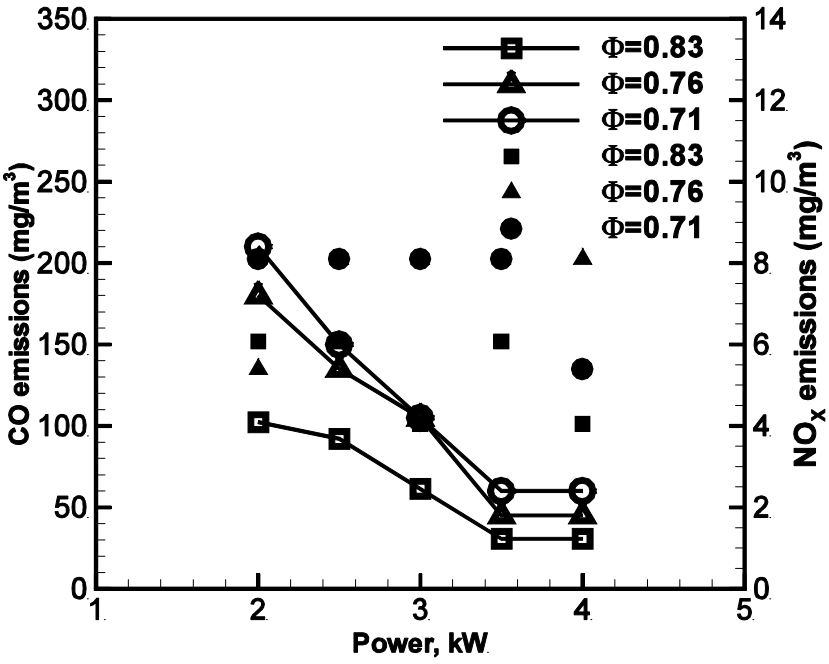

Fig. 5.5 Emissions from the Combinational burner when the PM is at 12 mm distance

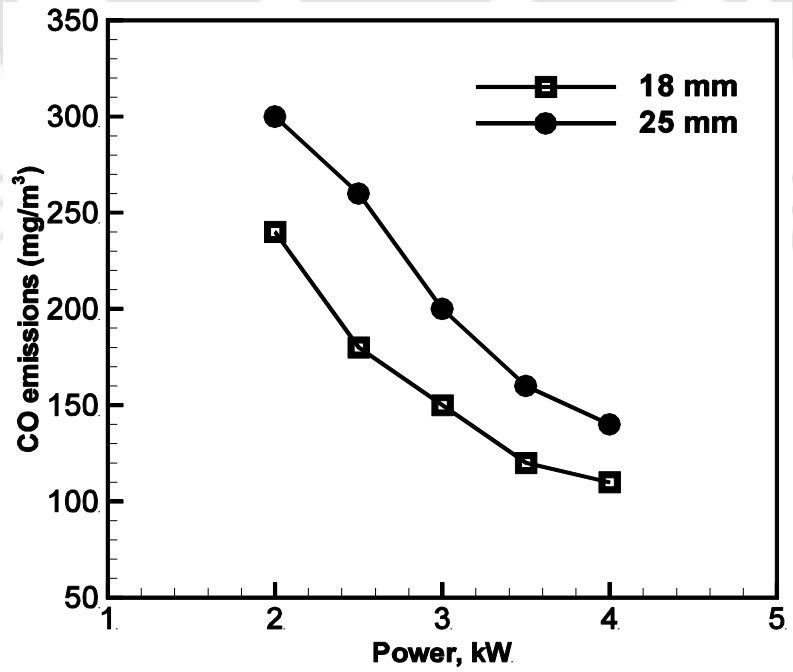

Fig. 5.6 CO emissions with the increase in height of PM on the surface of PSB at Φ = 0.71

Another set of emission readings were taken by varying the distance from 4 mm to 12 mm, which is illustrated in *Fig. 5.5*. In this arrangement, a considerable reduction in the CO emission levels was observed with further increase in the residence time. The emission levels reached below the lower limit of the conventional DB. When the distance was further increased, the CO emissions were found to increase significantly (shown *Fig. 5.6*). From Figs. 5.3 to 5.5, one can observe that the NO_x levels were reduced due to the radiative cooling of the flame from PSB with out PM and become insensitive for the power (2 - 4 kW) and also the distance between the PSB and PM.

5.3.2 Temperature distribution

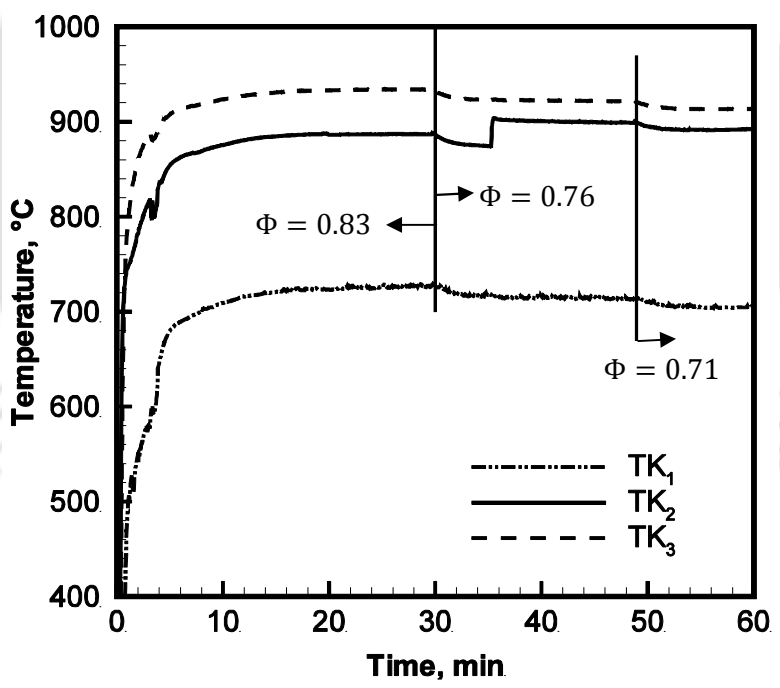

Fig. 5.7 Temperature distribution in the combinational burner at 2kW with different Φ

To further understand the combustion process within the combinational burner, the temperature distribution was recorded at different wattages. The measured temperature on the surface of the PSB was maximum 750 ℃ at 4 kW and Φ = 1.2. *Fig. 5.7* shows the temperature distributions in CB at 2 kW for different equivalence ratios. The temperature on

the surface of the PSB (TK_3) was already above 900°C and found to increase with power as shown in *Fig. 5.8*. It is observed from Figs. 5.5 and 5.6 that at a particular wattage as the Φ decreases, the surface temperature was also found to decrease. It is also observed that the CO emissions were found to increase with the decrease in Φ. The temperature difference between the points TK_2 and TK_3 was not too high even at a distance of 12 mm between the PM and PSB which was due to the back and forth radiation from the PM to the surface burner. The back radiation from the PM gradually increases with wattage and this limits the applicability range of the burner by inducing the flash back conditions.

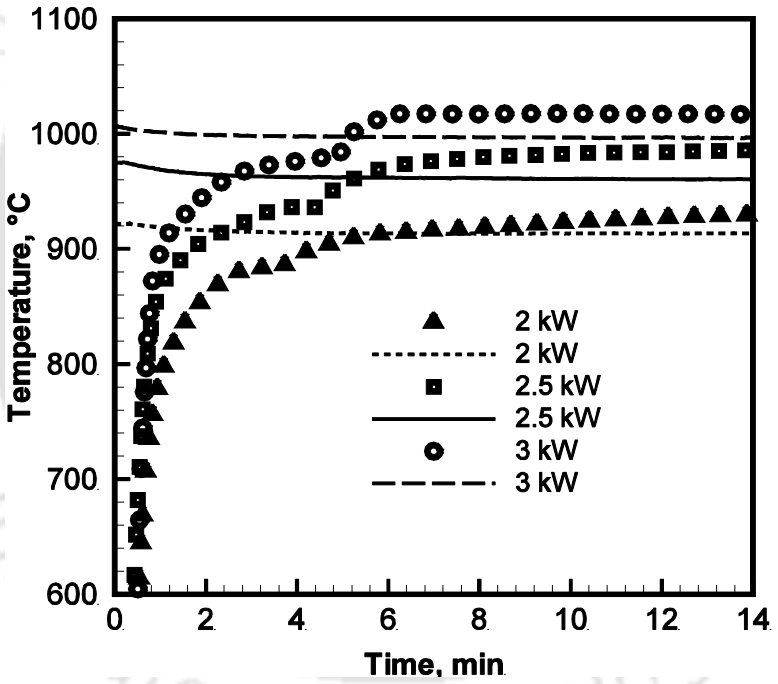

Fig. 5.8 Temperature distribution in the combinational burner at Φ = 0.83 (symbols) and 0.71 (solid lines) with different power

This is mainly due to the increased flame velocity above the air fuel mixture velocity. Generally, the flame velocity increases with the preheating of the air- fuel mixture. In the CB the increased back radiation from the PM on the PSB increases the preheating temperature of the incoming air fuel mixture with the increase in wattage which is unlike in the PSB. The

current combinational burner is able to run without any flashback conditions up to 3 kW which is the maximum wattage normally required for the domestic cooking purpose. At 3 kW, the temperature at point TK_2 and TK_3 overlapped each other due to the increased back radiation from both the surfaces as shown in *Fig. 5.9*. As illustrated in *Fig. 5.9*, the temperatures measured at the specified points for 3 kW were higher than those at 2 kW. From Figs 5.7 and 5.8, the stabilization period for CB was around 5 minutes at all conditions.

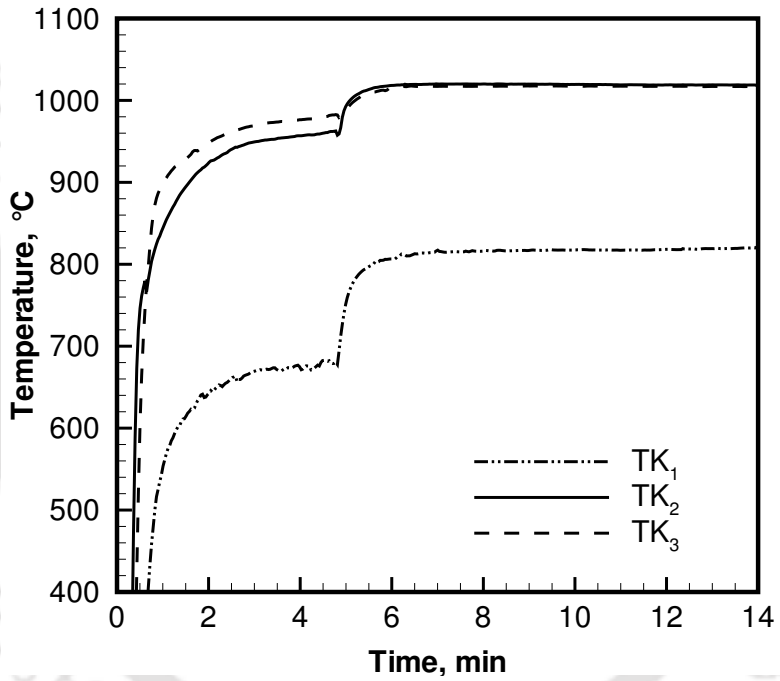

Fig. 5.9 Temperature distribution in the combinational burner at 3kW at Φ = 0.83

5.3.3 Thermal Efficiency characteristics

The efficiency of the experimental burner was estimated using the standard water boiling test. The results are illustrated in *Fig. 5.10*. As discussed in Section 3.2, the burner was tested up to the maximum possible wattage of 3 kW. The maximum efficiency achieved was around 50% which was quite low from the maximum efficiency of a conventional domestic burner (65%). The reason for a low efficiency for the combinational burner is attributed to the fact

that the burner surface area was too large in comparison to the vessel diameter which corresponds to increased radiation heat loss. The radiation output also increases with the wattage which decreases the thermal efficiency. The efficiency was found to decrease with Φ due to the high flow of flue gas which had greater possibility of wasting heat. To reduce the radiation heat losses further, the current maximum ratio of the burner surface area to the vessel bottom area should be reduced from 0.23 (145 x 145 mm^2) to 0.054 (80 x 80 mm^2).

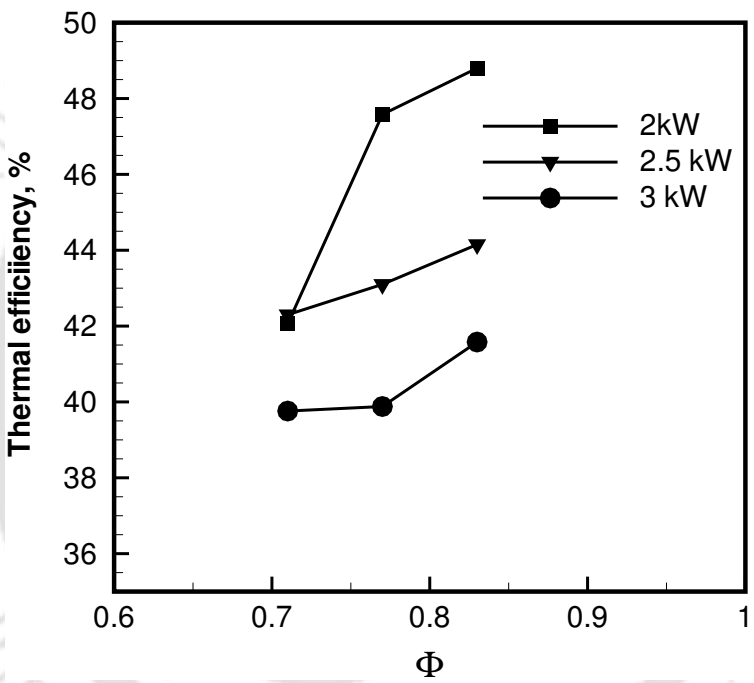

Fig. 5.10 Thermal efficiency of the combinational burner at different wattage and Φ

Chapter 6

CONCLUSIONS AND FUTURE WORK

6.1 CONCLUSIONS

This chapter presents the important conclusions obtained from the various stages of porous radiant burner developments for domestic cooking applications.

During the first phase developments, the modified conventional domestic cooking burner ascertained a path way for the application of the porous radiant burner for domestic cooking applications. The CO emissions have been reduced to 180 mg/m^3 which are still on the higher side of the lower limit of the conventional domestic burners (90 mg/m^3). The NO_X emissions have been found in the range of 150 to 270 mg/m^3 which are well below the conventional domestic cooking burner (162 - 216 mg/m^3). The modified burner (Case4) shows a maximum thermal efficiency of 73% which is about 8% higher than the domestic burner. At higher thermal efficiency, the burner was able to run in a very narrow power range of 1.5 to 1.8 kW due to the increased flame velocity than the gas mixture velocity. The experiments revealed the need for the changing of burner casing and burner materials to avoid the red hot conditions, hot spots, any flame on the surface of the burner.

During the second phase developments, the newly developed PMBs were investigated at different wattages and equivalence ratios. The effect of geometrical parameters viz. burner diameter and wall thickness of the burner casing on thermal efficiency and emission characteristics were studied. The different burners are named as B6, B7, B8, B9, and B10

based on the burner diameter in centimetres. In case of B6 and B7 burners, the CO emission was in the range of 90 mg/m^3 to 220 mg/m^3 and further brought down to 60 mg/m^3 to 300 mg/m^3 and for B8 and B9 burners, the same was lower than the range of conventional domestic cooking burner (90 mg/m^3 - 1050 mg/m^3). The NO_X levels were reduced drastically to a maximum of 30 mg/^{3} which is far from the range of the conventional domestic burner (162 - 216 mg/m^3). The thermal efficiencies of B6 and B7 burners were in the range of 50% to 65%. However B8 and B9 burners showed the thermal efficiency in the range of 54% to 68%. The highest thermal efficiency is 3% higher in comparison with the domestic cooking burner. The further modifications in B8 burner for proper temperature distribution increased the thermal efficiencies up to a maximum value of 72% which is 7% higher than the conventional burner. However, no distinguished change in the CO and NO_X emissions were observed.

Thermal efficiencies of all the burners gradually decreased with increase in the equivalence ratios which is due to increased in the radiation output (radiation heat loss) from the burner. For B10 burner, the thermal efficiency dropped to the range of 52% to 60%. The CO emissions were also found to decrease with increase in equivalence ratio which is mainly due to the gap in between the inside wall of the burner casing and the porous matrix. However, there was no significant variation in NO_x emissions with respect to equivalence ratios observed. However, the emissions for B10 burner were found to increase drastically with equivalence ratios and power due to formation of cold and hot spots (improper distribution of heat). The burners, B6 to B8, are able to operate within the equivalence ratio and power range of 0.3 - 0.5 and 0.55 - 2 kW (as per the demand), respectively. The newly developed burners are found to be safe within the specified operating limits.

The temperature distribution within the burner showed that the reaction zone was formed near to the interface of the two layers and moved to downstream of the burner with increase in wattage. The temperature profile measured on the surface of the burner shows the uniform distribution of the combustion.

During the third phase developments, a new combinational burner has been proposed for domestic cooking purpose and tested in the power range of 2 - 3 kW and equivalence ratios of 0.83, 0.76 and 0.71. In CB, the PM above PSB acts as a second stage combustor for the complete combustion with increase in residence time. The lowest possible CO emissions achieved are in the range of 200 mg/m^3 to 30 mg/m^3, when the distance between the PM and surface of PSB is 12 mm. NO_X emissions were reduced to the range of 5 mg/m^3 to 8 mg/m^3. In the CB, the CO emissions were decreased with the increase in the power and equivalence ratio.

The surface temperature of the PSB in CB has rose to above 900°C and gradually increased with the power due to the effect of the back radiation from the PM. In turn increases the preheating temperatures of air fuel mixture in the CB. The raise in temperatures of the air-fuel mixture raised the flame velocities beyond the (air-fuel) mixture velocities making the CB prone to the flash back conditions with the increase in wattage, which is in contrast with the PSB. However, within the specified range (2 - 3 kW) no flash back was observed. In fact, 3 kW is sufficient enough for cooking purpose.

The thermal efficiency of the combinational burner was reached to a maximum value of about 50% which is below in comparison with 65% of conventional domestic burner. This can be improved by reducing the dimensions of the burner. It is observed that the thermal

efficiency of the CB decreases with the increase in wattage and decrease in equivalence ratio. These results can be used as a benchmark for further developments. It is suggested that the burner's dimensions should be reduced in the interest of the end user demand for a low wattage of up to 0.5 kW and also for the possible increase of the thermal efficiency. Further, the vessel bottom should be concave with surface indentation for achieving high thermal efficiencies.

In general the results obtained confirmed that the research strategy was well conceived, thus giving a basis for further experimental and theoretical research on the optimal use of PMBs as well as the new combinational burner for cooking applications.

6.2 FUTURE WORK

The following are the scope for the future research work in the development of porous burners for domestic cooking applications.

- The PMBs need to be tested further to understand the effect of burner surface temperature distribution on the thermal efficiency of the burner.
- The present work may be extended to test the burners at higher wattage up to 10 kW for medium-scale applications.
- The combinational burner needs to be tested for reduced dimensions.
- The PMB and CB can be used for further studies with biogas and also methane combustion.

REFERENCES

Andersen F (1992), Heat transport model for fiber burners, *Prog. Energy Combust. Sci.* 18, 1-12.

Antonette D'Sa and Narasimha Murthy KV (2004), Report on the use of LPG as a domestic cooking fuel option in India, *Int. Energy Initiative*, June.

Arai N, Shinoda M and Churchill SW (1999), The characteristics of heat recirculating burner, *Trans. CSME*, 23 (1B), 147-58.

Avdic F (2004), Application of the porous medium gas combustion technique to household heating systems with additional energy sources, *Ph.D thesis*, Universität Erlangen-Nürnberg, Germany.

Babkin VS, Korzhavin AA and Bunaev VA (1991), Propagation of premixed gaseous explosion flames in porous media, *Combust. Flame*, 87, 182-90.

Baek SW (1989), The premixed flame in a radiatively active porous medium, *Combust. Sci. Technol.*, 64, 277-87.

Barra AJ, Diepvens G, Ellzey JL and Henneke MR (2003), Numerical study of the effects of material properties on flame stabilization in a porous burner, *Combust. Flame*, 134, 369-79.

Barra AJ and Ellzey JL (2004), Heat recirculation and heat transfer in porous burners, *Combust. Flame*, 137, 230-41.

Basu P, Kefa C and Jestin L (2000), Boilers and Burners: Design and Theory, Springer, New York, 563.

Bellucci V, Meili F, Paschereit OC and Schuermans B (2006), Premixburner, *United States Patent* No. 20060101825.

Bernstein MH and Churchill SW (1977), Multiple stationary states and NO_x production for turbulent flames in refractory tubes, *16th Int. Symp. on Combust., The Combust. Inst.*, 1737-45.

Bingue JP, Saveliev AV, Fridman AA, and Kennedy LA (2002), Hydrogen production in ultra-rich filtration combustion of methane and hydrogen sulfide, *Int. J. Hydrogen Energy*, 27, 643-49.

Bingue JP, Saveliev AV and Kennedy LA (2004), Optimization of hydrogen production by filtration combustion of methane by oxygen enrichment and depletion, *Int. J. Hydrogen Energy*, 29, 1365-70.

Bone WA (1912), Surface combustion, *J. Franklin Inst.*, 173, 101-31.

Bouma PH and De Goey LPH (1999), Premixed Combustion on ceramic foam burners, *Combust. Flame,* 119, 133-43.

Bouma PH, Eggels RL, DE Goey LPH, Nieuwenhuizen JK and Vander Drift AA (1995), Numerical and experimental study of the NO-emission of ceramic foam surface burners, *Combust. Sci. Technol*., 108, 193-203.

Bowman CT (1975), Kinetics of Pollutant Formation and Destruction in Combustion, *Prog. Energy Combust. Sci.*, 1, 33-45.

Brenner G, Pickenacker K, Pickenacker O, Trimis D, Wawrzinek K and Weber T (2002), Numerical and experimental investigation of matrix-stabilized methane/air combustion in porous inert media, *Combust. Flame,* 123, 201-13.

Bubnovich V and Toledo M (2007), Analytical modelling of filtration combustion in inert porous media, *Appl. Therm. Eng.,* 27, 1144-49.

Buckmaster J and Takeno T (1981), Blow off and flashback of an excess enthalpy flame, *Combust. Sci. Technol.*, 1981, 25, 153-58.

Chen YK, Hsu PF, Lim IG, Lu ZH, Matthews RD, Howell JR and Nicholas SP (1988), Experimental and theoretical investigation of combustion within porous media, *22nd Int. Symp. on Combust.*, *The Combust. Inst.*, Seattle, U.S.A, Aug 14 -19 Poster Paper: 22, 207.

Chen YK, Matthews RD and Howell JR (1987), The effect of radiation on the structure of a premixed flame within a highly porous inert medium, *Radiation, Phase Change Heat Transfer and Thermal Systems,* ASME-HTD, 81, 35-42.

Cho KW, Han K, Lee YK, Noh DS, Yoon HM, Riu KJ and Lee KH (2001), Premixed combustion of coke oven gas in a metallic fibre mat, *Fuel*, 80, 1033-36.

Choi B and Churchill SW (1979), A model for combustion of gaseous and liquid fuels in a refractory tube, *17th Int. Symp. on Combust., The Combust. Inst.*, 917-25.

Churchill SW (1989), Thermally stabilized combustion, *Chem. Eng. Technol.*, 12, 249-54.

Cookson EJ and Floyd II DE (2005), Application of reticulated metal foam to gas fired infrared burners, *4th Int. Conf. Porous Metals and Metal Foaming Technol. (JIMIC-4)*, Tokyo, Japan, September 21-23, 69-72.

Delalic N, Mulahasanovic Dz and Ganic EN (2004), Porous media compact heat exchanger unit–experiment and analysis, *Exp. Therm Fluid Sci.*, 28, 185-92.

Dillon J (1999), Combustion in porous media, LA-SUB-99-56 Final report. California Institute of Technology, Los Alamos National Lab, 1-27.

Dobrego KV, Gnezdilov NN, Kozlov IM, Bubnovich VI and Gonzalez HA (2005), Numerical investigation of the new regenerator–recuperator scheme of VOC oxidizer, *Int. J. Heat Mass Transfer*, 48, 4695-703.

Dobrego KV, Gnezdilov NN, Kozlov IM and Shmelev ES (2006), Numerical study and optimization of the porous media VOC oxidizer with electric heating elements, *Int. J. Heat Mass Transfer*, 6, 1-10.

Dobrego KV, Gnezdilov NN and Kozlov IM (2007), Parametric study of recuperative VOC oxidation reactor with porous media, *Int. J. Heat Mass Transfer*, 50, 2787–94.

Du L and Xie M (2006), The influences of thermophysical properties of porous media on superadiabatic combustion with reciprocating flow, *Heat transfer-Asian Research*, 35, 336-50.

Durst F, Trimis D, and Dimaczek G (1996a), Burner having material of varying porosity, *United States Patent*, No: 5522723.

Durst F and Trimis D (1996b), Compact porous medium burner and heat exchanger for household applications, *E C project report* (contract no. JOE3-CT95-0019).

Durst F and Weclas M (2001), A new type of internal combustion engine based on the porous-medium combustion technique, *J. Automobile Eng. IMechE Part D*, 215, 63-81.

Durst F and Trimis D, (2002), Combustion by free flames versus combustion reactors, *16th Int. Clean Air and Environ Conf. (Clean Air 2002)*, Christchurch, Newzland, August 19-22, 3, 1-20.

Echigo R (1982), Effective energy conversion method between gas enthalpy and thermal radiation and application to industrial furnaces, *Proc. 7th Int. Heat Transfer Conf.*, Munich, Germany, September 6-10, VI, 361-66.

Echigo R (1984), Method and device for combustion, Application No. 57-160456, Int. CI. F23C11/00, 8, 154.

Echigo R, Yoshizawa Y, Hanamura K and Tomimura T (1986), Analytical and experimental studies on radiative propagation in porous media with internal heat generation. *Proc. 8th Int) Heat Transfer Conf.*, San Francisco, U.S.A, March 16-20, II, 827-32.

Echigo R, Kurusu M, Ichimiya K and Yoshizawa Y (1987), Combustion augmentation of extremely low calorific gases, *Proc. of ASME/JSME Therm. Eng. Joint Conf.*, Honolulu, U.S.A., March 22-27, 99-103.

Echigo R. (1991), Radiation enhanced/controlled phenomena of heat and mass transfer in porous media, *Proc. ASME/JSME Thermal Eng. Joint Conf.*, Reno, U.S.A., September 30-October 2, 4, xxi-xxxii.

Echigo R, Yoshida H, Tawata, H and Tada S (1993), *12th Int. Conf. on Thermoelectrics*, Yokohama, Japan, November 9-11, VI-5, 1993.

Echigo R, Yoshida H, Tawata K, Koda M and Hanamura K (1994), Transient heat and mass transfer with condensable vapor in porous media, *Proc. 10th Int. Heat Transfer Conf.*, Brighton, UK, August 14-18, 5, 231-236.

Echigo R, Yoshida H, Tawata K and Tada S. (1995), Effective heating/cooling method for porous thermoelectric device in reciprocating flow combustion system, *Proc. 4th ASME/JSME Therm. Eng. Joint Conf.*, Lahaina, U.S.A, March 19-24, 4, 389-96.

Eleverum PJ, Ellzey JL and Kovar D (2005), Durability of YZA ceramic foams in a porous burner, *J. Mater. Sci.*, 40, 155-64.

Ellzey JL ad William Jr M (2003), Porous burner for gas turbine applications, *United States Patent* No. 2003024655.

Escobedo F and Viljoen HJ (1994), Modeling of porous radiant burners with large extinction coefficients, *Canadian J. Chem. Eng.*, 72, 805-14.

Fleming DK (1987), Non-catalytic porous-phase combustor, *United States Patent* 4643667.

Fu X, Viskanta R and Gore JP (1998a), Measurement and correlation of volumetric heat transfer coefficients of cellular ceramics, *Exp. Therm Fluid Sci.*, 17, 285-93.

Fu X, Viskanta R and Gore JP (1998b), Prediction of effective thermal conductivity of cellular ceramics, *Int. Comm. Heat Mass Transfer*, 25, 151-60.

Goeckner BA, Helmich DR, McCarthy TA, Arinez JM, Peard TE, Peters JE, Brewster MQ and Buckvis RO (1992), Radiative heat transfer augmentation of natural gas flames in radiant tube burners with porous ceramic inserts, *Exp. Therm Fluid Sci.*, 5, 848-60.

Goretta KC, Brezny R and Dam CQ (1990), High temperature mechanical behaviour of porous open-cell Al_2O_3, *Mater. Sci. Eng.*, 124, 151-58.

Hackert CL, Ellzey JL and Ezekoye OA (1999), Combustion and heat transfer in 2-D model porous burners. *Combust. Flame*, 116, 177-91.

Hale MJ and Bohn MS (1992), Measurement of the radiative transport properties of reticulated alumina foams, *ASME/ASES Joint Solar Eng. Conf.*, Washington D.C., U.S.A., April 4-8, Paper 92-v-842.

Hanamura K and Echigo R (1991), An analysis of flame stabilization mechanism in radiation burners, *Heat Mass Transfer*, 26, 377-83.

Hanamura K, Echigo R and Zhdanok SA (1993), Superadiabatic combustion in a porous medium, *Int. J. Heat Mass Transfer*, 36, 3201-09.

Hardesty DR and Weinberg FJ (1974), Burners producing large excess enthalpies, *Combust. Science Technol.*, 8, 201-14.

Hashimoto T, Yamasaki S and Takeno T (1982), An excess enthalpy flame stabilized in ceramic tubes, in flames, lasers, and reactive systems, *Prog. in Aeronautics and Astronautics*, 88, 57-77.

Hayashi TC, Malico I and Pereira JCF (2004), Three-dimensional modeling of a two-layer porous burner for household applications, *Comput. Struct.*, 82, 1543-50.

Hays JW (1933), Surface combustion process, *United States Patent,* No. 2095065.

Hendricks TJ and Howell JR (1994), Inverse radiative analysis to determine spectral radiative properties using the discrete ordinates method, *Proc. 10th Int. Heat Transfer Conf.*, Brighton, UK, August 14-18, 75-80.

Hendricks TJ and Howell JR (1996), Absorption/scattering coefficients and scattering phase functions in reticulated porous ceramics, *J. Heat Transfer*, 118, 79-87.

Henneke MR, Ellzey JL (1999), Modelling of filtration combustion in a packed bed, *Combust. Flame*, 117, 832–40.

Hoetger M and Thiele W (2006), Pore-type burner with silicon-carbide porous body, *United States Patent* No. 20060035190.

Hoffmann JG, Echigo R, Tada S and Yoshida H (1995),, Analytical study on flammable limits of reciprocating superadiabatic combustion in porous media, *Proc. 8th Int. Symp. Transport Phenomena in Combust.*, San Francisco, U.S.A, July 16-20. 2, 1430-40.

Hoffman JG, Echigo R, Yoshida H and Tada S (1997), Experimental study on combustion in porous media with a reciprocating flow system, *Combust. Flame*, 11, 32-64.

Howell JR, Hall MJ and Ellzey JL (1996), Combustion of hydrocarbon fuels within porous inert media, *Prog. Eng and Combust. Sci.*, 22, 121-45.

Hsu PF, Howell JR and Matthews RD (1991a), A numerical investigation of premixed combustion within porous inert media, *Proc. ASME /JSME Thermal Engg. Joint Conf.*, 4, Reno, U.S.A., March 17-22, 225-31.

Hsu PF (1991b), Analytical and Experimental study of combustion in porous inert media, *Ph.D. dissertation*, University of Texas.

Hsu PF, Evans WD and Howell JR (1993a), Experimental and numerical study of premixed combustion within non homogeneous porous ceramics, *Combust. Sci. Technol.*, 90, 149-72.

Hsu PF, Howell JR and Matthews RD (1993b), A numerical investigation of pre-mixed combustion within porous inert media, *J. Heat Transfer,* 115, 744-50.

Hsu PF and Matthews RD (1993c), The necessity of using detailed kinetics in models for premixed combustion within porous media, *Combust. Flame*, 93, 457-66.

Hsu PF and Howell JR (1993d), Measurements of thermal conductivity and optical properties of porous partially stabilized zirconia, *Exp. Heat Transfer*, 5, 293-313.

Huang Y, Chao CYH and Cheng P (2002), Effects of preheating and operation conditions on combustion in a porous medium, *Int. J. Heat Mass Transfer*, 4, 4315-24.

Hunt TK, Ivanenok JF and Sievers RK (1994), AMTEC auxiliary power unit for hybrid electric vehicles, *Proc. 29th Intersociety Eng. Conversion Engg. Conf.*, Monterey, U.S.A, August 7-11.

Hunt TK, Sievers RK and Ivanenok JF (1995), Low emission AMTEC automotive power system, *Proc. 30th Intersociety Eng. Conversion Engg. Conf.*, Orlando, U.S.A, July 30 July-August 4, 145-50.

Itaya Y, Miyoshi K, Maeda S and Hasatani M (1992), Surface combustion of a premixed methane-air gas on a porous ceramic, *Int. Chem. Eng.*, 32, 123-31.

Itaya Y, Jinno K and Hasatani M (1994), Methane premixed combustion behavior of a porous ceramic surface burner in a furnace, *J. Chem. Eng. Japan*, 20, 301-5.

Jugjai S and Rungsimuntuchart N (2002), High Efficiency heat-recirculating domestic gas burners, *Exp. Therm. Fluid Sci.*, 26, 581-92.

Jugjai S and Anantachai Sawananon (2004), The surface combustor-heater with cyclic flow reversal combustion embedded with water tube bank, *Fuel*, 83, 2369-79.

Kamal MM and Mohamad AA (2005), Enhanced radiation output from foam burners operating with a non premixed flame, *Combust. Flame*, 140, 233-48.

Kamijo T, Suzuki Y, Kasagi N and Okamasa T (2009), High-temperature micro catalytic combustor with Pd/nano-porous alumina, *Proc. Combust. Inst.*, 32, 3019-26.

Kandpal B, Maheswari RC and Kandpal TC (1995), Indoor air pollution from domestic cooking stoves using coal kerosene and LPG, *Energy Convers. Manage.*, 36, 1067-1072.

Kendall RM, DesJardin ST and Sullivan JD (1992), Basic research on radiant burners, Final report, *Gas Research Inst.*, Chicago, GRI Report No. 92-7027-171.

Kesting A, Pickenäcker O, Trimis D and Durst F (1999), Development of a radiation burner for methane and pure oxygen using the porous burner technology, *Proc. 5th Int. Conf. Technologies and Combust. Clean Environ. (Clean Air V)*, Lisbon, Portugal, July 12-15, 1999.

Khanna V, Goel R and Ellzey JL (1994), Measurements of emissions and radiation for methane combustion within a porous medium burner, *Combust. Sci. Technol.*, 99, 133-142.

Kline SR and Mc Clintock (1953), Describing uncertainties in single sample experiments, *Mech Engg.*, 75, 1-3.

Koester GE, Kennedy LA and Subramaniam VV (1994), Low temperature wave enhanced combustion in porous systems, *Proc. Central States Section meeting. The Combust. Inst.*, Madison, U.S.A, June 5-7, 55-60.

Korzhavin AA, Bunev VA and Babkin VS (1997), Dynamics of gaseous combustion in closed system with an inert porous medium, *Combust. Flame*, 109, 507-20.

Kotani Y and Takeno T (1982), An experimental study on stability and combustion characteristics of an excess enthalpy flame, *19th Symp. Int. on Combust., The Combust. Inst.*, Pittsburgh, Aug 8-13, 1503-09.

Kotani Y, Behbahani HF and Takeno T (1984), An excess enthalpy flame combustor for extended flow ranges, *20th Int. Symp. Combust., The Combust. Inst.*, Michigan, U.S.A, August 11-19, 2025-33.

Kulkarni MR and Peck RE (1996), Analysis of bilayered porous radiant burners, *Numerical Heat Transfer*, 30, 219-32.

Lammers FA and De Goey LPH (2004), The influence of gas radiation on the temperature decrease above a burner with a flat porous inert surface, *Combust. Flame*, 136, 533-547.

Lee KB and Howell JR (1991), Theoretical and experimental heat and mass transfer in highly porous media, *Int. J. Heat Mass Transfer*, 34, 2123-32.

Leonardi SA, Viskanta R and Gore JP (2002), Radiation and thermal performance measurements of a metal fiber burner, *J. Quant. Spectrosc. Radiat. Transfer*, 73, 491-501.

Leonardi SA, Viskanta R and Gore JP (2003), Analytical and experimental study of combustion and heat transfer in submerged flame metal fiber burners/heaters, *Trans. ASME*, 125, 118-25.

Li BX, Lu YP, Liu LH, Kudo K and Tan HP (2005), Analysis of directional radiative behavior and heating efficiency for a gas-fired radiant burner, *J. Quant. Spectrosc. Radiat. Transfer*, 92, 51-9.

Li Y-H, Chao Y-C and Dunn-Rankin D (2008), Combustion in a meso-scale liquid-fuel film combustor with central-porous fuel inlet, *Combust. Sci. Technol.*, 180, 1900-19.

Lim IG (1997), Effect of properties on CO and NO emission in premixed combustion within porous ceramic burner, *Proc. 4th Int. Conf. on Technologies and Combust. Clean Environ.*, Portugal, July 7-10, II, 28.

Liu JF and Hsieh WH (2004), Experimental investigation of combustion in porous heating burners, *Combust. Flame,*138, 295-303.

Lucke CE (1913), Design of surface combustion appliances, *J Indus Eng Chem.*, 1913, 5, 801-24.

Malico I and Pereira JCF (1999), Numerical predictions of porous burners with integrated heat exchanger for house hold applications, *J. Porous Media*, 2, 153-62.

Malico I, Zhou XY and Pereira JCF (2000), Two-dimensional numerical study of combustion and pollutants formation in porous burners, *Combust. Sci. Technol.*, 152, 57-9.

Malico I and Pereira JCF (2001), Numerical study on the influence of radiative properties in porous media combustion, *J. Heat Transfer*, 123, 951-57.

Marbach TL and Agrawal AK (2006), Heat-recirculating combustor using porous inert media for meso-scale applications, *J Propul Power*, 22, 145-150.

Marbach TL, Sadasivuni V and Agrawal AK (2007), Investigation of a miniature combustor using porous media surface stabilized flame, *Combust Sci Technol.*, 179:1901-22.

Mare L. di, Mihalik TA. Continillo G and Lee JHS (2000), Experimental and numerical study of flammability limits of gaseous mixtures in porous media, *Exp. Therm Fluid Sci.* 21, 117-23.

Min DK and Shin HD (1991), Laminar premixed flame stabilized inside a honeycomb ceramic, *Int. J. Heat Mass Transfer*, 34, 341-56.

Mishra SC, Steven M, Nemoda S, Talukdar P, Trimis D and Durst F (2006), Heat transfer analysis of a two-dimensional rectangular porous radiant burner, *Int. Commu. Heat Mass Transfer*, 33, 467-74.

Mital R, Gore JP and Viskanta R (1997), A study of the structure of submerged reaction in porous ceramic radiant burners, *Combust. Flame*, 11, 175-84.

Mital R, Gore JP and Viskanta R (1998), A radiant efficiency measurement procedure for gas fired radiant burners, *Exp Heat Transfer*, 11, 3-21.

Mjaanes HP, Chan L and Mastorakos E (2005), Hydrogen production from rich combustion in porous media, *Int. J. Hydrogen Energy*, 30, 579-92.

Mohamad AA, Ramadhyani S, Viskanta R (1994), Modelling of combustion and heat transfer in a packed bed with embedded coolant tubes, *Int. J. Heat Mass Transfer,* 37, 1181-91.

Mößbauer S, Pickenäcker O, Pickenäcker K, Trimis D (1999), *5th Int. Conf. Technologies and Combust. for a Clean Environ. (Clean Air V)*, Lisbon, Portugal, July 12-15, I, 519-23.

Mößbauer S, Grüber W and Trimis D (2001), Exhaust gas recirculation in porous burners for the target application zero emission steam engines, *Proc. 6th Int. conf. on technologies and combust. for a clean Environ*, Porto, Portugal, July 9-12, 2, 213-18.

Nakamura Y, Itaya Y, Miyoshi K, Hasatani M (1993), Mechanism of methane-air combustion on the surface of a porous ceramic plate, *J. Chem. Eng. Japan*, 26, 205-11.

Nemoda S, Trimis D and Zivkovi G (2004), Numerical simulation of porous burners and hole plate surface burners, Thermal Science, 8, 3-17

Orenstein RM and Green DJ (1992), Thermal shock behavior of open cell ceramic foams, *J. Am. Ceram. Soc.*, 75, 1899-1905.

Pickenacker O, Pickenacker K, Wawrzinek K, Trimis D, Pritzkow WEC, Muller C, Goedtke P, Papenburg U, Adler J, Standke G, Heymer H, Tauscher W and Jansen F (1999), Innovative ceramic materials for porous-medium burners, *Interceram*, Freiburg, Germany, 48, 424-33.

Qui K and Hayden ACS (2006), Premixed gas combustion stabilized in fiber felt and its application to a novel radiant burner, *Fuel*, 85, 1094-1100.

Qiu K and Hayden ACS (2007), Thermophotovoltaic power generation systems using natural gas-fired radiant burners, *Solar Energy Mater. Solar Cells*, 91, 588-96.

Raviraj SD and Janrt LE (2006), Numerical and experimental study of the conversion of methane to hydrogen in a porous medium reactor, *combust. Flame*, 144, 698-709.

Sadasivuni V and Agrawal AK (2009), A novel meso-scale combustion system for operation with liquid fuels, *Proc. Combust. Inst.*, 32, 3155-62.

Sahraoui M and Kaviany M (1994), Direct simulation vs volume-averaged treatment of adiabatic, premixed flame in a porous medium, *Int. J. Heat Mass Transfer*, 37, 2817-34.

Sanmiguel JE, Mehta SAR and Moore RG (2003), An experimental study of controlled gas-phase combustion in porous media for enhanced recovery of oil and gas, *Trans. ASME*, 125, 64-71.

Sathe SB, Peck RE and Tong TW (1989a), A numerical analysis of combustion and heat transfer in porous radiant burners, *Heat Transfer Phenom. Radiat. Combust. Fires*, ASME HTD, 107, 461-68.

Sathe SB, Kulkarni MR, Peck RE and Tong TW (1989b), An experimental study of combustion and heat transfer in porous radiant burners, *Meeting of Western Sates Section, The Combust. Inst.*, Livermore, U.S.A, Oct 23–24, 1-19.

Sathe SB, Kulkarni MR, Peck RE and Tong TW (1990a), An experimental and theoretical study of porous radiant burner performance, *23rd Symp. Int. on Combust., The Combust. Inst.,* Pittsburgh, U.S.A, May 21-23, 1011-18.

Sathe SB, Peck RE and Tong TW (1990b), Flame stabilization and multi-mode heat transfer in inert porous media-a numerical study, *Combust. Sci. Technol.*, 70, 93-109.

Scribano G, Solero G and Coghe A (2006), Pollutant emissions reduction and performance optimization of an industrial radiant tube burner, *Exp. Therm Fluid Sci.,* 30, 605-12.

Seinfeld JH (1986), Atmospheric Chemistry and Physics of Air Pollution, John Wiley and Sons, New York, 1986.

Semenov NN (1928), On the theory of the combustion process, *Z. Physics*, 48, 571.

Sharafat S, Ghoniem N, Williams B and Babcock J (2004), An innovative solid breeder material for fusion application, *16th ANS Topical Meeting on the Technol. of Fusion Energy*, Madison WI, U.S.A, September 14-16.

Shinoda M, Maihara R, Kobayashi N, Arai N and Churchill SW (1998), The characteristics of a heat-recirculating ceramic burner, *Chem. Eng. J.*, 71, 207-12.

Shinoda M, Tanaka R and Arai N (2002), Optimization of heat transfer performances of a heat-recirculating ceramic burner during methane/air and low-calorific-fuel/air combustion, *Energy Convers. Manage.*, 43, 1479-491.

Singh R, Kasana HS (2004), Computational aspects of effective thermal conductivity of highly porous metal foams, *Appl. Therm. Eng.*, 24, 1841-49.

Singh S, Ziolkowski M, Sultzbaugh J and Viskanta R (1991), Mathematical model of a ceramic burner radiant heater, *Foss. Fuel Combust.* ASME-PD, 33, 111-16.

Soete G (1966), Stability and propagation of combustion waves in inert porous media, *11th Symp. Int. on Combust., The Combust. Inst.*, Pittsburgh, U.S.A, July 11-15, 959-66.

Suzukawa Y, Sugiyama S, Hino Y, Ishioka M and Mori I (1997), Heat transfer improvement and NOx reduction by highly preheated air combustion, *Energy Convers. Manage.*, 38, 1061-71.

Takeno T, Sato K (1979), An excess enthalpy flame theory, *Combust. Sci. Technol.*, 20, 73-84.

Takeno T, Sato K and Hase K (1980), A theoretical study on an excess enthalpy flame, *Proc. of 18th Symp. Int. on Combust.*, *The Combust. Inst.*, Waterloo, Canada, August 17-22, 465-72.

Takeno T and Hase K (1983), Effects of solid length and heat loss on an excess enthalpy flame, *Combust. Sci. Technol.,* 31, 207-15.

Takeno T and Murayama M (1986), One-dimensional flame with extended reaction zone, *Progr. Astro. Sci.*, 105, 246-62.

Talukdar P, Mishra SC, Trimis D and Durst F (2004) Heat transfer characteristics of a porous radiant burner under the influence of a 2-D radiation field, *J. Quant. Spectrosc. Radiat. Transfer*, 84, 527-37.

Tanaka R, Shinoda M and Arai N (2001), Combustion characteristics of a heat recirculating ceramic burner using low-calorific fuel, *Energy Convers. Manage.*, 42, 1897-1907.

Tomimura T, Hamano K, Honda Y, Echigo R (2004), Experimental study on multi-layered type of gas-to-gas heat exchanger using porous media, *Int. J. Heat Mass Transfer*, 47, 4615-23.

Tong TW and Sathe SB (1988), Heat transfer characteristics of porous radiant burners, *ASME HTD*, 104, 147-55.

Tong TW, Lin WQ and Peck RE (1987), Radiative heat transfer in porous media with spatially-dependent heat generation, *Int. Comm. Heat Mass Transfer,* 14, 627-37.

Tong TW, Sathe SB and Peck RE (1990), Improving the performance of porous radiant burners through use of sub-micron size fibres, *Int. J. Heat Mass Transfer*, 33, 6, 1339-46.

Tong TW and Li W (1995), Enhancement of thermal emission from porous radiant burners, *J. Quant. Spectrosc. Radiat. Transfer,* 53, 235-48.

Trimis D and Durst F (1996), Combustion in a porous medium-advances and applications, *Combust. Sci. Technol.*, 121, 153-68.

Turns SR (2000), An Introduction to Combustion: Concepts and Applications, Second edition, McGraw-Hill, New York.

Viskanta R (1996), Interaction of combustion and heat transfer in porous inert media, *Transport Phenonm. Combust.*, 1, 64-87.

Viskanta R and Gore JP (2000), Overview of cellular ceramics based porous radiant burners for supporting combustion, *Int. J. Environ. Combust. Technol.*, 3, 167-203.

Volkert Jochen and Goebel Peter (2006), Burner for a gas and air mixture, *United States Patent* No. 6997701.

Weclas M (2005), Porous media in internal combustion engines, Cellular ceramics-structure, manufacturing, properties and applications, Wiley-VCH-Publication.

Wei M, Wang Y and Reh L (2002), Experimental investigation of the pre vaporized premixed (vpl) combustion process for liquid fuel lean combustion, *Chem. Eng. Process*, 41, 157-64.

Weinberg FJ (1971), Combustion temperatures: the future? , *Nature*, 233, 239-41.

Williams A, Woolley R, and Lawes M (1992), The formation of NOx in surface burners, *Combust. Flame*, 89, 157-166.

World Bank (2003), India: Access of the poor to clean household fuels, ESM 263, Joint United Nations Development Programme (UNDP)/World Bank Energy Sector Management Assistance Programme (ESMAP), July 2003.

Xiong T (1991), Experimental study of ultra-low emission radiant porous burner, *AFRC 1991 Spring Members Meeting*, Hartford, U.S.A, March 18-19.

Xiong Tian-Yu, Mark JK and Ferol F. Fish (1995), Experimental study of a high-efficiency, low emission porous matrix combustor-heater, *Fuel*, 74, 1641-47.

Yamamoto K, Takada N and Misawa M (2005), Combustion simulation with Lattice Boltzmann method in a three-dimensional porous structure, *Proc 4th Joint Meeting of the US Sections of the Combust. Inst.*, Philadelphia, U.S.A., March 20-23, 30, 1509-15

Yoshida H, Yun JH, Echigo R and Tomimura T (1990), Transient characteristics of combined conduction, convection and radiation heat transfer in porous media, *Int. J. Heat Mass Transfer*, 1990, 33, 847-57.

Yoshizawa Y, Sasaki K and Echigo R (1988), Analytical Study of the structure of radiation controlled flame, *Int. J. Heat Mass Transfer*, 31, 311-319.

Younis LB, Viskanta R (1993), Experimental determination of the volumetric heat transfer coefficient between stream of air and ceramic foam, *Int. J. Heat Mass Transfer*, 36, 1425-34.

Zeldovich Ya B, Barenblatt GI and Librovich VB (1985), Mathematical theory of combustion and explosions, Plenum Press, New York.

Zhang JM, Sutton WH and Lai FC (1997), Enhancement of heat transfer using porous convection-to-radiation converter for laminar flow in a circular duct, *Int. J. Heat Mass Transfer*, 40, 39-48.

Zhdanok SA, Martynenko VV and Shabunya SI (1993), Obtaining superadiabtic temperatures in combustion of gaseous fuel in a system of two porous plates with a periodic change of the direction of pumping, *J. Eng. Phys. Thermphys.*, 64, 463-69.

Zhdanok SA, Dobrego KV and Futko SI (1998), Flame localization inside axis symmetric cylindrical and spherical porous media burners, *Int. J. Heat Mass Transfer*, 41, 3647-65.

Zumbrunnen DA, Viskanta R and Incropera FP (1986), Heat transfer through porous solids with complex internal geometries, *Int. J. Heat Mass Transfer*, 29, 275-84.

LIST OF PUBLICATIONS AND PATENT

International Journals

1. **V. K. Pantangi**, A. S. S. R. Karuna Kumar, Subhash C. Mishra, N. Sahoo., *Performance Analysis of Domestic LPG Cooking Stoves with Porous Media.* International Energy Journal, 8, 139-144, 2007.

2. **V. K. Pantangi**, Subhash C. Mishra, P. Muthukumar, Franz Durst., *Experimental Investigations of a New Combinational Burner for Domestic Cooking Application.* Energy Conversion and Management. (Under review).

3. **V. K. Pantangi**, Subhash C. Mishra, P. Muthukumar, R. Reddy. *Performance Analysis of Porous Radiant Burners for Cooking Applications.* Applied Thermal Engineering. (Under review).

International Conferences

1. **V. K. Pantangi**, Subhash C. Mishra, Muthukumar P, Rajesh Reddy. *Experimental Study on Performance Improvement of a Domestic LPG Cooking Stove Using Porous Inert Media. Presented at* 20th National and 9th International ISHMT-ASME Heat and Mass Transfer Conference, January 4-6, 2010, Indian Institute of Technology Bombay, Mumbai.

2. **V. K. Pantangi**, Subhash C. Mishra. *Thermal Analysis of Low Wattage Porous Inert Media Radiant Burners. Presented at* 20th National and 9th International ISHMT-ASME Heat and Mass Transfer Conference, January 4-6, 2010, Indian Institute of Technology Bombay, Mumbai.

3. **V. K. Pantangi**, Subhash C. Mishra, P. Muthukumar, Franz Durst. *Experimental Investigations of New Combinational Burner for Domestic Cooking Application. Presented at* International Conference on Advances in Energy Research 2009, 9-11 December 2009, Indian Institute of Technology Bombay, Mumbai.

National Conferences

4. **V. K. Pantangi**, Subhash C. Mishra. *Improved Efficiency of Domestic LPG cooking Stove with Porous Media. Presented at* 22nd National Convention of Mechanical Engineers on Energy Technologies-Strategies for Optimal Utilization of Natural Resources, September 9 - 10, 2006, Guwahati.

5. **V. K. Pantangi**, Subhash C. Mishra. *Combustion Of Gaseous Hydrocarbon Fuels Within Porous Media – A Review. Presented at* National Conference on Advances in Energy Research, December4–5, 2006, Indian Institute of Technology Bombay, Mumbai.

PATENT

1. A national level patent titled "Development of porous radiant burner for domestic cooking applications" is under process.

APPENDIX – I

1. **Power/ Thermal load of a burner:**

To find the power/thermal load of the burner, kW = Mass flow rate of the fuel x calorific value of the fuel

For example:

If the flow meter shows a reading of 0.3 LPM = 1.23×10^{-5} kg/s

Then the power at which the burner is running = 1.23×10^{-5} kg/s x 45636.12 kJ/kg

= 0.56 kW

2. **Conversion of emissions from ppm to mg/m^3 in relation to the 3% O_2 reference index**

$$CO\ (mg/m^3) = \frac{21 - O_2\ reference}{21 - O_2} \times COppm \times 1.25$$

21 - Oxygen content of the air

O_2 – Measured oxygen content of the

$$NO_X\ (mg/m^3) = \frac{21 - O_2 reference}{21 - O_2} \times NO_X\ ppm \times 1.25$$

21 - Oxygen content of the air

O_2 – Measured oxygen content of the

APPENDIX – II

Estimation of Equivalence ratio (Φ)

The equivalence ratio $\Phi = \frac{(A/F)_{stoich}}{(A/F)_{actual}}$

Φ>1 fuel rich mixture

Φ<1 fuel lean mixture

Φ=1 stoichiometric mixture

The stoichiometric quantity of air is just that amount needed to completely burn a quantity of fuel. The stoichiometric air fuel ratio is determined by writing simple atomic balances, assuming that the fuel reacts to form an ideal set of products.

For a hydrocarbon fuel given by C_xH_y, the stoichiometric relation is expressed as [Turns, 2002]

$$C_xH_y + a(O_2 + 3.76N_2) \Leftrightarrow CO_2 + H_2O + 3.76 \times a \times N_2$$

$$(A/F)_{Stoich} = 4.76 \times a \frac{(MW)_{air}}{(MW)_{fuel}}$$

The main constituents of LPG are Propane (C_3H_8) – 60% and Butane (C_4H_{10}) – 40%

Stoichiometric relation:

$$\tfrac{3}{5}C_3H_8 + \tfrac{2}{5}C_4H_{10} + a(O_2 + 3.76N_2) \rightarrow cCO_2 + bH_2O + 3.76a\,N_2$$

After balancing,

$$\frac{3}{5}C_3H_8+\frac{3}{5}C_4H_{10}+\frac{28}{5}\left(O_2+3.76N_2\right)\rightarrow\frac{17}{5}CO_2+\frac{22}{5}H_2O+\left(3.76\times\frac{28}{5}\right)N_2$$

$$\left(A/F\right)_{Stoich}=4.76\times(28/5)\frac{29}{(248/5)}=15.58\approx15.6$$

For a required wattage, the fuel mass flow rate (F_{actual}) is known.

The equivalence ratio can be changed by changing the mass flow rate of air (A_{actual}) as per the requirement.

$$\Phi=\frac{15.6}{\left(A/F\right)_{actual}}$$

APPENDIX - III

Error Analysis

Klein and McClintock [1953] proposed a procedure for estimating the uncertainty of any measured quantity in experimental studies. If an estimated quantity, R depends on the independent variables like x_1, x_2, x_3,…….x_n then,

$$R = R\ (x_1, x_2, x_3, \ldots\ldots x_n)$$

Then the maximum value of uncertainty is given by:

$$W_R = W_R = \left[\left(\frac{\partial x_1}{x_1} \right)^2 + \left(\frac{\partial x_2}{x_3} \right)^2 + \left(\frac{\partial x_3}{x_3} \right)^2 \ldots\ldots\ldots\ldots\ldots \left(\frac{\partial x_n}{x_n} \right)^2 \right]^{1/2}$$

In the present case, the formula for efficiency is as given below:

$$\eta = \frac{[m_w C_w \Delta T_w] + [m_p C_p \Delta T_p]}{m_f \times CV}$$

Since $\Delta T_w = \Delta T_p = \Delta T$

$$\eta = \frac{[(m_w C_v) + (m_p C_p)][\Delta T]}{m_f \times CV_f}$$

$$m_f = m_1 - m_2$$

m_1 - Initial mass of the cylinder

m_2 - Final mass of the cylinder

The uncertainty in the thermal efficiency mainly comes due to the measured quantities of mass and temperature.

Assumptions:

1. Temperature rise of water and vessel are equal.
2. No error in values of specific heat of pan (C_p) and water (C_w), and Calorific value (CV) of fuel. The values considered are suggested in the standard (IS: 4246: 2002)

Hence the Calculation formula:

$$\frac{\partial \eta}{\eta} = \left[\left(\frac{\partial \eta}{\partial m_v} \Delta m_v \right)^2 + \left(\frac{\partial \eta}{\partial m_w} \Delta m_w \right)^2 + \left(\frac{\partial \eta}{\partial (\Delta T)} \Delta(\Delta T) \right)^2 + \left(\frac{\partial \eta}{\partial m_f} \Delta m_f \right)^2 \right]^{1/2}$$

where $\Delta m_v = \pm 1$ gm , $\Delta m_w = \pm 1$ gm

$\Delta(\Delta T) = \pm 1°C$, $\Delta m_f = \pm 0.1$ gm

At a condition of $m_v = 0.864$ kg, $m_w = 8$ kg

$\Delta T = (91\text{-}20) = 65°C$, $m_f = 0.1062$ kg

we get $\frac{\partial \eta}{\eta} = 0.0339$

Therefore the maximum uncertainty in efficiency is 3.39 ≈ ±3.4%.

APPENDIX – IV

Technical specifications of the instruments used in the experiments

1. Digital pressure gauges:

	P1		P2
Make	:DWYER (U.S.A.)	Make	: DWYER (U.S.A.)
Fluid	:LPG	Fluid	: Air
Models	: DPG-003	Models	: DPG-006
Range	: 0-2 bar	Range	: 0-13.8 bar
Wetted materials	: 316 SS.	Wetted materials	: 316 SS.
Housing Materials	: 300 Series SS.	Housing Materials	: 300 Series SS.
Accuracy	: ±0.05% full scale	Accuracy	: ±0.05% full scale
Pressure Limit	: 2 x FS range	Pressure Limit	: 2 x FS range
Temperature Limits	: -18 to 66°C	Temperature Limits	: -18 to 66°C
Power requirements	: 3 AAA batteries.	Power requirements	: 3 AAA batteries.
Weight	: 0.23 kg	Weight	: 0.23 kg

2. Pressure regulator

Make	: Norgren
Model	: R73G-2GK-RMN
Fluid	: Compressed air
Maximum pressure	: 10 bar
Operating temperature	: -20° to +50°C

3. Compressor

Make	: Ingersoll Rand
Type	: Reciprocating
Maximum Pressure	: 12 kg/cm^2
Free air delivery	: 400-450 lpm
Type	: 2 stage
Tank capacity	: 250 liters
Accessories	: Precise Pressure regulator, air filter

4. Weighing Balance (WB)

WB – I		**WB – II**	
Make	:SARTORIUS COMBICS LITE	Make	: TULA
Model	**:** CLWP1 – 30ED-I	Capacity	: 5kg
Capacity	: 30kg	Platform size	: 200 x 220 mm
Platform size	: 400X300mm	Readability	: 0.1 gm
Readability	: 1g		
Power Supply	: 90 to 260V AC & DC		
Indicator	:18mm LCD 7 segment backlit		

5. Rotameters

R1

Make	:Flow Tech Engineers Pvt. Ltd
Fluid	: LPG gas
Operating Pressure	: Ambient

Measuring range : 0-2.5 lpm

Least count : 0.1 lpm

Accuracy : ±2% FS

R2

Make :Flow Tech Engineers Pvt. Ltd

Fluid :Air

Operating Pressure :Ambient

Measuring range : 0-80 lpm

Least count : 2.5 lpm

Accuracy : ±1% FS

6. Thermocouples

T1

Make : Tempsens Instruments (I) Pvt. Ltd.

Type : metal sheathed K-type

Junction : Grounded

Range : 20 ºC to 1400 ºC

T2

Make : Tempsens Instruments (I) Pvt. Ltd.

Type : metal sheathed K-type

Junction : Exposed

Range : 20 ºC to 1400 ºC

7. Data Acquisition Unit (DAQ)

DAQ - 1

Make : VPL INFOTECH & CONSULTANTS

Model : V7520 A

Communication port : RS 232

Modules : 3

Module model : 7018

Channels : 45

DAQ – 2

Make : Omega

Model : OMB DAQ 55

Communication Port : USB

Module : 1

Channels : 8

8. Mass Flow meter

Make : Analyt MTC

Fluid : Propane

Model : 358

Communication Port : RS 232

Accuracy : ±1% on full scale

Flow range : 0 - 20 LPM

Response time : ±10 ms

Output voltage : 0 -5 V dc

9. Mass Flow Controller

Make	: Bürkert
Fluid	: Air
Model	: 8626
Accuracy	: ±1.5%
Communication port	: RS 232
Flow Range	: 25 – 1000 LPM
Output voltage	: 0 – 10 V dc

10. Portable Gas Analyser (PGA)

PGA 1		**PGA 2**	
Make	: TESTO	Make	: TESTO
Model	: 350 XL	Model	: 330 - 2
O_2	: 0 – 25 Vol%	O_2	: 0 – 21% Vol
Resolution	: 0.1 Vol%	Resolution	: 0.1 Vol%
Accuracy	: < 0.2 Vol%	Accuracy	: ± 0.2 Vol%
CO	: 0 – 10000 ppm	CO	: 0 – 8000 ppm
Accuracy	: < 5 ppm (0 – 99 ppm)	Accuracy	: ± 10 ppm (0 – 200 ppm)
Resolution	: 0.1 Vol%	Resolution	: 1ppm
NO	: 0 – 3000 ppm	NO	: 0 – 300 ppm
Accuracy	: < 5 ppm (0 – 99 ppm)	Accuracy	: ± 2 ppm (0 – 40 ppm)
Resolution	: 0.1 ppm	Resolution	:0.1 ppm
NO_2	: 0 – 500 ppm	NO_2	: 0 – 500 ppm
Accuracy	: < 5 ppm (0 – 99 ppm)	Accuracy	: < 5 ppm (0 – 99 ppm)